University of Turin

Department of Medical Sciences

PhD Biomedical Sciences and Oncology (XXXIV cycle)

Curriculum: Advanced techniques for the localization of human tumours

Simultaneous inhibition of the B-cell receptor signalling pathway and NAMPT enzyme activity shows potent antitumour activity in xenografts derived from patients with Richter syndrome

PhD coordinator: Prof. Emilio Hirsh

Supervisor: Prof. Silvia Deaglio

Candidate: Vincenzo Gianluca Messana

SSD: MED/03

A.A. 2021/2022

Abstract

This works defines for the first time a molecular circuit connecting NAMPT activity to the B cell receptor (BCR) pathway. Using four distinct Richter syndrome patient derived xenograft models (RS-PDX), we show that ligation of the BCR results in transcriptional activation of the NAD-biosynthetic enzyme nicotinamide mononucleoside phosphoriblsyl transferase (NAMPT), with increased protein expression, in turn positively affecting global cellular NAD^+ levels and sirtuin activity. Blocking NAMPT by using the novel OT82 inhibitor in combination with the PI3K δ/γ inhibitor duvelisib induces rapid and potent apoptotic responses in all four models, independently of their mutational profile and of the expression of the other NAD^+ biosynthetic enzymes, including nicotinate phosphoribosyltransferase (NAPRT). The connecting link in the circuit is represented by AKT, which is both tyrosine- and serine-phosphorylated by PI3K activity and deacetylated by sirtuin 1 and 2 to obtain full kinase activation. Acetylation (i.e., inhibition) of AKT following OT82 administration was shown by 2D gel electrophoresis. Consistently, pharmacological inhibition or silencing of sirtuin 1 and 2 impair AKT activation and induce apoptosis of RS cells in combination with duvelisib. Lastly, treatment of RS-PDX mice with the combination of OT82 and duvelisib results in significant inhibition of tumor growth, with evidence of *in vivo* activation of apoptosis. Collectively, these data highlight a novel application of NAMPT inhibitors in combination with duvelisib in aggressive lymphomas.

Abbreviations Used

ABVD = Doxorubicin, Bleomycin, Vinblastine, Dacarbazine

ADCs = Antibody-drug conjugates

ADPR = ADP ribose

ARTs = Mono adenosine diphosphate-ribose transferases

BCL-2 = B-cell lymphoma 2

BCR = B lymphocyte antigen receptor

BTK = Bruton's tyrosine kinase

cADPR = cyclic ADP ribose

CDK4/6 = Cyclin-dependent kinase 4 and 6

CLL = Chronic lymphocytic leukemia

CR = Complete response

CT = Computed tomography

DLBCL = Diffuse large B-cell lymphoma

ECOG= Eastern Cooperative Oncology Group

ECOG PS = ECOG performance status

eNAMPT = Extracellular NAMPT

FDG = Fluorodeoxyglucose

GAPDH= Glyceraldehyde 3-phosphate dehydrogenase

GSSG = Oxidized glutathione

GSH = Reduced glutathione

GM-CSF = Macrophage colony-stimulating factor

GRs = Glutathione reductases

HL = Hodgkin lymphoma

IDH= Isocitrate dehydrogenase

LDH = lactatedehydrogenase

LRF CLL4 = Leukemia Research Foundation Chronic Lymphocytic Leukaemia 4

LRP4 = lipoprotein receptor-related protein 4

MMAE = Antimicrotubular agent monomethyl auristatin E

Na = Nicotinic acid

NAAD = Nicotinate adenine dinucleotide

NAADP = Nicotinic acid adenine dinucleotide phosphate

NAD^+ = Nicotinamide adenine dinucleotide

NADH= Reduced NAD^+

NADPH = Reduced $NADP^+$

NAM = Nicotinamide

NAMPT = Nicotinamide phosphoribosyl transferase

NAPRT = Nicotinate phosphoribosyltransferase

NMN = Nicotinamide mononucleotide

NMNAT = Nicotinamide nucleotide adenyltransferase

NR = Nicotinamide riboside

NRK= Nicotinamide riboside kinase

OFAR1 = Oxaliplatin, fluradabine, ara-C and rituximab

OGD = Oxoglutarate dehydrogenase

ORR = Overall response rate

PAR = Mono-ADP-ribose from poly (ADP-ribose)

PARPs = Poly ADP-ribose polymerases

PET = Positron emission tomography

PDX = Patient derived xenograft

PPM1D = Protein phosphatase Mg2+/Mn2+-dependent 1D

PRPP =5-phosphoribosyl-1-pyrophosphate

Prx = Peroxiredoxin

PSF = Progression free survival

QA = Quinolinic acid

QPRT = Quinolinate phosphoribosyltransferase

R-CHOP = Rituximab, Cyclophosphamide, Doxorubicin, Vincristine and Prednisone

ROR1 = Receptor tyrosine kinase–like orphan receptor 1

RS = Richter syndrome

SASP = Senescence-associated secretory

SBS-RT = Single base substitution

SCT = Stem cell transplantation

SLL = Small Lymphocytic Lymphoma

TCA = Tricarboxylic acid cycle

TLR4 = Toll-like receptor 4

trisomy 12 = Third chromosome 12

Trx = Reduced thioredoxin

TrxRs = Thioredoxin reductases

Table of Contents

INTRODUCTION **7**

1. NAD^+ metabolism **7**

1.1 The multiple roles of NAD^+ 7

1.2 NAD+ biosynthesis 10

1.3 NAD^+ in cancer 13

1.4 Sirtuin in cancer 17

1.5 Targeting NAD^+ metabolism in cancer 20

2. Richter Syndrome **24**

2.1 Definition 24

2.2 Clonally related RS 24

2.3 Histopathologic features of Richter syndrome 26

2.4 Incidence 28

2.5 Pathogenetic mechanism 29

2.6 Risk factors for Richter transformation 33

2.7 Clinical presentation 35

2.8 Prognosis of Richter Syndrome 36

2.9 Current treatment of Richter Syndrome 39

2.10 Novel therapeutic approaches in Richter Syndrome patients 41

2.11 Combination strategies in Richter Syndrome patients 43

2.12 RS-Patient derived xenograft (PDX) 46

AIM OF THE WORK **50**

MATERIALS AND METHODS **51**

4.1 Reagents and antibodies 51

4.2 RS-PDX Models 51

4.3 Ex-vivo treatment of RS cells 52

4.4 RNA sequencing analysis 53

4.5 RNA extraction and qRT-PCR 53

4.6 Western Blotting 53

4.7 Enzymatic assays 54

4.8 Apoptosis evaluation and combination index 54

4.9 Immunoprecipitation 54

4.20 2D Electrophoresis (IEF/SDS-PAGE) 55

4.11 Gene silencing 55

4.12 Immunohistochemistry 56

RESULTS 57

5.1 NAD biosynthetic pathways in RS 57

5.2 NAMPT is dynamically modulated upon BCR signaling 57

5.3 Functional cooperation between NAMPT and PI3Kδ/γ inhibitors 58

5.4 PI3Ki and NAMPTi converge on AKT in fully blocking the BCR signalling pathway 59

5.5 SIRT1 or SIRT2 inhibition of in combination with Duvelisib leads to increased apoptosis 60

5.6 In vivo combination of OT-82 and Duvelisib treatments induce a significant block in tumor growth and reduction in cellular sirtuins activity 61

DISCUSSION 63

REFERENCES 69

FIGURES 95

PUBLICATIONS OF THIS PHD THESIS 108

LIST OF PUBLICATIONS 109

(chronological order, 2018-to date, during PhD) 109

Introduction

1. NAD^+ metabolism

1.1 The multiple roles of NAD^+

Nicotinamide adenine dinucleotide exists in two forms, including an oxidized (NAD^+) and a reduced (NADH) form, and plays a vital role in intermediary metabolism, as obligatory partner in numerous oxidation/reduction reactions.[1,2] NAD^+ was discovered over 100 years ago and went through a period of relative anonymity until was improved the knowledge about its chemistry and function by Otto Warburg in 1930s.[3] The relevance of findings concerning the centrality of NAD^+ reactions in cell physiology, strongly encouraged studies on NAD^+ metabolism in the last decades, leading to the validated evidence of the dual role of NAD^+ as energy cofactor and signalling molecule.[2] As energetic co-enzyme, NAD^+ is first essential as electron acceptor donor in various metabolic pathways including cytosolic glycolysis, serine biosynthesis, mitochondrial tricarboxylic acid cycle (TCA) and in mitochondrial oxidative phosphorylation.[4] Moreover, the balance between the NAD^+/reduced NAD^+ (NADH) and $NADP^+$/reduced $NADP^+$ (NADPH) redox couples are essential for maintaining cellular redox homeostasis and for modulating cellular antioxidation mechanisms, energy metabolism and mitochondrial functions.[5] NAD^+ is used as a redox coenzyme by almost 300 dehydrogenases and it is primarily used during glycolysis.

In glycolysis, the first enzyme utilizing NAD^+ is glyceraldehyde 3-phosphate dehydrogenase (GAPDH). It is the sixth step in glycolysis, wherein glyceraldehyde 3-phosphate is oxidized into 1,3-bisphosphoglycerate are required two molecules of NAD^+, which in turn is reduced to NADH per molecule of glucose.[6]

The products of glycolysis are two moles of pyruvate, 2 moles of NADH and two moles of ATP. Pyruvate has multiple possible fates. The final glycolytic product pyruvate can be converted to lactate in condition of low oxygen tension or metabolized to produce acetylCoA thus entering the TCA cycle for maximal energy production. In lactate dehydrogenase reaction pyruvate is reduced to lactate with concomitant interconversion of NADH and NAD^+.[7] For maximal energy yield pyruvate is alternatively acted upon by the pyruvate dehydrogenase complex to form acetylCoA with concomitant NAD^+ reduction to NADH.[8] AcetylCoA can then enter the TCA cycle, where NAD^+ equivalents are reduced to NADH moieties in several key steps by isocitrate dehydrogenase (IDH), oxoglutarate dehydrogenase (OGD) and malate dehydrogenase. The next enzyme in the cycle, OGD, catalyzes the reaction from α-ketoglutarate to succinyl CoA, with reduction of NAD^+ to NADH. Lastly, NADH formed from glycolysis (via the malate-aspartate shuttle) or the TCA cycle can react at Complex I, in the mitochondrial electron transport chain to regenerate ATP.[9] In addition, a higher ratio between NAD^+/NADH and their relative phosphorylated form ($NADP^+$/NADPH), is essential to maintain a reducing environment for both enzymatic and non-enzymatic scavengers defence systems against oxidative stress.[10] Intriguingly, both enzymatic and non-enzymatic antioxidant system components use NADPH as the ultimate donor of reductive power.[11] Two classes of enzymatic components, glutathione reductases (GRs) and thioredoxin reductases (TrxRs) use electrons from NADPH to reduce a disulfide to a dithiol. Specifically, GRs catalyze the conversion of oxidized glutathione (GSSG) into reduced glutathione (GSH), while TrxRs enzymes maintain the reduced thioredoxin (Trx) concentration that supports peroxiredoxin (Prx) to remove H2O2.[12] Therefore, through supplying electrons for

bioreductive synthesis and the regeneration of GSH and reduced thioredoxin, NADPH plays critical roles in the maintenance of redox homeostasis and modulating redox signaling.[13]

Beyond its vital role as a coenzyme in energy metabolism, the important role of NAD^+ has expanded to be a co-substrate for various enzymes with fundamental roles in gene expression and cell signaling.[14] In these reactions, NAD^+ contributes as a donator of ADP-ribose and, through its consumption, the energetic cofactor acquires the characteristic of an intracellular or extracellular signaling molecule. Unlike the metabolic redox reactions, which reversibly oxidize or reduce pyridine nucleotides, NAD^+-dependent signaling processes continuously consume NAD^+.

There are different NAD-consuming enzymes (Figure 1), among them (i) mono adenosine diphosphate (ADP)-ribose transferases (ARTs) and poly ADP-ribose polymerases (PARPs), which transfer the ADP ribose moiety to acceptor proteins resulting in their modification and function regulation; (ii) sirtuins (1-7), which catalyze the NAD-dependent deacetylation of metabolic enzymes and transcription factors, thus controlling their activity; (iii) NAD glycohydrolase (CD38/CD73) that generates different NAD^+ metabolites, including ADP ribose (ADPR), cyclic ADP ribose (cADPR) and nicotinic acid adenine dinucleotide phosphate (NAADP), all molecules with calcium (Ca^{+2}) mobilizing activity.[15,16] These enzymes through their functional activities of calcium (Ca^{2+}) signaling activation or post-translational modifications (deacetylation and ADP-riboposylation reactions) are implicated in the regulation of extended biological processes. Among others, gene transcription, cell differentiation, cell cycle progression, DNA repair, chromatin stability, cell adaptation to stress signals, immune response, and represent coupling elements between the metabolic state of a cell and

its signaling and transcriptional activities.[17] Considering the cellular impact of NAD-consuming enzymes, especially sirtuins, has led to the hypothesis that these enzymes may act as "energy sensors", and consequently, regulating the triggering of adaptive responses. These enzymes are considered "energy sensors" as they respond to changes in NAD^+ levels, a complex and not fully understood phenomenon involving NAD^+ pool sub-cellular compartmentalization and NAD^+ transport across the cell and organelle membrane.[2]

1.2 NAD+ biosynthesis

NAD^+ levels are finely regulated, as it is highly compartmentalized in the cytoplasm, mitochondria and nucleus, which represent its main subcellular pools. These different pools are regulated independently of each other. When cellular NAD^+ levels fall below a critical threshold, regeneration processes are triggered. The two main ones are re-oxidation by NADH, or through the synthesis of active NAD^+ from pyridine nucleotides.[18–21]

NAD^+ can be made *de novo* from L-tryptophan via the kynurenine pathway or from vitamin B3 precursors, such as nicotinamide (Figure 1).

The kynurenine pathway is composed from 8-steps biosynthesis reaction, starting from tryptophan/quinolinic acid (QA) and controlled by the rate limiting enzyme quinolinate phosphoribosyltransferase (QPRT).[2] In particular, the contribution of this biosynthesis pathway is not yet fully elucidated. The kynurenine pathway is particularly active in liver cells, as most cells do not express all the enzymes of this pathway. In the liver, most tryptophan is metabolised into NAM, from which it is then released into the serum and taken up by peripheral cells, where it is subsequently conferred into NAD^+ by the salvage pathway. Recent evidence has shown that some cells of the immune system, such as

macrophages, as well as renal, endocrine and nervous system cells, produce NAD^+ via tryptophan, contributing to systemic NAD^+ levels.[22–24]

In order to maintain the physiological concentration of the vital pyridine cofactor, rather than being generated de novo, most NAD^+ is recycled via the three salvage pathways from nicotinic acid (Na), nicotinamide (Nam) or nicotinamide riboside (NR) present in NAD^+ metabolites or from food sources.[17,25] The salvage pathways predominate in most cell types and each of them is controlled by a rate-limiting enzyme. Specifically, NR is used to generate NMN by nicotinamide riboside kinase (NRK); Na is converted to NAMN through nicotinate phosphoribosyltransferase (NAPRT); Nam is converted to NMN by nicotinamide phosphoribosyl transferase (NAMPT).

NR is a newly discovered NAD^+ precursor that feeds the recovery pathway and it has been detected in cow's milk as a natural nutrient. NR is first phosphorylated into NMN by NR kinases (NRK1-2), after which NMNATs catalyse the production of NAD^+.[26] The Preiss-Handler pathway was first discovered in human erythrocytes. In this pathway, NA can be converted to NAD^+ in a three-step process that produces NAMN and NAAD as intermediate metabolites. In mammals, the key enzyme in this biosynthetic pathway is NAPRT as it catalyses the first conversion reaction of NA to NAMN.[27]

NAMPT catalyzes the reaction between NAM and 5-phosphoribosyl-1-pyrophosphate (PRPP) to form nicotinamide mononucleotide (NMN).

NMN is then converted to NAD^+ by nicotinamide nucleotide adenyltransferase (NMNAT1-3), using ATP as the donor of adenylyl moiety.[25] Again the final steps of these reactions are carried out by NMNATs which convert NMN to NAD^+, and NAMN to nicotinate adenine dinucleotide (NAAD). NAAD is finally amidated to NAD^+ by the enzyme NAD^+ synthetase.[28]

Several lines of evidence support the evidence that in mammalian cells, the NAM salvage pathway controlled by NAMPT is the most relevant.[29,30]

In fact, NAM is the most abundant NAD^+ precursor in the bloodstream.[21] Moreover, NAMPT, catalyses the NAD^+ synthesis reaction from NAM, which is also the product of all the reactions of NAD-consuming enzymes, such as sirtuins and PARP.[31] For these reasons, NAMPT links the biosynthesis and degradation process in a functional loop in which NAD^+ is consumed and regenerated. NAMPT is considered the master regulator of NAD^+ biosynthesis in all mammalian cells, as well as a vital gene whose absence of expression has been correlated with drastic lethality in mice.[32,33]

NAMPT not only plays a key role within cells, but it also has a role at the extracellular space. NAMPT has been found in plasma and in the supernatants of different type of cells (tumor cells but also differentiated adipocytes, primary hepatocytes, cardiomyocyte, leucocytes, neutrophils, monocytes and macrophages), where exerts cytokine-like properties.[33,34]

It was reported an increased extracellular (e)NAMPT levels in conditions of acute or chronic inflammation, including tumours, correlating with worse prognosis and increased tumour aggressiveness.[34] Furthermore, eNAMPT is involved in several biological functions, as it acts as a cytokine, independent of its enzymatic activity, modulating the activation of inflammatory programmer and the immune response.[35–37]

Specifically, eNAMPT also exerts pro-oncogenic effects by modulating the tumor microenvironment, enhancing tumor metabolism, and promoting EMT.[38,39]

Although the modalities leading to its secretion are still unknown, it has recently been shown that Toll-like receptor 4 (TLR4) is a receptor for Enampt.[40] Finally, eNAMPT, as an adipokine, also known as visfatin, plays a critical role in metabolic diseases.[35]

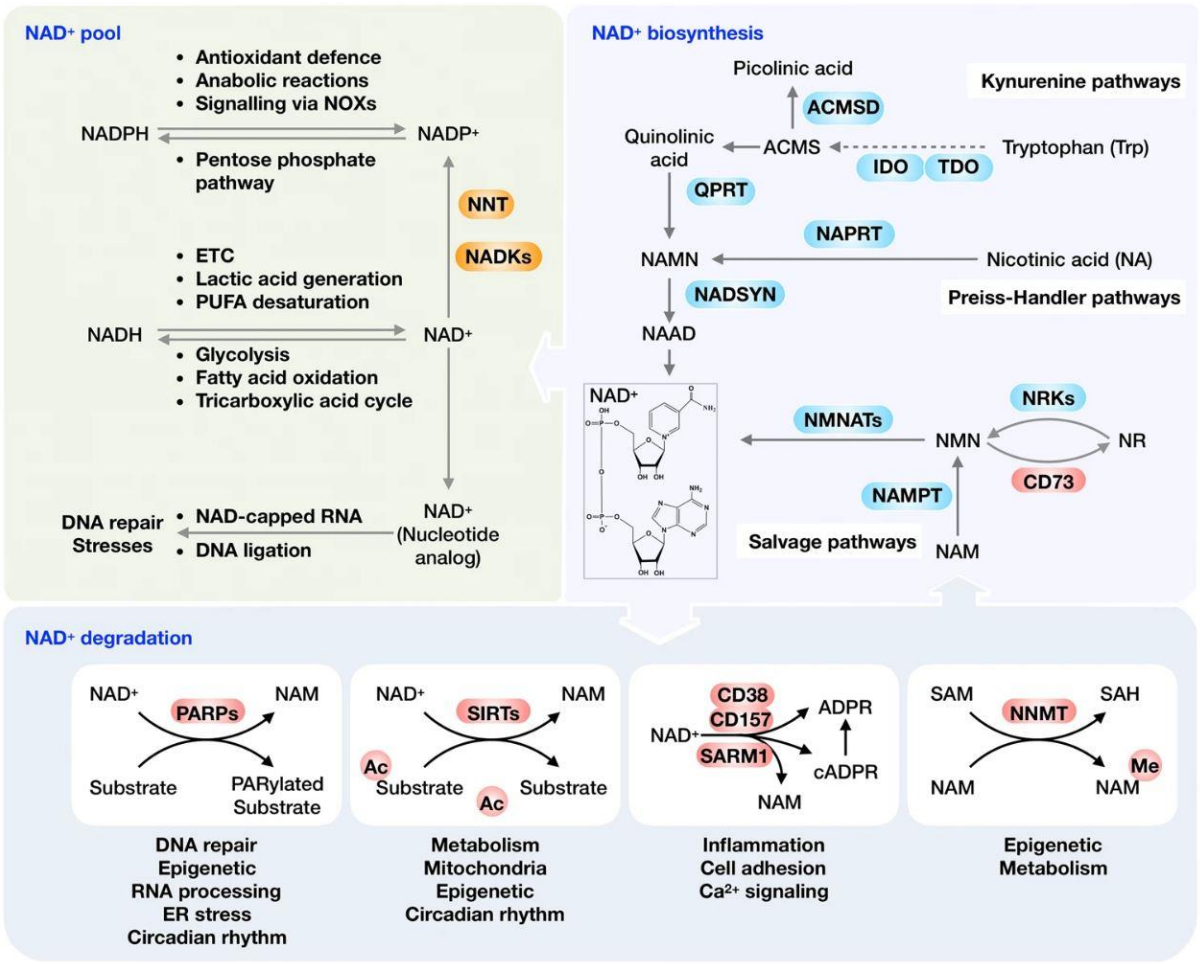

1.3 NAD$^+$ in cancer

One of the main hallmarks established by cancer cells is the metabolic reprogramming, a process that support and enable the metabolic adaptation and cancer growth. The aim of the metabolic adaptation is to satisfy the adaptive needs during tumor progression, including growth in the nutrient-altered and oxygen-deficient microenvironment.[41]

There are multiple molecular mechanisms underlying the metabolic reprogramming processes, which involve the activation of different oncogenic pathways, specific in various cancer type (e.g., the B-receptor signaling pathway in chronic lymphatic leukemia or the pathways driven by RAS, BRAF and MEK in metastatic melanoma). The activation of these oncogenic signaling pathways directly influences the expression and activity of metabolic

enzymes, so that cancer cells can continue to proliferate in unfavorable environments.[37] The classic example of metabolic reprogramming in cancer cells is the 'Warburg effect', defined as an increase in the rate of glycolysis and lactate production even in the presence of oxygen, whose ultimate scope of this metabolic change is the increase in ATP synthesis. The Warburg effect is closely related to the need that cancer cells have to sustain a higher production and availability of NAD^+, since it can directly promote cancer proliferation by enhancing the activity of GADPH.[17]

Certainly, the tissue-specific expression and modulation of the NAD^+ biosynthetic and consuming enzymes play a pivotal role in these energetic adaptation processes, since the continuous replenishment of NAD^+ is essential for both energy for new energetic and signal transduction necessities of cancerous cells.[28]

Regardless of tumour type, the processes of neoplastic initiation and progression are directly influenced by intracellular NAD^+ levels and consequently by the activity of NAD-consumption enzymes. Specifically, as described above, PARPs directly modulate DNA repair and chromatin stabilisation processes, while sirtuins are involved in epigenetic regulation and post-translational regulation of some proteins. Increased NAD^+ pool consequently led to an increase in the activity of both families of these enzymes, which in turn activate several pro-cancer pathways involved in the first step of carcinogenesis and in the development of drug resistance as well.[4,42]

Among the other NAD-consuming enzymes, Sirtuins have key roles in normal and diseased cells, including cancer cells.[42,43] SIRT1 is predominantly nuclear and is known as a tumor-promoter protein.[43] In both solid and hematological cancer have been reported that it is upregulated.[44–46] In fact, SIRT1 deacetylate and repress the activity of the tumour suppressor p53 and the FOXO transcription factors reducing their pro-apoptotic effect.[47,48]

Furthermore, it is known that the two mains cellular NADases, CD38 and CD73, are overexpressed in several cancer types, where they control the activation of different signaling pathways and influence cancer immune tolerance.[49]

Moreover, in pancreatic ductal adenocarcinoma, upregulation of some PARPs protein increases consumption of NAD^+ results in increased sensitivity on NAD^+ depletion thought small molecule inhibition.[50]

The molecular basis and genetic mechanisms that underlie the selection of the NAD^+ biosynthetic pathway in cancer cells have not been fully uncovered. Notably, NAMPT overexpression was initially observed in a wide range of solid tumors, including colorectal, ovarian, breast, prostate, well-differentiated thyroid cancers, endometrial carcinomas, melanoma, gliomas and astrocytomas.[51]

Clinically, higher NAMPT expression increases the tumor aggressiveness. Indeed, it is associated with worse prognosis and correlates with increased tumor growth, metastases, and cellular dedifferentiation in astrocytoma/glioblastoma and metastatic melanoma.[52,53]

Increased NAMPT expression has also been observed in hematological malignancies, particularly in lymphomas such as: diffuse large B-cell lymphoma, follicular B-cell lymphoma, Hodgkin's lymphoma, and peripheral T-cell lymphoma and is associated with a more aggressive malignant lymphoma phenotype.[53]

NAMPT overexpression is also often associated with the acquisition resistance to chemotherapeutic agents, including fluorouracil and doxorubicin.[54,55] In addition, it was elucidated that NAMPT overexpression also increased steaminess and invasiveness properties of cancer cells by regulating epithelial to mesenchymal transition and the proinflammatory senescence-associated secretory (SASP) phenotype.[56]

Remarkable, NAPRT is frequently amplified and overexpressed in a subset of human tumors such as ovarian prostate, ovarian, and pancreatic cancers.[57] On the contrary, gastric, renal, and several leukemia cell lines, were reported to have low or no NAPRT expression.[58] In colorectal cancer cells have been highlighted that both NAPRT and NAMPT are negative prognostic marker in these patients and their highest expression is associate with vascular invasion, lymph node metastasis and advanced TNM stage. In colorectal cancer patients NAMPT is mainly regulated by miRNAs binding its promoter, while NAPRT gene is amplificated as well as its promoter is methylated, both these two-event result in NAPRT up-regulation.[59] On the other hand, in other kind of cancer the mutations in the protein phosphatase $Mg2^{+}$/$Mn2^{+}$-dependent 1D (PPM1D) or isocitrate dehydrogenase 1 (IDH1) genes, are involved in the hypermethylation of NAPRT promoter inducing its silencing. [60]

Due to their dependency on the Nam salvage pathway for survival, NAPRT-deficient cancers are extremely relayed on NAMPT activity to regenerate NAD^{+}.[61,62]

Additionally, NAPRT was also found to exist as an extracellular protein, which mediates inflammation by binding to TLR4 and by activating the NF-κB pathway. Consistent with these findings, NAPRT serum levels were strikingly elevated in septic patients.[63]

Importantly, Chowdhry et al, demonstrated the NAD-producing pathway in cancer cells is based upon the healthy tissues from which they originate.[64] Accordingly, during malignant transformation, tissues with a high expression of NAPRT remain dependent on this pathway in NAD^{+} regeneration. On the other hand, salvage-dependent tumors originate from tissues that do not express NAPRT and, consequently, their NAD^{+} supply relies mainly on NAMPT. Indeed, when NAMPT was depleted in salvage-dependent tumors, they were still able to maintain the NAD^{+} supply through the alternative salvage NR-NMRK1 pathway, and dual NMRK1 and NAMPT inhibition resulted in more effective NAD^{+} reduction and significant

tumor suppression *in vivo*. Overall, this finding provides insights into the essential role that NAD^+ plays in energetic and transcriptional cancer cell metabolism, growth and survival. Based on NAD^+ metabolism, targeting the activity of NAD^+ biosynthetic machinery was conceived as a promising therapeutic strategy against cancer. [17]

1.4 Sirtuin in cancer

Sirtuins (SIRT1–7) are a family of deacetylase proteins for which NAD^+ is a coenzyme for the removal acetyl modifications of lysine residues on histones and other proteins, generating o-actyl-ADP-ribose and NAM as the reaction products.[1,2] The best characterized member is SIRT1, which has been associated with longevity. There is evidence showing that resveratrol, a potent antioxidant with anti-aging effects, is able to increase NAD^+ levels, leading to SIRT1 activation.[1,2,20]

The NAD+-consuming enzyme SIRT1 strongly depends on the NAD^+/NADH ratio and can be inhibited by high NAM levels and DBC1, an endogenous SIRT1 inhibitor. Most of the evidence shows that SIRT1 can act as a tumor promoter. It is well known that SIRT1 has an anti-aging effect and that its activity can be increased by calorific restriction, which can also reduce cancer risk.[17]

SIRT1 also acts as a deacetylase and inhibits HIF-1α, one ofthe factors needed to activate the Warburg effect.[65] However, SIRT1 has been found to be upregulated in several human cancers. The relationship between SIRT1 and NAMPT has been well established; that is, NAMPT promotes SIRT1 activity through a NAD^+ pool increase and NAM level reduction.[66]

In addition to HIF-1α, SIRT1 regulates other important factors, such as p53, c-Myc, FOXO3, E2F1, BAX, and NF-κB. The most important antitumoral effects of p53 are cell cycle arrest

and apoptosis. P53 can also inhibit G6PDH in the PPP pathway. SIRT1 deacetylates and inhibits p53, ensuring R5P and NADPH production, and promotes cell survival.[4]

SIRT1 is also involved in the promotion of cancer cell proliferation, angiogenesis, and metastasis through the activation of the MAP kinase pathway by deacetylation.[67] All these data corroborate the oncogenic role of SIRT1, which strongly depends on the NAD^+ pool and NAMPT activity.

Another major cytosolic NAD^+-consuming enzyme is SIRT2, originally considered a tumor suppressor.[68] SIRT2 inhibits the peroxidase activity of peroxiredoxin-1 (Prdx-1) by deacetylation, increasing oxidation, and sensitizing breast tumor cells to further increase ROS.[69] Another target of SIRT2 is HIF1α in the cytosol, promoting the hydroxylation and degradation of HIF1α and suppressing the tumor growth dependent on hypoxia. However, other works have demonstrated that SIRT2 promotes cancer growth by stabilizing the Myc family of oncoproteins and enhancing the signaling of the Notch pathway.[70–72]

Mutations in the SIRT2 gene have also been reported in human cancers, impairing genome maintenance and promoting tumorigenesis.[73,74]

SIRT2 has also been described as a sensor for the amount of nutrients available in the cell and regulating metabolic activity to adapt the energy need for cancer growth.[75]

SIRT3, similar to SIRT4, has both oncogenic and tumorsuppressive activities. SIRT3 is localized in the mitochondria but is also localized in the nucleus and translocated to mitochondria upon DNA damage. This translocation contributes to the downregulation of genes involved in mitochondrial function.[76] SIRT3, on the other hand, inhibits apoptosis and promotes cell growth, increases glycolytic metabolism, maintains mitochondrial membrane integrity, promotes mitochondrial DNA repair, and increases cell resistance to environmental

stress.[77–83] SIRT3 can act as a tumor suppressor by inactivating HIF1α and decreasing oxidative stress.[84] SIRT3 activation correlates with an increase in mitochondrial NAD^+ and a number reduced of glioblastoma-initiating cells.[85] In contrast, the reduction of mitochondrial NAD^+ levels inhibits SIRT3 activity, increasing ROS levels through the deactivation of superoxide dismutase 2 (SOD2), facilitating the metastasis of hepatocellular carcinoma cells.[86] SIRT4 functions as an ADP-ribosyltransferase, promoting tumorigenicity when induced under oncogenic stress and maintaining metabolic homeostasis.[87,88] On the other hand, SIRT4 suppresses tumor growth by inhibiting glutamine metabolism and upon downregulation, it inhibits apoptosis and desensitizes cancer cells to chemotherapy.[89–91]

SIRT5 and SIRT6 are master regulators involved in metabolic reprogramming during tumorigenesis.[92] SIRT5 regulates the NAD^+-dependent elimination of the succinyl, glutaryl, or malonyl groups from lysine residues and, in contrast, is an inefficient deacetylase.[93] SIRT5 confers chemotherapy resistance to CCR cells through the elimination of malonyl groups from succinate dehydrogenase complex subunit A (SDHA). SIRT6 also suppresses the Warburg effect through the inhibition of the pyruvate kinase M2 (PKM2), thereby regulating glucose homeostasis.[94,95] SIRT6, on the other hand, maintains genome integrity during tumorigenesis.[96] In this regard, high SIRT6 levels have been reported in colon cancer samples, which correlate with worse prognosis.[97]

The role of SIRT7 in cancer is poorly understood. SIRT7 regulates RNA metabolism and the biogenesis of ribosomes. SIRT7 deacetylates CDK9, a subunit of the P-TEFb elongation factor, leading to the activation of RNA polymerase IIdependent transcription.[98,99]

SIRT7 is also a prognostic factor indicating a poor outcome in colorectal cancer because it induces the EMT and cell invasion.[98] However, SIRT7 inhibits breast cancer metastasis by promoting SMAD4 degradation and antagonizing TGF-β signaling.

1.5 Targeting NAD^+ metabolism in cancer

Considering the key role of NAD^+ metabolism in tumor progression, many efforts have been made to develop drugs that can reduce the availability of NAD^+ levels by targeting NAD-biosynthesis enzymes (Table 1). Deregulating NAD^+ homeostasis in the cancer cells through NAD^+ synthesis inhibitors was shown to result in anti-proliferative and cytotoxic effects via different mechanisms. The main effect of targeting NAD^+ metabolism involve the direct depletion of NAD^+ levels and dramatic ATP reduction, followed by an excessive ROS accumulation, as well as inhibition of DNA repairing mechanism. As a result, treated cells showed mitochondrial stress, cell cycle arrest, induction of apoptosis and autophagy processes. Such events are cancer type-specific and regulated in a dose- and time-dependent manner.

Given its pleiotropic role in cancer pathogenesis, NAMPT has long been considered an attractive therapeutic target for cancer treatment. In this section, we provide a brief overview of NAMPT inhibitors, which have shown preclinical efficacy and some of them entered in clinical trials, as well as of other inhibitors of NAD^+ biosynthesis reported over the last years. The treatment with NAMPT inhibitors demonstrated marked antineoplastic efficacy across a wide range of tumor murine models, either used a single agent or in combination with other anticancer treatments. FK866 (also known as APO866) is the first chemical compound reported as an NAMPT inhibitor. It demonstrated antitumor, antiangiogenic, and antimetastatic effects in renal cancer murine models.[100]

As previously mentioned, IDH1-mutant tumors down-regulate the expression of NAPRT and therefore depend on NAMPT for NAD^+ regeneration. This dependence has also been observed in vivo, where significant antitumor activity has been observed against IDH1-

mutant gliomas and fibrosarcomas xenografts.[20] Also, in IDH1-mutant tumors, a recent approach has shown that acting directly on the regeneration of mono-ADP-ribose from poly(ADP-ribose) (PAR) via inhibition of poly(ADP-ribose) glycohydrolase (PARG), the enzyme responsible for PAR cleavage, increased sensitivity against NAMPT inhibitors.[101]

Concerning the antileukemic activity of NAMPT inhibitors, OT-82 showed in vivo efficacy against hematological malignancies in a dose-dependent manner.[102]

OT-82 suppressed the tumor growth of subcutaneous xenografts of acute myeloid leukemia (AML) (MV4-11), erythroleukemia (HEL92.1.7), Burkitt lymphoma (Ramos), and multiple myeloma (RPMI 8226), and prolonged survival of mice with systemic xenografts of AML (MV4-11), erythroleukemia (HEL92.1.7), infant MLL-arranged ALL (MLL-2) and with patient-derived xenografts (PDX) of high risk ALL.[102,103]

In the latter model, OT-82 was found to delay leukemia growth in 95% (20/21), and cause disease regression in 86% (18/21), of the pediatric ALL PDXs. Additionally, OT-82 alone showed comparable efficacy to an induction-type chemotherapeutic regimen used to treat pediatric ALL and improved the efficacy of cytarabine and dasatinib against pediatric ALL in mice.[103] OT-82 was also reported to reduce tumor growth and to prolong mouse survival in Ewing sarcoma xenograft (TC71 and TC32)-bearing mice, although tumors were found to grow again upon treatment discontinuation.[104] Notably, the combination of low doses of OT-82 and drugs that augment DNA damage, such as Irinotecan or niraparib, improved the anticancer efficacy of OT-82 in orthotopic xenografts (TC32) and patient-derived xenografts of Ewing sarcoma.[104]

Consistent with these reports, earlier studies had shown that also FK866 elicited potent *in vivo* antitumor activity in human xenograft models of ATL, AML, Burkitt leukemia, and lymphoma.[105,106] Additionally, in a Burkitt lymphoma (Ramos) xenograft model, combining

FK866 with rituximab resulted in prolonged mouse survival and reduced tumor burden as compared to mice receiving the single agents.[107]

KPT-9274, a novel NAMPT/PAK4 inhibitor, showed remarkable antitumor effect in a broad panel of tumor mouse models, including multiple myeloma B-cell acute lymphoblastic leukemia, acute myeloid leukemia, Ewing sarcoma, colon cancer and melanoma.[108–111]

Overall, compelling results from preclinical studies built a strong rationale for the evaluation of these two inhibitors in the clinic. However, adverse effects have been associated with NAMPT inhibitors.

The early-generation NAMPT inhibitors, FK866 (APO-866), GMX1778 (CHS-828), and its prodrug GMX1777, were investigated in early-phase clinical trials. Thrombocytopenia was the common dose-limiting toxicity associated with the three NAMPT inhibitors.[112] In fact, in an acute toxicological study, treatment of mice with high doses of FK866 (60 mg/kg bid for 4 days) resulted in thrombocytopenia and severe lymphopenia which were reverted by NA co-treatment.[113] Similarly, in non-tumor-bearing mice, NA infusion reduced the mortality associated with the administration of toxic doses of GMX1777 (650 mg/kg and 750 mg/kg).[114] These data encourage the use of NA as an 'antidote' to at least partially prevent the most damaging effects of NAMPTi. However, safety studies conducted in rodents treated with GNE-617 and GMX1778 showed effects of retinal and cardiac toxicity, both fatal.

Of note, systemic NA treatment did not mitigate the retinal toxicity associated with GNE-617 and GMX1778 in rodents and only partially protected them from the NAMPTi (GNE-617)-induced cardiotoxicity.[51,115]

In contrast, in another study in dogs, co-administration of a NAMPT inhibitor and NA showed a protective effect.[116] Altogether, these findings suggest that NAMPTi-induced retinal

damage and its mitigation by NA could be chemotype-specific and might show species variability depending on the used animal model.

Lastly, the recently reported NAMPT inhibitor OT-82 showed a favorable toxicological profile

Target enzymes	Compound name	Property	Implication in cancer treatment
Nampt	FK866 (APO866)	Non-competitive inhibitor	Phase I study in advanced solid tumors: Thrombocytopenia was the dose limiting toxicity. No objective tumor responses were observed
	GMX-1778 (CHS-828)	Pyridyl cyanoguanidine	Phase I study in advanced resistant solid tumors: Gastrointestinal toxicitiy and thrombocytopenia were observed. No objective tumor responses were observed
	GMX-1777	Pro-drug of GMX-1778	Phase I study in advanced malignancies: Thrombocytopenia and gastrointestinal hemorrhage was the dose limiting toxicity. No objective tumor responses were observed
	STF-31	Dual inhibitor of Nampt and Glut1	Deplete NAD levels, and inhibit glucose uptake and glycolysis
	STF-118804	Competitive inhibitor	Induce apoptosis antecedent cell cycle arrest
	GNE-617	Competitive inhibitor	Deplete NAD and ATP levels, and promote cell death
	GNE-618	Competitive inhibitor	Deplete NAD and ATP levels, and promote cell death
	LSN3154567	Competitive inhibitor	Alone or coadministered with NA exhibits a potent antitumor activity in tumor xenograft models. The retinopathy associated with LSN3154567 could be mitigated with NA coadministration
	KPT-9274	Dual inhibitor of Nampt and PAK4	KPT-9274 decreases G2/M transit and causes apoptosis
Nmnat2	VAD	NAD analog inhibiting both Nampt and Nmnat2	Induce NAD depletion, glycolytic block, energy failure, and necrotic death.

with no cardiac, neurological, or retinal toxicities in mice and cynomolgus monkeys (non-human primates), thus apparently avoiding the side effects of other NAMPT inhibitors.[102]

Table 1. Small molecules targeting NAD^+ synthesis enzymes.[2]

Noteworthy, a combined low-dose OT-82 and niraparib therapy for one month led to several unexpected deaths in Ewing sarcoma-bearing mice, raising the concern of potential toxicities associated with prolonged combination treatments with this compound.[104] Notably, OT-82 is being currently investigated in phase I trials. In a two-stage (dose escalation and dose expansion) phase 1 study, the safety and efficacy of OT-82 are being evaluated in participants with relapsed or refractory lymphoma (NCT03921879). So far, no results have been disclosed.

2. Richter Syndrome

2.1 Definition

The development of an aggressive lymphoid malignancy in a patient with chronic lymphocytic leukemia (CLL) and/or small Lymphocytic Lymphoma (SLL) is called Richter syndrome/Richter transformation.[117] The phenomenon was first reported by Richter in 1928 as" reticular cell sarcoma" associated with lymphocytic leukemia.[118] Lortholary et al. introduced the clinicopathological term" Richter transformation" 40 years later.[119]

The aggressive lymphoma has different histology than the underlying CLL. RS differs from both accelerated phase of CLL and prolymphocytic transformation. The associated lymphoid malignancies described over the time are diffuse large B-cell lymphoma (DLBCL), Hodgkin lymphoma, lymphoblastic lymphoma, plasmablastic lymphoma, and composite lymphoma.[120,121] The RS definition, as described in the WHO classification, is typically recognized in two different variants: DLBCL variant in the major of cases (95%), or, rarely, the hodgkin lymphoma (HL) variant in a minority of cases (0.5–5%).[122–124]

2.2 Clonally related RS

Two distinct types of RS have been identified based on the relationship to pre-existing CLL, defined clonally related and clonally unrelated. The clonal relationship representing true transformations to the preceding CLL phase, is characterized by identical immunoglobulin heavy- and light-chain rearrangements in the CLL and lymphoma cells (Figure 2).[125]

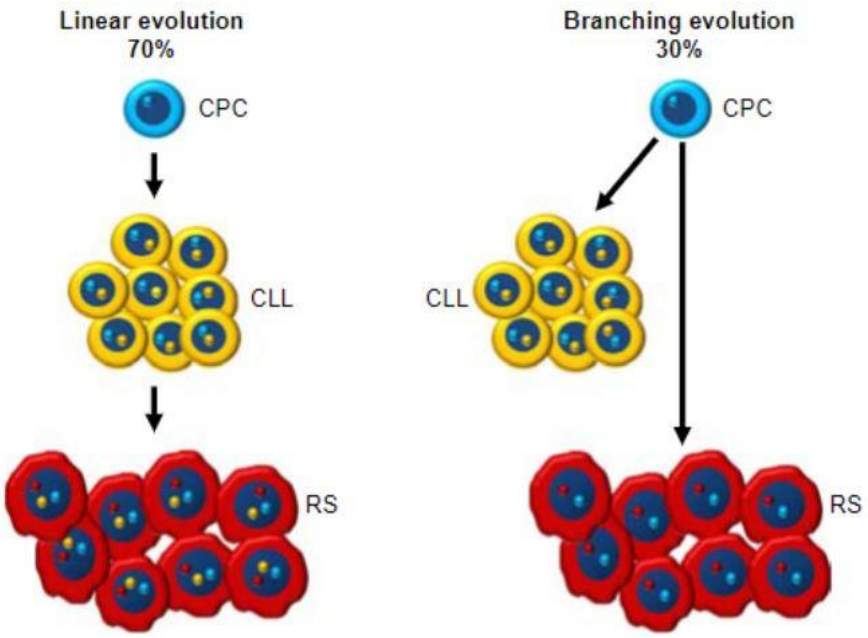

Clonally related RS is found in the most (~60-80%) of the DLBCL variants. The clonal relationship is clinically important: patients with true transformations have worse prognosis, with a median survival of approximately 12 months, than patients in which RS is clonally unrelated to CLL showing a similar survival to de novo DLBCL cases, of nearly 65 months.

On the other hand, clonally unrelated DLBCL variant responds to therapy as de novo DLBCL with a longer median survival (5 years) compared with patients with a clonally related DLBCL (8–16 months).[126,127] Clonally unrelated RS of both DLBCL and HL variants merely represents a secondary lymphoid cancer in the context of CLL. The mechanisms underlying the development of an aggressive lymphoma that is clonally unrelated to CLL cells are not fully

understood and may be related, at least in part, to the condition of immune deregulation that frequently characterizes patients affected by CLL.

2.3 Histopathologic features of Richter syndrome

RS transformation involves most frequently (60–70 % of cases) the lymph nodes, but extranodal localizations are also common and may affect the gastrointestinal tract (10 %), tonsil (10 %), and bone marrow (10 %) among other sites.[125,126]

The morphology of the DLBCL variant of RS is characterized by confluent sheets of large neoplastic B lymphocytes resembling either centroblasts (60–80% of cases) or immunoblasts (20–40% of cases).[125] In addition, it is important to note that RS cases derived from a previous CLL possess numerous proliferation centres and a high number of prolymphocytes and paraimmunoblasts, but do not have clear features of DLBCL.[128,129]

For this reason, new criteria for distinguishing between accelerated CLL and RS have been proposed. These characteristics include the presence of (i) a tumour of large B-cells with a nuclear size equal to or larger than the nuclei of macrophages or more than twice the size of a normal lymphocyte and (ii) a diffuse growth pattern of these large cells (not just the presence of small foci). Applying these criteria, up to 20% of cases diagnosed as RS will be correctly classified as 'accelerated' CLL.[129] Moreover, the histological report requires a biopsy to confirm the suspected lesion.

In CLL patients with suspected transformation, the fluorodeoxyglucose (^{18}FDG) positron emission tomography (PET)/computed tomography (CT) characteristics of the lesion, in particular the standardized uptake value (SUV [maximum SUV(SUVmax)]), may guide the choice of whether to perform a biopsy because sites affected by RS are expected to have SUVs overlapping with those of de novo DLBCL. The main contribution of ^{18}FDG PET/CT in RS

diagnosis relies on its high (97%-98%) negative predictive value, meaning that in the presence of a negative ^{18}FDG PET/CT, the final probability of RS transformation is only 2-3%. For these reasons, if PET/CT ^{18}FDG is negative, biopsy is usually not performed. On the contrary, in patients with higher uptake of ^{18}FDG the biopsy is mandatory.[130]

Phenotypically, although the CD5 and CD23 antigens are invariably expressed in CLL cells, their expression is frequently lost at the time of transformation.[98] Indeed, CD5 expression is present in only a fraction (~30 %) of cases, while CD23 expression is even more rare (~15 % of cases). CD20 is generally expressed by transformed cells and represents an important target for immunotherapy with anti-CD20 monoclonal antibodies.[125]

Based on immunophenotypic markers of de novo DLBCL, most cases of DLBCL transformation (90–95 %) have a post-germinal center phenotype (IRF4-positivity), whereas only 5–10 % display a germinal center phenotype (CD10 and/or BCL6 expression).[125]

Two types of HL transformation have been described.[120,131]

Type 1 HL transformation usually mimics the pathologic features of classical HL, being characterized by the presence of mononuclear Hodgkin cells and multinuclear Reed–Sternberg cells residing in a polymorphous background of small T cells, epithelioid histiocytes, eosinophils, and plasma cells. In type 1 transformation, the Hodgkin–Reed–Sternberg cells show the typical CD30-positive/CD15-positive/CD20-negative phenotype.[120,131] In contrast, type 2 HL transformation is characterized by the presence of Hodgkin–Reed–Sternberg-like cells in a background of CLL cells lacking the polymorphous reactive infiltrate of classic HL. In type 2 transformation, Hodgkin–Reed–Sternberg-like cells express both CD30 and CD20 but lack CD15. [120,131]

Based on the analysis of the rearrangement of IGHV-D-J genes, only a fraction (~40–50 %) of the HL variants of RS are clonally related to CLL.[132,133] Consistently, a number of RS cases

(~20 % showing a DLBCL morphology and ~50–60 % showing a classical HL morphology) harbour distinct IGHV-D-J rearrangements compared to the paired CLL, representing de novo lymphomas arising in a CLL patient.[132,133]

2.4 Incidence

The frequency of RS in CLL patients ranges from 2 to 12% in reports from the period prior to targeted therapy.[134] The incidence of RS is determined by several variables, including the different selection of patient cohorts, duration of follow-up, biopsy vigilance and the mixing of clonally related and unrelated patients. Incidence estimations are overwhelmingly reported retrospectively and derived from selected patient materials.[135]

Most of the studies report on the occurrence of both clonally related and unrelated RS due to a lack of attempts to disclose clonal relationship. The largest study of RS was reported from the MD Anderson Cancer Center in 2006.[127]

Of 3986 retrospectively assigned CLL patients, 148 (3.7%) had histologically proven RS and 204 patients (5.1%) had possible RS. A cohort study of 1641 newly diagnosed CLL patients at the Mayo Clinic estimated RS incidence of 2.3 % (37/1641).[123] Interestingly, the occurrence of RS was significantly higher in patients younger than 55 years (5.9%) compared to patients older than 55 years (1.2%) as reported on an retrospective, Italian single-institution study published in 1999.[136] The incidence of RS has been 4-20% in patients treated by novel targeted agents, especially patients with TP53 disrupted CLL clones seem to have a high risk of transformation.[137] Incidence in these cohorts usually refers to clonally related RS. However, the frequency of RS does not seem to decrease in the era of targeted therapy. Highest occurrence of RS has been reported in cohorts of patients who are refractory to treatment.[137,138]

2.5 Pathogenetic mechanism

Pathogenetic mechanisms for development of RS have not been clarified. Genetic predisposition, impaired immunological cancer surveillance and possible cancerogenic effect of CLL treatment are mechanisms suggested and studied. The obstacles with research on RS have been the rarity of the disease and thus, difficulty to study in a prospective manner in unselected populations. However, in recent years, reports based on larger patient cohorts appeared thanks to worldwide institutional collaborations.[139]

Transformation to DLBCL has been the most studied type of Richter syndrome. Somatic mutations appearing during haematopoiesis can lead to dysregulation followed by transformation and have been the focus for studies on RS pathophysiology.[140]

Researchers have found somatic mutations in genes coding for regulators of proliferation and apoptosis in a proportion of RS patients, even though the spectrum of mutations is broad, and no RS unique mutation has been found.[137]

Two previous studies have identified common evolutionary genetic pathways that CLL cells undertake during Richter's clonal transformation (Figure 3).

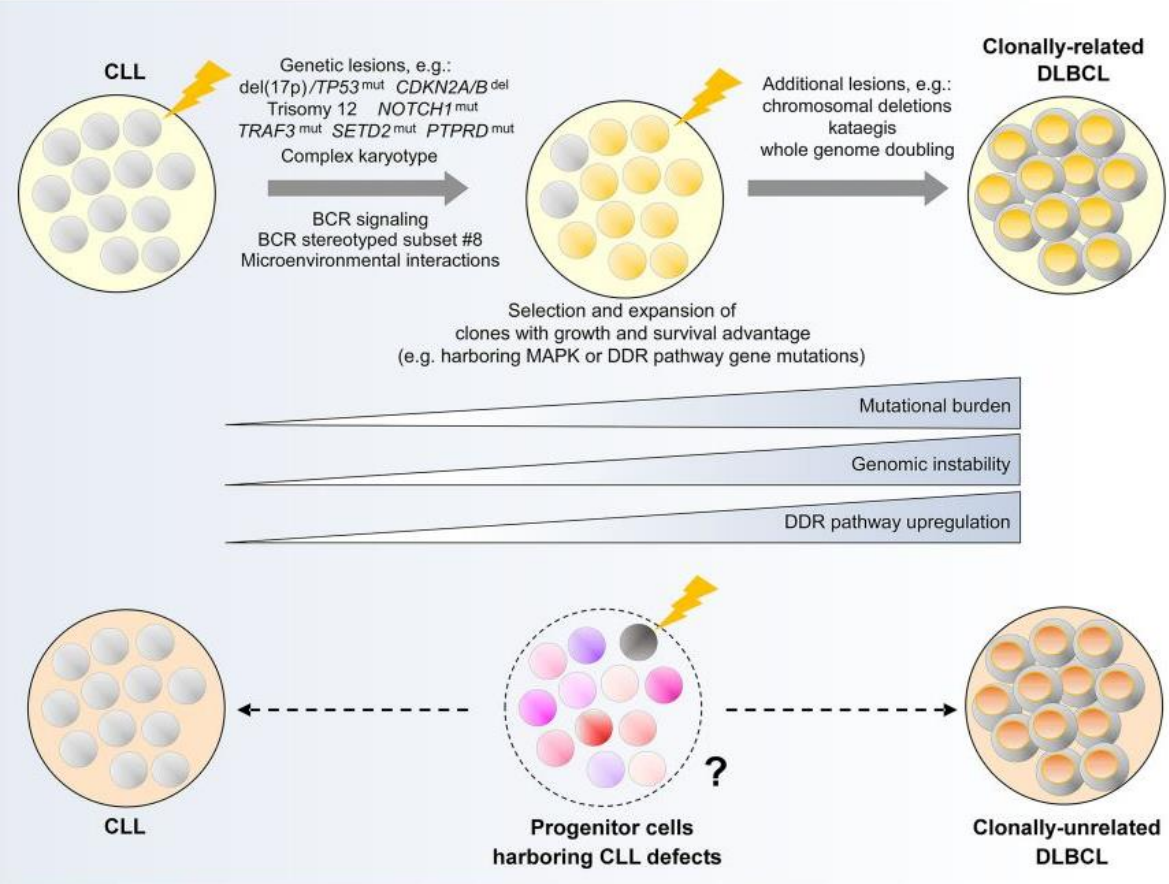

The first study, conducted by Chigrinova et al. analysed CLL and DLBCL samples, some of which developed RS. Using SNP arrays and targeted gene sequencing, the main genetic lesions acquired during transformation in RS were identified.[139]

Chigrinova et al. found that RS patients could be separated into two distinct subgroups according to most frequent genetic lesions. About 50% of patients were characterized by TP53 inactivation and/or CDKN2A/B loss and alongside MYC activation, and in some cases 13q deletion together with other lesions. The second group was characterized by acquisition of a third chromosome 12 (trisomy 12) and was found in 28% of 59 studied patients. NOTCH1 mutations have been frequently found in patients with RS, particularly among individuals who also have trisomy 12.[139]

The heterogeneous lesions identified by Chigrinova et al. were confirmed by a second study conducted by Fabbri et al, using the WES method to analyse CLL-RS pairs and other Richter-transformed lymphomas.[141] This study confirmed a clonal linearity observed during transformation into RS. Indeed, many of the generic alterations were already present in the CLL clone and were maintained in the RS clone, together with the acquisition of an additional heterogeneous lesions.[141]

Analysis of CLL/DLBCL paired samples have shown that TP53 disruption is acquired at transformation in most cases (55 %).[126] TP53 gene is located on a short arm of chromosome 17 and codes for tumor suppressor protein, a central regulator of the DNA-damage response pathway. Activation of p53 protein leads to cell-cycle arrest and apoptosis. Disruption of p53 protein pathway is associated with poor response to chemo-immunotherapy and remains the most negative prognostic marker characterizing the transformation to clonally related DLBCL.[142] TP53 disruption often coexist with mutations that activate MYC oncogene and with CDKN2A/B disruptions.[143] CDKN2A/B is a tumour suppressor gene involved in cell cycle regulation. MYC family genes activation plays a role in initiation and progression of several haematological cancers.[143] MYC deregulation characterizes a significant fraction (40-60 %) of cases of clonally related and may be sustained by genetic lesions affecting the MYC network or by mutations affecting MYC trans-regulatory factors, as exemplified by mutations of NOTCH1.[144–146] Somatic structural lesions activating the MYC gene are observed in approximately 30-40% of clonal transformations of DLBCL.

NOTCH1 mutations recur in approximately 30% of clonal transformations of DLBCL, causing the removal of the C-terminal PEST domain of the protein, necessary for switching off the signalling pathway.[146] The NOTCH1 gene codes for a protein central in NOTCH signalling pathway, which, depending on the context, has both oncogenic and tumor-suppressor

function.[145,147,148] Interestingly, NOTCH1 mutations are not coexistent with TP53 mutations and thus, these two groups distinctly separate about 75% of studied RS cases. Different studies demonstrated the early acquisition of chromosome 12 trisomy in 173 of RS patients and the consequently acquisition of NOTCH1 mutations.[149]

The use of murine models of CLL made possible to assess the role of the main generic alterations found in RS. In the Eμ-TCL1 model, the concomitant loss of TP53 and CDKN2A/B functions causes the loss of all cell cycle regulatory signals, leading to uncontrolled proliferation driven by the activation of the BCR pathway causing a transformation process like that of RS.[150]

In the study conducted by Kohlhaas et al, they showed that the gain-of-function mutation in NOTCH1 causes constitutive activation of Notch1 in Eμ-TCL1 mice recapitulating the RS phenotype. Furthermore, at least in the Eμ-TCL1 model, in the absence of mutation in NOTCH1, constitutive activation of AKT, downstream of the BCR pathway, drives transformation to RS via constitutive activation of Notch1.[150,151] This work suggests that both genetic and non-genetic mechanisms could lead to the same phenotype. Indeed, certain stereotyped BCR subpopulations, in particular subpopulation #8, have been shown to confer an increased risk of RS.[152]

Lastly, in a recent work by Nadeu et al, discovered a new driver gene in RS mainly involving cell cycle regulators (89%), chromatin modifiers (79%), MYC (74%), nuclear factor (NF)-κB (74%) and NOTCH (32%).[153] These genetic aberrations were present simultaneously in most RS cases, but alterations in the MYC and NOTCH pathways in only 2 out of 19 cases. Specifically, the newly observed alterations included deletions of CDKN1A and CDKN1B in five RS cases, an immunoglobulin (IG)-CDK6 translocation and a CCND2 mutation already present at the time of CLL diagnosis. Furthermore, an unsupervised analysis showed that the

mutation profile of RS patients was completely different from M-CLL and U-CLL patients before treatment or at post-treatment relapse (independent cohort of 27 post-treatment CLL samples)[154] Nadeu et al, identified 11 different mutational signatures, including a completely new one called single base substitution (SBS-RT) not yet identified in any tumour type, including CLL and DLBCL.[154–159] Specifically, all cases in which the novel SBS-RT mutational signature was found had been previously treated with alkylating agents, such as bendamustine (n=5) or chlorambucil (n=2). In contrast, RS cases lacking SBS-RT did not receive alkylating agent therapy during their CLL phase. The results of this study demonstrate that RS can arise from several sub-clones and that some of them can be positively selected following exposure to certain therapies.

Recent findings have shown that clonal evolution from high-risk CLL, apparently heterogeneous from a genetic point of view, leads to clonal selection and enrichment of certain mutations, due in part, to the acquisition of resistance to treatment-associated therapies in these patients. However, further research is needed to highlight which targeted therapies will need to be used according to the mutation profile.[160]

2.6 Risk factors for Richter transformation

Several studies addressed possible risk factors in CLL patients, but none have been able to clearly identify a patient at high risk of development RS.[122,161] Small cohorts from selected CLL populations and mixing true transformation with de novo DLBCL together with the retrospective character of the studies have been major limitations in risk factor studies.

A pilot study reported by Rossi et al in 2008 involving 185 CLL patients and paired samples (CLL and Richter's transformation in the same patient) has shown that the following factors predispose to Richter's transformation in a patient with CLL:[133,162]

1. CD38 expression (CD38 ≥ 30%)
2. Stereotyped B-cell receptor
3. IGHV4-39 gene usage
4. Telomere length < 5000 base pairs
5. Lymph node size > 3 cm
6. Absence of del13q14

Other studies have reported that polymorphisms with B-cell lymphoma 2 (BCL-2), CD38 and low-density lipoprotein receptor-related protein 4 (LRP4) gene have been associated with increased risk of RS.[161–163] CD38 GG homozygous patients had a 30.6% increased risk compared with patients having the GC or CC genotype and patients having the LRP4 TT genotype (which is related to Wnt signaling pathways in CLL).[163] NOTCH1 mutations were recently shown to predict for the development of Richter's transformation, while SF3B1 mutations did not.[137] CLL patients with unmutated IGHV gene are more likely to develop RS than patients with mutated IGHV gene.[164]

Importantly, inactivating lesions in CDKN2A, CDKN2B, and TP53 frequently co-occur in Richter syndrome (RS), and BCR stimulation of human RS cells with such lesions is sufficient to induce proliferation. Chakraborty et al showed that tumor cells with combined TP53 and CDKN2A/2B abnormalities remain sensitive to BCR-inhibitor treatment and are synergistically sensitive to the combination of a BCR and cyclin-dependent kinase 4 and 6 (CDK4/6) inhibitor both *in vitro* and *in vivo*.[150] These data provide evidence that BCR signals are driving CLL cell proliferation and reveal a novel mechanism of Richter transformation.

Symptoms and signs at CLL diagnosis have been studied, and only advanced stage and large lymph nodes have been associated with increased risk of transformation.[122,161]

Association between CLL treatment and RS is not clarified. DNA damage induced by alkylating agents (chlorambucil, cyklofosfamide) and impaired DNA repair caused by purine analogs (fludarabine) has, in theory, potential to trigger RS transformation. In a single-institution cohort study with prospective follow up of 1641 newly diagnosed CLL patients, the rate of transformation increased from 0.5% to 1% per year after receiving treatment for CLL.[165] Among patients who received the combination of alkylating agents and purine analogs, the risk of RS increased 3-fold (Odds ratio = 3.26; p=0.0003). No significant increase in RS rate among patients treated with single agent was found. In contrast, no difference in the rates of RS in patients treated with either chlorambucil alone (2%), fludarabine alone (1%), or the combination of cyklofosfamide and fludarabine (1%) was seen after a median follow up of 3.5 years in Leukemia Research Foundation Chronic Lymphocytic Leukaemia 4 (LRF CLL4) Trial.[166] Similarly, no difference in transformation rate was observed between patients treated with either fludarabine monotherapy (7%), chlorambucil monotherapy (5%) or combination of fludarabine and chlorambucil (8%) in the Cancer and Leukemia Group B 9011 study.[135] Remarkably large variation in RS frequency in these studies is truly due to the high grade of patient selection and varying length of follow up. Thus, the impact of CLL therapy on risk of RS is still unclear. A prospective study comparing untreated and treated patients would compare two biologically distinct groups, however it would not be ethically acceptable because treatment improves prognosis.

2.7 Clinical presentation

The clinical presentation of RS in a CLL patient varies and none of the symptoms are specific. Thus, the vigilance of the physician considering CLL patient is crucial. In CLL patients, the clinical features suspected of a transformation are the development of new B symptoms, the

asymmetric rise of bulky lymph nodes, and/or the sudden rise of lactatedehydrogenase (LDH) levels.[167] Patients with RS can deteriorate rapidly and promote constitutional symptoms like fever and night sweats. A rapidly progressive discordant lymphadenopathy; or cytopenia can be initial symptoms. RS could also develop in extra-nodal sites, and it might be included in the differential diagnosis of an extra-nodal mass developing in patients with a known CLL. The specificity of these clinical findings for transformation is only 50–60%, with the remaining cases showing either progressive or "accelerated" CLL, or even a solid cancer.[130] To establish the diagnosis of a new, more aggressive lymphoma in a CLL patient, biopsy is essential. These facts, e.g., nonspecific symptoms and the necessity of a biopsy to establish a diagnosis can potentially play a role in the measured incidence of RS, introducing selection bias.[121]

2.8 Prognosis of Richter Syndrome

In general, the prognosis in RS is poor, as observed by a median survival ranging between 8 and 16 months in clonally related patients.[127] However, the prognosis is not uniform among patients and depends on several clinical and biological factors. These allowed the development of an RS prognostic score based on five adverse risk factors: Zubrod performance status >1, elevated LDH levels, platelet count 100,000, tumor size 5 cm and more than two previous lines of therapy. These five adverse risk factors help to predict the survival once transformation (Figure 4).[131]

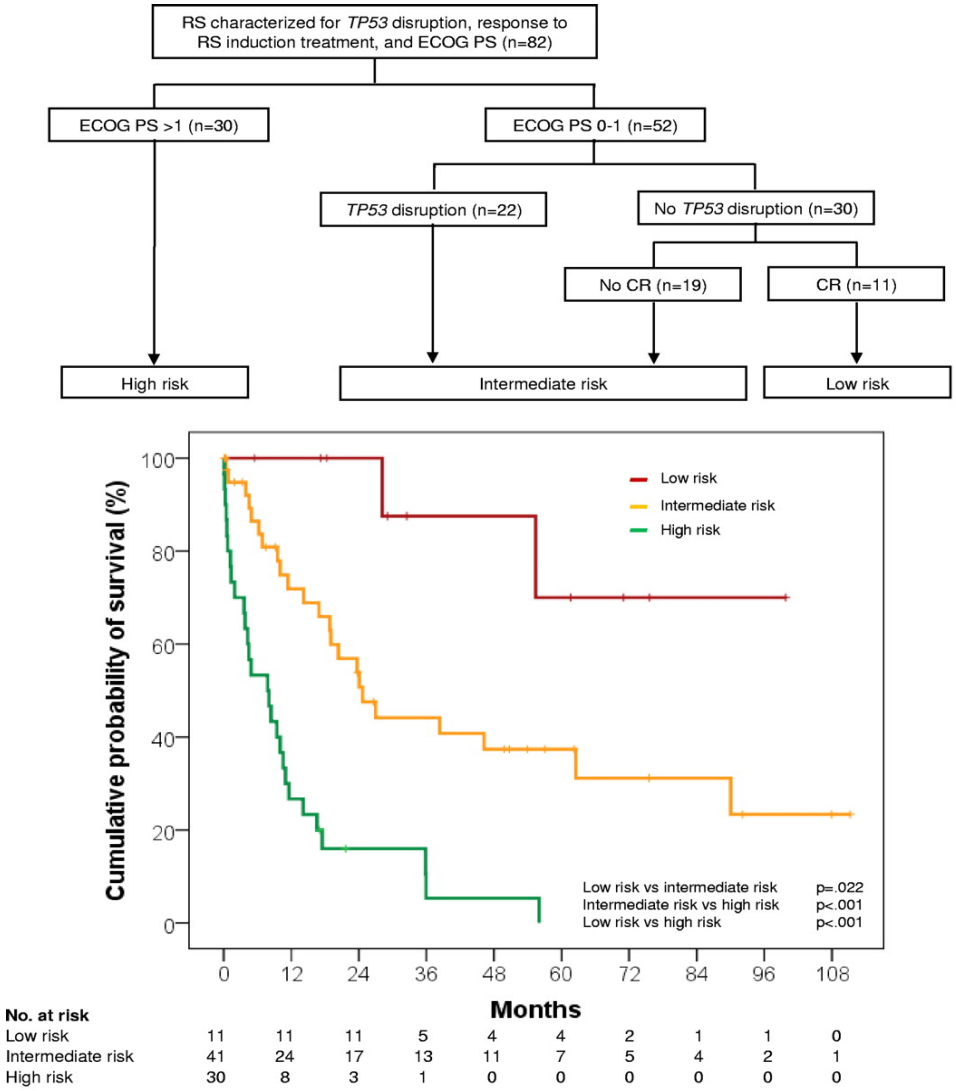

Based on the prognostic score, patients are assigned to one of four risk groups: 0 or 1, low risk (median survival: 13 months); 2, low-intermediate risk (median survival: 11 months); 3, high-intermediate risk (median survival: 4 months); 4 or 5, high risk (median survival: 1 month).[127] The median survival of patients after Richter transformation takes into account clinical parameters reflecting bone marrow dysfunction and immune system exhaustion, as

well as the enrichment of chemoresistant clones reflecting previous therapies. Other factors influencing median survival are TP53 mutational status, treatment response and ECOG performance status (ECOG PS), which are used to construct an algorithm for classifying patients according to risk of death.[126] Low-risk patients presented with a good ECOG PS 1 and had no genetic alterations in TP53, showing a good complete response (CR) to treatment with a median survival of 5 years in 70% of cases. Patients belonging to the intermediate risk presented a good ECOG PS 1, but with an alteration in TP53 and did not achieve CR after treatment, showing a median survival of 24 months. Patients belonging to the high-risk category presented with an ECOG PS >1 and showed a median survival of only 4 months.[126] In fact, these patients are not responsive to the major lines of treatment, showing a negative impact on performance status. As noted above, the clonal relationship directly impacts the clinical course of the disease. Clonally unrelated patients have a significantly longer median survival (62 months), like de novo DLBCL.[126] The differences in survival reflect genetic differences in the disease. Clonally unrelated patients have a low frequency of TP53 alteration (20%), as well as stereotyped VH CDR3, an immunogenetic feature that is frequent in clonally related DLBCL (~50% of cases) but very rare in de novo DLBCL, is virtually absent.[126] For these reasons, patients presenting with a clonally unrelated RS should be considered as a secondary DLBCL arising de novo in a CLL context, rather than a true Richter transformation. In the HL variant of RS, the few available cases have shown that the median survival of these patients ranges from 10 to 20 months, presenting clinical features of a high-risk disease.[168] The RS score developed for DLBCL transformation, is not useful to stratify the outcome of HL transformation.[127]

2.9 Current treatment of Richter Syndrome

CLL patients with transformation into Richter's syndrome are commonly treated the same therapeutic regimens commonly adopted for aggressive B-cell non-Hodgkin lymphomas or de novo DLBCL, mainly based on chemo-immunotherapy and stem cell transplantation (SCT), depending on the fitness of the patients, showing worse toxic effects with a short remission. Treatment with hyper-CVAD, a fractionated regimen of cyclophosphamide, vincristine, doxorubicin and dexamethasone, induced a response in only 41% of DLBCL treated patients with a median survival of only 10 months. Moreover, this treatment regimen showed severe hemotoxicity in all cases, causing a high rate of infection in 50% of cases, and a mortality rate of 14%.[169] The combination of hyper CVAD alternating with methotrexate and ara-C regimen with rituximab showed a response rate of 43% showing a median survival of 8 months. However, this combination was highly toxic, showing a 22% mortality rate, despite the prophylaxis with granulocyte macrophage colony-stimulating factor (GM-CSF).[170]

A good balance between activity and toxicity was observed in less intensive chemotherapy regiments. A prospective multicenter phase II trial (NCT00309881) from Langerbeins et al, in 2014, evaluated efficacy and tolerability of R-CHOP (rituximab, cyclophosphamide, doxorubicin, vincristine and prednisone) regiment resulted in a response rate of 67% in 15 RS patients showing a median progression free survival (PSF) of 10 months and a median survival of 21 months. The overall response rate (ORR) was significantly associated with a longer time from CLL diagnosis to transformation, higher levels of hemoglobin and lower levels of LDH. The treatment-related mortality was low (3 %). In the 65% of patients were observed hematotoxicity, while infection occurred in 28% of patients.[171]

In a retrospective study, it was observed that the R-CHOP treatment regimen in 12 RS patients showed a 50% response rate and a median survival of 15 months.[127]

The first results of phase I–II clinical trial of platinum-containing regimens, oxaliplatin, fluradabine, ara-C and rituximab (OFAR1), showed a response rate of 40% with a remission of only 3 months leading to a median survival of 6-8 months. A high rate of haematotoxicities accompanied by severe infections and mortality in the range of 3-8% was also observed with the OFAR regimen.[172,173]

In other to improve the clinical outcomes and decrease the toxicities the OFAR 2 trials was designed introducing modification of oxaliplatin and cytarabine doses. However, despite this adjustment the hematologic toxicity and infection were still higher. The ORR was 39%, the median PFS was 3 months, the median OS was 7 months and at 2 years only 19.7% of patients with RS were alive.[173]

Based on these results, chemo-immunotherapy regimens, both with rituximab a human/murine chimeric anti-CD20 monoclonal antibody, have shown promising activity in the treatment of the DLBCL variant of RS in terms of complete response rate. Although the response rate of both treatments is high, both treatments induced a high rate of severe toxicities and the short-lasting remission durations (3-15 months).

Despite the unsatisfactory results obtained using chemo-immunotherapy for RS patients remains the frontline therapy, underlining the urgent need for novel and more effective therapeutic strategies.[174]

An alternative approach to chemo-immunotherapy is either the autologous or allogenic- SCT, explored as post-remission therapy in RS patients because of the short duration of responses with the sole chemotherapy. Although, SCT approach can be adopted only in a minority of patients with RS (~10–15%), due to limitations imposed by age, performance status, and donor availability.[127]

Several clinical data showed that patients who underwent allogeneic SCT as post-remission therapy had a longer survival compared to patients who received no salvage therapy, revealing a 5-year OS of 58% and long-term efficacy of SCT.[175–177]

The main factor influencing post-transplant outcome is disease activity at the time of stem cell transplantation. In fact, RS patients sensitive to chemo-immunotherapy have shown superior survival compared to resistant ones. The greatest benefit was observed in patients younger than 60 years of age. [127]

There are limited clinical data on the treatment of HL variants. Patients diagnosed with de novo HL are treated with multi-agent chemotherapy, such as doxorubicin, bleomycin, vinblastine, dacarbazine (ABVD) being the most effective regimen. The response rate is 40-60%, but patients end up developing recurrent disease after a short period of time, showing a median overall survival of 4 years.

Since the outcome of the HL variant of RS appears to be longer than that observed in the DLBCL variant of RS, SCT is less used for consolidation of this condition.

In summary, these results show that for young patients with chemo-sensitive Richter syndrome, stem cell transplantation is a viable alternative.

2.10 Novel therapeutic approaches in Richter Syndrome patients

As noted above, chemotherapy is one of the most effective therapeutic options in the treatment of cancer, although it is accompanied by numerous side effects.

In recent years, progress has been made with small molecule inhibitors, focusing on tumor-specific molecular alterations. In this way, the therapy is adapted to the patient, leading to improved benefits. The treatment of CLL has been revolutionized with the introduction of small molecule inhibitors, such as BTK, PI3K and BCL2 inhibitors (Figure 5).[178]

Bruton's tyrosine kinase (BTK), a member of the Tec kinase family, is an important molecule in the B lymphocyte antigen receptor (BCR) and cytokine receptor signalling pathways. Ibrutinib, a reversible BTK inhibitor, showed good tolerability, although it showed partial clinical responses in small cohort of CLL patient and a complete response in only one patient.[179–182] Similarly, acalabrutinib, an irreversible BTK inhibitor, showed a good tolerability profile, but poor clinical effects when used as monotherapy.[155]

Another reversible BTK inhibitor, AR1 531, showed a better pre-clinical efficacy compared to Ibrutinib, in mouse models of CLL and aggressive B-cell lymphomas. Currently, a phase I study (NCT03162536), enrolling CLL and RS patients, is ongoing to test the efficacy and tolerability of ARQ 531.[182]

Another element of the BCR signaling pathway cascade is AKT, downstream of PI3K. It has been shown that in mouse models of Eμ-TCL1, constitutive activation of AKT causes the onset of an aggressive lymphoma that mimics the clinical features of RS, suggesting a role of PI3K/AKT in RS transformation.[150] In CLL patients, treatment with Idelalisib, a PI3Kδ inhibitor, has shown great clinical efficacy while exhibiting severe toxic effects, even in relapsed/refractory patients when combined with bendamustine-based regimens or rituximab.[150] Treatment of RS patients with idelalisib showed one complete response and two partial responses without disease progression in a small cohort study (4 patients).[183,184]

In addition, another study confirmed its clinical efficacy in the treatment of RS, showing a complete response after three weeks, although a rapid relapse after discontinuation of treatment was evidenced.[158]

In several hematological malignancies, including CLL and RS, have been observed the overexpression or mutation of XPO1, a nuclear export protein, making it an interesting target in target therapy.[185] In a phase I study, including 6 refractory/recurrent RS patients,

the treatment with selinexor, an XPO1 inhibitor, showed a partial response in 2 out of 5 patients and showed a good tolerability profile.[186]

A promising approach for the treatment of haematological malignancies is CD19-targeted antigen receptor T (CAR-T) against CD19.[187,188] CAR-t therapy was evaluated in 24 patients, 19 of them with high-risk CLL and previously treated with ibrutinib, five of them with RT.

The results of this study showed an ORR of 71% at 4 weeks post administration.[188]

The same study group then tested this therapy on 19 patients simultaneously treated with ibrutinib, four of them with RT; they found a 4-week ORR of 83%, and a 1-year OS and PFS of 86%.[188,189] Due to the results of this study in 2019, an Israeli study included eight high-risk CLL patients with RT, treated with CAR-T cell therapy during 2019-2020; they reported an ORR of 71% (5/8).[189]

However, no other studies are currently available and its efficacy in the treatment of RS needs to be further proven.

2.11 Combination strategies in Richter Syndrome patients

The clinical efficacy of small molecule inhibitors in CLL has allowed their use in the treatment of RS patients, although many of these new compounds are associated with poor or partial responses, probably due to the more complex karyotype or genetic background that determines, at least in part, a more aggressive behavior of these cells. Therefore, a strategy that could be effective for treating RS patients could be the combination of drugs targeting different molecules or molecular pathways.

BTK inhibitors have already been tested in combination with several other agents.

In 2015, Jaglowski and colleagues performed a phase 1b/II trial using ibrutinib and ofatumumab, an anti-CD20 monoclonal antibody (NCT01217749). The result of this study

demonstrated a reduction of tumor burden in lymph nodes in 3 treated patients, two of them had a stable disease for a median time of 10 months, while the other had a partial response, before undergoing disease progression 5 months later.[190]

Similarly, another study reported the case of a patient with RS, who underwent several cycles of chemotherapy, before and after transformation, a temporary reduction of disease within 1 month after treatment with Ibrutinib and rituximab.[191]

A further study, which included 20 RS cases and other patients with relapsed/refractory B-cell haematological malignancies, tested the efficacy of Ibrutinib in combination with the anti-PD-1 agent nivolumab. This therapeutic combination showed the best clinical responses in the RS cohort with an ORR of 65% and two patients in complete remission. However, treatment was discontinued due to severe side effects observed in most patients.[192]

In 2019, the STELLAR (NCT03899337) trial started in a large cohort of RS patients. The results of the prospective randomised phase II trial of R-CHOP alone or in combination with Acalabrutinib demonstrated the feasibility and clinical activity of adding Acalabrutinib to R-CHOP.[193]

Venetoclax, an inhibitor of the anti-apoptotic protein BCL2, showed interesting results in CLL patients relapsed/refractory to chemo-immunotherapy, showing durable response rates.[194] Therefore, the clinical efficacy of Venetoclax was evaluated in a cohort of 26 RS patients in combination with chemo-immunotherapy regimen based on R-EPOCH. The results of the phase II study (NCT03054896) showed that 13 RS patients achieved a complete response and 3 a partial response, with an ORR of 62% and a median survival of 19 months. The main side effects observed were neutropenia and thrombocytopenia.[195]

Despite significant advances in treatment options, only a few phase I/phase II clinical trials are ongoing, mostly based on different drug combinations, but without any first-line

therapy.[196] For this reason, RS remains a devastating end-stage complication that represents an unmet need for patients. One of the main problems in the study of RS is the lack of murine models of RS, as well as the reduced availability of primary samples. Based on this observation, understanding the genetics and biology of RS is a necessary step to identify new targets.

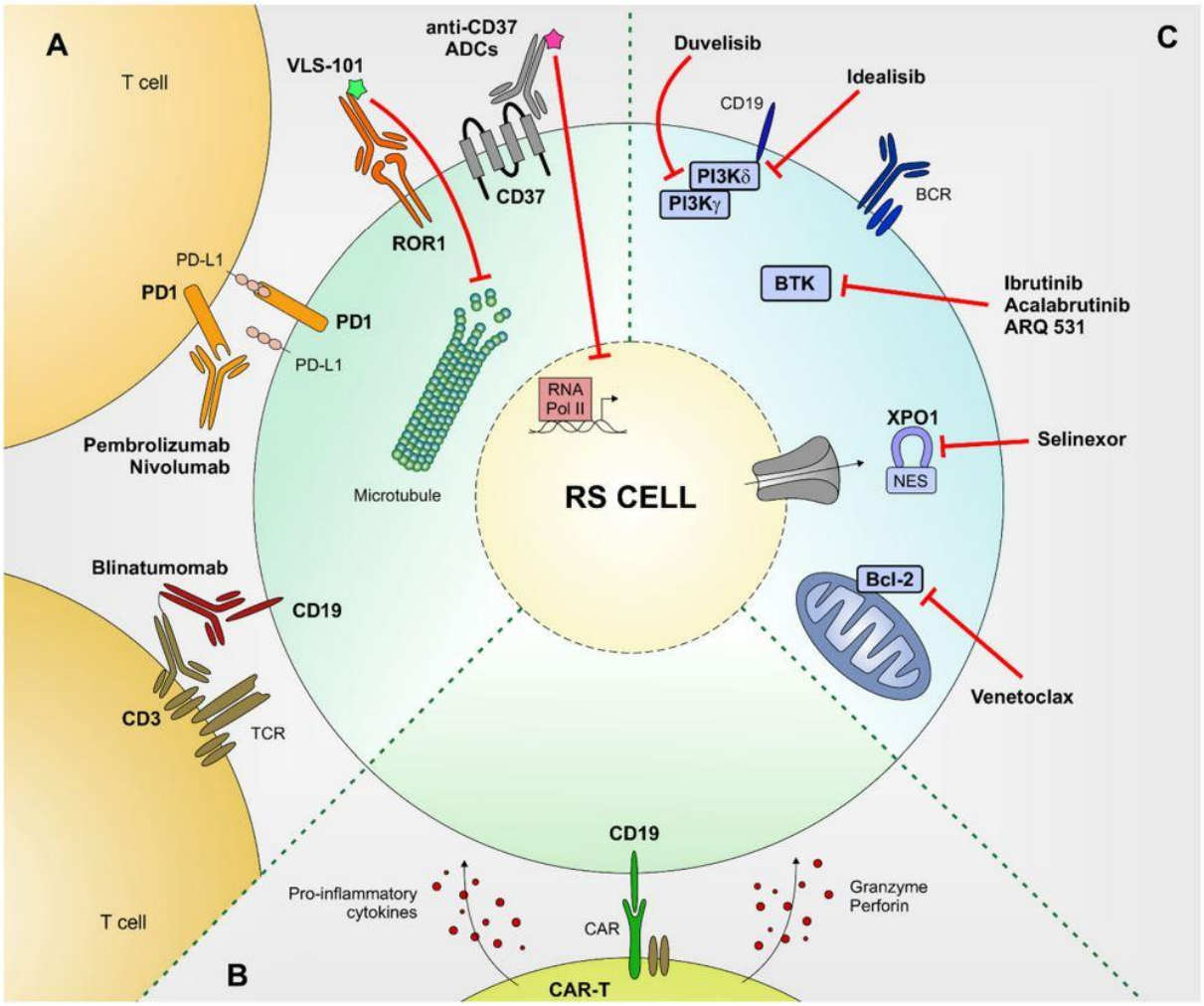

Figure 5: Schematic representation of novel therapeutic approaches to treat RS patients.[196]

The main novel therapeutic approaches to treat RS patients are summarized. Small molecules targeted therapies (A), antibody-based therapies (B), and CAR-T (C). Bcl-2 (Bcell lymphoma 2), XPO1 (exportin 1), BTK (Bruton tyrosine kinase), BCR (B-cell receptor), PI3K (phosphoinositide 3-kinase), ADC (antibody-drug conjugate), ROR1 (receptor tyrosine kinase-like orphan receptor 1), PD1 (programmed death 1), PD-L1 (programmed death 1 Ligand), TCR (T-cell receptor), RNA Pol II (RNA polymerase 2), CAR (chimeric antigen receptor), NES (nuclearexport signal)

2.12 RS-Patient derived xenograft (PDX)

Recently, our group had for the first time established four different PDX models of Richter syndrome (RS9737, RS1316, IP867/17 and RS1050).[197] The neoplastic cells derived from lymph node or peripheral blood biopsies of diagnosed patients with Richter syndrome.

Three of the models (RS9737, RS1316, and RS1050) were established from patients who had a previous history of CLL and were resistant to conventional chemo-immunotherapy, as R-CHOP and/or Ibrutinib treatment. In contrast, IP867/17 was obtained from a patient who received no therapy. The neoplastic cells from RS patients were subcutaneously injected in NSG mice and the cells from tumor masses were reimplanted for a minimum of 10 passages.

Phenotypically, all the RS-PDX models were positive for B-cell markers (CD19, CD21, and CD23), while CD5 is expressed only by RS1316, in agreement with the phenotype characteristic of primary RS samples. Immunohistochemistry analyses confirmed the robust expression of CD20, CD23, and of PAX5, in accordance with a diagnosis of DLBCL.

All the RS-PDX models maintain a close relationship with the primary RS clone, maintaining the same phenotypic and genotypic characteristics, remaining stable over time. Importantly, most of the single or multi-nucleotide variations present in the 4 PDX models were already present in the primary samples. RS-PDXs carry a complex pattern of somatic mutations. Specifically, all RS-PDX models have point mutations or deletions on chromosome 17p, causing biallelic inactivation of the TP53 gene. In addition, IP867/17 has an amplification of the MYC gene involving the 8q24 region. RS-PDX models offered a new opportunity to highlight pathogenic mechanisms and discover driver signaling pathways of therapeutic interest. A promising therapeutic strategy recently approved by the FDA for the treatment of solid and hematological cancers is therapy based on antibody-drug conjugates (ADCs).

The clinical success of these therapies depends on selectivity towards neoplastic cells, reducing off-target effects. These engineered therapies are based on combining the toxicity of a drug with the selectivity of mAb. For these reasons, the preclinical impact of two ADC molecules was explored in the four RS xenograft models targeting two molecules, ROR1 and CD37, which are highly and selectively expressed by these neoplastic cells.

The receptor tyrosine kinase–like orphan receptor 1 (ROR1) has a key role during embiogenesis, but its expression decreases during fetal development and is absent or low in adult tissues.[198–200] The expression of ROR1 has been observed in both solid and hematological tumors, including CLL, making it an interesting tumor-specific therapeutic target to explore in RS.[201,202] Vaisitti et al, evaluated the pre-clinical effect of the ADC, VLS-101 comprising UC-961, a humanised monoclonal immunoglobulin G1 antibody that binds an extracellular epitope of human ROR1, linked to the antimicrotubular agent monomethyl auristatin E (MMAE).[203] When VLS-101 binds the ROR1 receptor, the entire complex is internalized and transported to the lysosomes where it is released, at which point it is free to inhibit cell cycle progression and induce apoptosis.

Ex-vivo use in RS-PDX models has shown significant efficacy in cell cycle arrest and induction of apoptosis. These promising results were also observed in murine models, with a reduction in tumor burden and consequently an increase in animal survival. Of note, VLS-101 showed high selectivity as no clinical effects in RS9737, the only ROR1-negative model. Furthermore, no toxic effects were observed in all treated mice.

Thanks to the contribution also of this work, a phase I clinical study is now testing VLS-101 in RS and other hematological malignancies (NCT03833180). The results of this study have not yet been made available.

The second target explored by Vaisitti et al. in RS to be targeted with ADC is CD37, a leukocyte surface antigen belonging to the tetraspanin family.[204]

This antigen is expressed at high levels in mature B cells and in their transformed leukaemia/lymphoma counterpart. Since CD37 expression is peculiar in B cells and absent in normal T cells, NK cells and plasma cells, it has recently been proposed as a target for the treatment of CLL and DLBCL.[205–207] The surface expression of CD37, both in primary samples and in established PDX models of RS, showed levels comparable to that observed in follicular lymphoma cells and DLBCL. Specifically, the analysis of CD37 expression by flow cytometry analysis and immunohistochemically staining in the PDX models showed that two of them (RS1316 and IP867/17) were characterized by significantly higher expression than the other two models (RS9737 and RS1050). The efficacy of three different anti-CD37 ADCs was evaluated, all generated using amanitine as payload, a toxin that once internalized in CD37 positive cells binds RNA polymerase II inhibits its activity and the cellular transcription.

Ex vivo treatment of RS cells with the three different anti-CD37 ADCs showed significant induction of apoptosis in all PDX models and increased survival of single dose treated mice. In addition, all three anti-CD37 ADCs showed high specificity and selectivity with no toxic effects. The results of this work showed the pre-clinical efficacy of these anti-CD37 DCAs, making it an attractive target for patients with RS.

Lastly, a recent work from my group demonstrated the pre-clinical efficacy of Duvelisib, a dual PI3Kδ/γ inhibitor, and the BLC-2 inhibitor, Venetoclax, in RS-PDX models expressing the target molecules.[208] Inhibition of PI3K by Duvelisib showed a downregulation of the AKT signaling pathway and subsequent GSK3β activation, which causes the ubiquitination and degradation of c-Myc and Mcl-1 via proteasome, making RS cells more sensitive to BCL-2 inhibition. *Ex-vivo* treatment of RS-PDX models with Duvelisib, Venetoclax and their

combination showed a variable induction of apoptosis in RS-PDX models. Importantly, the use of the two drugs in combination showed a significant effect in the induction of apoptosis compared to the two single drugs. In *in vivo* models, treatment in combination led to a significant reduction in tumor volume and increased survival of the mice, particularly in RS1316 and IP867 the two best responsive models. Contrarily, RS9737, the fastest growing model, has shown partial responses to the combination treatment. Finally, RS1050, characterized by very low levels of PI3K-γ and lacking Bcl-2, proved to be completely resistant to treatment.[208] As demonstrated by the results of this work, preventive molecular profiling of RS patients shows increased therapeutic efficacy, highlighting the preclinical efficacy of Duvelisib and Venetoclax in combination in the treatment of RS. Notably, the results of this work provided a rationale for the clinical use of Duvelisib in patients with RS, in combination with the anti-PD1, Nivolumab (NCT03892044).

Aim of the work

Since the metabolic reprogramming is a key process during cancer progression, my PhD project focused on studying the connection between the BCR signalling pathway and NAD^+ metabolism in Richter syndrome.

The aim of this work was to understand the metabolic dependencies of RS cells to identify critical and actionable pathways for RS cells to exploit them therapeutically.

This work stems from the observation that BCR cross-linking in CLL is followed by an increase in NAMPT expression and NAD^+ levels,[37] leading the way for the use of BCRi in combination with NAMPTi. Furthermore, using the four PDX models we explored the preclinical efficacy of OT-82, a novel NAMPT inhibitor in combination with Duvelisib, a PI3K δ/γ. Both OT-82 and Duvelisib are currently used in two clinical trials for the treatment of patients with relapsed or refractory lymphoma (NCT03921879, NCT03892044).

Materials and Methods

4.1 Reagents and antibodies

OT-82 was kindly made available by OncoTartis (Buffalo, NY); Duvelisib, FK866, Selisistat (EX-527) and Thiomyristoyl (TM) were from Selleckchem (Munich, DE); Nicotinamide (NAM) and Trichostatin A (TSA) were from Sigma-Aldrich (St. Louis, Missouri, US).

For western blot analyses the following primary antibodies were used: anti-p-Akt (Thr308) (#4056), -p-AKT (Ser473) (#4060), -AKT (#2920S), -p-GSK3β (#5558), -GSK3β (#12456), -PARP1 (#9532S), -Cleaved Caspase 3 (#9664S), -Caspase 3 (#9662), -SIRT1 (#8469S), -SIRT2 (#12672), -Acetyl-Histone H3 (Lys9) (#9649), -Histone H3 (#4499S), -Acetyl-Histone H4 (Lys16) (#13534), -Histone H4 (#2935), -Acetyl-α-Tubulin (Lys40) (#5335), -α-Tubulin (#3873), -Acetylated-Lysine (9814S), -HSP90 (#4877), -β-Actin (#12620S) all from Cell Signaling Technologies (Milan, IT). Anti-NAPRT (#90725) was from Merck (St. Louis, Missouri, US). Anti-QPRT (#ab57125) and anti-NRK1(#ab169548) were both from Abcam (Cambridge, UK). Anti-NAMPT (#A300-779A) is from Bethyl (Waltham, MA).

The following secondary antibodies were used: donkey anti-rabbit IgG-horseradish peroxidase (HRP)- conjugated (GE Healthcare; Milan, IT), goat anti-mouse IgG HRP-conjugated (Perkin Elmer; Milan, IT).

4.2 RS-PDX Models

RS-PDX models were established and maintained as described by Vaisitti et al. [173]

Briefly, RS cells (5×10^6) were resuspended in Matrigel (Becton Dickinson, Milan, IT), injected (double flank) into 8-week-old NOD/SCID/γ-chain−/− (NSG) mice, and left to engraft. When a

mass could be detected (volume of ~0.2 cm), animals were randomly assigned to 4 different groups and treated by oral gavage for nine non-consecutive days (three rounds of treatments and four stops) for three weeks with Vehicle (5% DMSO, 90% PEG300 and 5% Tween 80 or 30% hydroxypropyl-b-cyclodextrin; all from Sigma-Aldrich), Duv (100 mg/Kg), OT-82 (40 mg/Kg) or their combination. Four days before the start of treatment, animals were fed a commercial niacin-free rodent diet (2018S, Harlan or rat and mouse premium breeder diet 23% protein, Gordon's Specialty Stockfeeds, Australia) or custom designed diets (Harlan). During drug administration and after treatment discontinuation, mice were monitored, and tumor masses regularly measured twice a week by caliper. Mice were euthanized two days after the last treatment. The Institutional Animal Care and Use Committee approved all the experiments involving mice. Mice were treated following the European guidelines and with the approval of the Italian Ministry of Health (authorization #664/2020-PR).

4.3 Ex-vivo treatment of RS cells

RS cells, freshly purified from tumor masses, were exposed to drugs for the indicated time points, depending on the read-out considered. Specifically, we used: Duvelisib (5 uM; 24, 48 and 72 hours); OT-82 (0.625, 1.25 and 2.5nM; 24, 48 and 72 hours). All cells were maintained in RPMI-1640 medium supplemented with 10% heat-inactivated fetal calf serum (FCS) (referred to as "complete medium") and penicillin/streptomycin (P/S, 100 IU/ml) plus one additional antibiotic among gentamicin (10 mg/mL), kanamycin (50 mg/mL) and tylosin (8 mg/mL).

4.4 RNA sequencing analysis

RNA sequencing analysis for RS-PDX models was performed as reported 13. RNA sequencing on a cohort of primary RS samples was performed on RNA extracted from formalin-fixed paraffin-embedded lymph nodes biopsies. RNA was purified with Qiagen Kit and RNA sequencing performed using the total mRNA stranded Illumina kit.

4.5 RNA extraction and qRT-PCR

Total RNA was extracted using Qiagen Kit and retrotranscribed to cDNA using the High-Capacity cDNA Reverse Transcription Kit (Thermo Fisher). qRT-PCRs were performed using NAMPT, NMRK1, QPRT, B2M, CCL3 and MYC primers all obtained from Thermo Fisher Scientific, expect for NAPRT and B2M primers obtained from Eurofins Genomics. For each gene, expression levels were computed as a ratio of the number of copies of the target gene over 105 copies of β2- microglobulin (B2M).

4.6 Western Blotting

Proteins were resolved by SDS-PAGE and transferred into a 0.2 µm nitrocellulose Trans-Blot Turbo Transfer membrane using the Trans-Blot Turbo Transfer System (all from Bio-Rad). The optical density (OD) of the bands was determined with the Image Lab 3.0 software (Bio-Rad Laboratories). Protein levels were normalized using the β-actin or non-phosphorylated protein signal.

4.7 Enzymatic assays

NAD^+ and ATP levels were measured using bioluminescent assay (NAD/NADH-Glo Assay and CellTiter-Glo Luminescent Cell Viability Assay, Promega, Milan, IT). Both NAD^+ and ATP levels were normalized on protein levels (RLU x µl/µg). Sirtuin activity was evaluated using a fluorimetric assay (EPI018, Sigma-Aldrich, St. Louis, Missouri, US) and normalized on protein levels (pmol/min/ µg).

4.8 Apoptosis evaluation and combination index

RS cells were cultured in vehicle (0.1% DMSO), Duvelisib, FK866, OT-82, Selisistat (EX-527) and Thiomyristoyl (TM) or their combination (Duvelisib/OT-82, Duvelisib/FK866, Duvelisib/ Selisistat, Duvelisib/TM) for 24, 48 and 72 hours. Viability was then assessed by Annexin V-APC Apoptosis Kit (Thermofisher, Milan, IT). Samples were analyzed by flow cytometry using FACS Celesta (BD Bioscience, Franklin Lakes, NJ USA).

The synergistic effects on RS cells of the dual administration of Duvelisib/OT-82 (EDuvelisib/OT-82) compared to the single agents (EDuvelisib/EOT-82) in terms of apoptosis induction were evaluated by calculating the combination index (CI).[185]

4.9 Immunoprecipitation

500 mg of protein was precleared with immunoglobulin G–coated protein A magnetic Sepharose beads (30 minutes, 4°C) from GE Healthcare (Milan, IT). Precleared lysates were then incubated with anti-AKT-coated beads (3 hours, 4°C) using AKT (#2920S) from Cell Signaling Technologies (Milan, IT). Immunocomplexes were then washed 3 times with a Tris buffer (50 mM Tris, 150 mM NaCl, pH 7.5), eluted with sodium dodecyl sulfate 2%, and analyzed by western blot.

4.20 2D Electrophoresis (IEF/SDS-PAGE)

Cells were washed once with cell washing buffer (10 mM Tris-HCl, 250 mM sucrose, pH 7.0), lysed in 2D Sample Solution (7M urea, 2M thiourea, 4% (w/v) CHAPS, 2% 3-10 NL IPG Buffer, GE Healthcare), and incubated at room temperature for 20 mins. Samples were centrifuged (13'000 for 15 mins) and quantified. We prepared the sample mix with 100 µg of lysate, 5 µl of DTT, 2.5 µl of 3-10 NL IPG Buffer, 1.42 µl of Destreak Reagent (GE Healthcare) and added RH Buffer (7 M urea, 2 M thiourea, 4% (w/v) CHAPS, 0.002% bromophenol blue) to 125 µl. Supernatants were then removed and layered in the equilibration tray, and the 3-10 NL 7-cm IPG strips were placed on top of them and left rehydrating, covered in mineral oil to prevent drying. After 18 hours of incubation, the strips were removed and placed in the focusing tray of the PROTEAN i12 for the first dimension IEF, again covered in mineral oil. the strips were incubated in 1% DTT in Equilibration Buffer (6 M Urea, 2% SDS, 0.05 M, 20% glycerol, Tris-HCl, pH 8.8) and then in 2.5% iodoacetamide in Equilibration Buffer, both for 15 mins, while rocking. The second dimension was performed as described in western blot.

4.11 Gene silencing

For sirtuins silencing we used freshly isolated RS cells ($6x10^6$) transfected with validated siRNA for SIRT1 (sc-40986), SIRT2 (sc-40988) or scramble siRNA (sc-37007), obtained from Santa Cruz Biotechnology (Dallas, Texas, US) using the NEPA21 Super Electroporator (Nepagene, Chiba, Japan). Following transfection, RS cells were cultured in complete medium, and harvested at 24h for protein and RNA extraction, or treated with Duvelisib for 24 and 48 hours.

4.12 Immunohistochemistry

For IHC staining, anti-Cleaved Caspase-3 antibody (#9664S) from Cell Signaling Technologies (Milan, IT) was used to detect RS cells, followed by an anti-mouse HRP-conjugated antibody and 3,3'-diaminobenzidine (EnVision™ System, Dako) to visualize the reaction. Slides were analyzed using an AXIO Lab.A1 microscope (Zeiss), equipped with a Canon EOS600D reflex camera and the images acquired using the ZoomBrowserEX software (Canon).

Results

5.1 NAD^+ biosynthetic pathways in RS

NAD^+ is a vital molecule for regulating redox reactions, as well as the activity of intracellular and extracellule NAD-dependent enzymes. Its biosynthesis is controlled through the activity of four rate-limiting enzymes, namely NAMPT, which controls the biosynthetic pathway from nicotinamide, NRK, from nicotinamide riboside, NAPRT, from niacin and QPRT from tryptophan, considered the only de novo pathway. By using RNA sequencing data from a cohort of 14 primary RS samples and 4 RS-PDX models (RS9737, IP867/17, RS1316, and RS1050), we show that NAMPT is invariably expressed by all samples, while NRK and NAPRT show heterogeneous levels (Figure 1A). QPRT constitutive expression is low to undetectable, supporting the notion that de novo biosynthesis does not occur in lymphocytes.[34] Expression data were confirmed in RS-PDX samples at both transcript and protein levels (Figure 1B), clearly showing that NAMPT protein levels are elevated in all 4 models. Intriguingly, RS9737 and RS1316 cells show high constitutive expression of NAPRT, an enzyme associated to intrinsic resistance to treatment with NAMPT inhibitors in different cancer models.[64]

5.2 NAMPT is dynamically modulated upon BCR signaling

We next investigated the effects of BCR signaling on NBE expression in RS cells, using RS-PDX cells obtained from mice and cultured for up to 4 days. Ligation of the BCR using plate-bound anti-IgM antibodies was followed by significant increase in NAMPT mRNA and protein levels after 24 hours of IgM stimulation (Figure 2A). Correct activation of the BCR pathway was confirmed by showing increased expression of both CCL3 and MYC, known downstream effectors 29 (Figure 3A-B). It is important to note that in these conditions no statistically

significant changes in NMRK and NAPRT expression levels could be observed, confirming that NAMPT is the enzyme that responds to environmental needs (Figure 3C-D).

NAMPT up-regulation was completely inhibited by treating RS cells with the PI3K δ/γ inhibitor Duvelisib, which effectively blocks BCR signaling (Figure 2A-B). In line with previous observations, treatment with Duvelisib at 5 µM for 24 hours did not induce apoptosis.[208]

Consistent with NAMPT upregulation, cellular NAD^+ levels were markedly increased 24 hours after BCR ligation compared to unstimulated cells in all 4 RS models (Figure 2C). Increased bioavailability of NAD^+ levels fuelled activity of NAD-dependent sirtuins, as documented using a sirtuin activity assay (Figure 2D). Pre-treatment of cells with duvelisib completely inhibited this effect, implying that it is specifically related to BCR activation (Figure 2C-D). These findings highlight a molecular circuit connecting BCR activation to NAD^+ biosynthesis through NAMPT upregulation, in turn positively affecting activity of NAD-dependent situins.

5.3 Functional cooperation between NAMPT and PI3Kδ/γ inhibitors

Given the functional link between BCR signalling and NAMPT expression, we evaluated the effects of the combination of dual PI3K (with Duvelisib) and NAMPT (with OT-82) inhibitors, using ex vivo cultured RS-PDX cells. For Duvelisib, we used a non-lethal concentration (5 µM), while for OT-82, we performed a dose-escalation assay (0.625 nM, 1.25 nM, 2.5 nM) and observed a significant decrease in cell viability, as determinate by APC-Annexin V/PI staining after both 48 and 72 hours of treatment (Figure 4A-B), in line with a decrease in NAD^+ and ATP levels after 24 and 48 hours (Figure 4C-D). As expected, on the basis of enzyme expression, RS9737 and RS1316 were partially resistant to OT-82, confirming that NAPRT can compensate for NAMPT block.[57] On the other hand, IP867 and RS1050, which were NAPRT-negative, showed significant apoptosis already at the lowest dose (0.625 nM).

Exposure to the combination of PI3Ki (Duvelisib, 5uM) and NAMPTi (OT-82, 2.5nM for RS9737 and RS1316; 0.625nM for RS1050 and IP867/17) for 48 and 72 hours induced a strong reduction in cell viability, compared to both drugs used alone.

On average, viability in combined treatment samples dropped to 50% after 48 hours (Figure 5A) and to 20% after 72 hours (Figure 4B), without differences based on NAPRT expression. By calculating the combination index (CI) of Duvelisib and OT-82 co-treatment, we highlighted a strong synergic effect (CI<1) in all RS-PDX models (Figure 5C). These results were confirmed by showing that FK866, a different and well-known NAMPTi, showed overlapping apoptotic responses alone and in combination with Duvelisib (Figure 6A-D).

In line with apoptosis data, we observed higher levels of cleaved Caspase 3 and PARP1 in the combination treatment compared to single treatments (Figure 5D). Taken together, these results highlight a synergy between PI3Kδ/γ and NAMPT inhibitors in RS cells in inducing apoptosis, independently of the underlying genetic lesions and of the expression of NAPRT.

5.4 PI3Ki and NAMPTi converge on AKT in fully blocking the BCR signalling pathway

Examining potential convergence points to explain the synergy between Duvelisib and OT-82, we focused on AKT, a central effector in the BCR signalling pathway. To achieve full activation, AKT needs to be phosphorylated at different amino acid residues, an event mediated by the PI3K and deacetylated at lysines 14 and 20 (K14/20), a second post-translational modification regulated by sirtuins. AKT acetylation at specific lysine residues suppresses its activity by preventing its PIP3-mediated recruitment at the inner leaflet of the plasma membrane. SIRT-mediated deacetylation of K14/20 is a necessary step for its activation.[209,210] Several studies have demonstrated how NAD^+ depletion via NAMPT inhibition results in the decrease in PIP3-bound and phosphorylated AKT levels.[211212]

For these reasons, we investigated BCR-mediated AKT activation upon NAMPT and PI3K inhibition. Upon BCR crosslinking, AKT was robustly phosphorylated at both Thr308 and Ser473 in all RS models, an event that was partially blocked in the presence of OT-82 or of Duvelisib, with their combination being the most effective in blocking AKT activation. Consistently, also the activation of GSK3b, which is directly downstream of AKT was significantly blocked with combination treatment (Figure 7A).

To validate the hypothesis of a sirtuin-dependent activation of AKT we performed immunoprecipitation experiments, followed by western blotting using an anti-acetyl-lysine residue, demonstrating that the active form of AKT is de-acetylated (Figure 7B).

Pre-treatment of cells with OT-82 increased the levels of AKT acetylation, consistent with effective sirtuin inhibition and indicating that the molecule is inactive (Figure 7B). By using 2D WB for total AKT, we show four AKT-immunoreactive spots: by using the acetyl-lysine blot signal, we identified the first one on the right as AKT without any post-translational modifications, the second one to singly modified AKT (either acetylated or phosphorylated), and the third and fourth as doubly- and triply-modified AKT molecules (Figure 7C).

As shown by the WB (Figure 7D), the levels of p-AKT (both p-Thr308 and p-Ser473) decreased upon treatment and, at the same time, proteome-wide acetylation levels increased, shown by the increasing acetyl-α-tubulin signal. Correspondingly, in the 2D blot we observed a shift in intensity, upon treatment, towards the spots on the left, which correspond to AKT, either at a single or double lysine residue, corresponding to its inactive form.

5.5 SIRT1 or SIRT2 inhibition of in combination with Duvelisib leads to increased apoptosis

AKT acetylation is regulated through the activity of SIRT1, which deacetylates AKT at lysines 14 and 20, and SIRT2, which deacetylates AKT at lysine.[209–213]

Both these enzymes are expressed by primary RS cells and by the PDX models, as verified by RT-PCR and western blotting (Figure 8A). Treatment of RS cells with either SIRT1-specific (Selisistat, EX-527) or SIRT2-specific [Thiomyristoyl (TM)] inhibitors triggered a potent apoptotic response after 72 hours of treatment, which was further increased by the addition of Duvelisib (Figure 8B). In line with these findings, genetic knock-down of either SIRT1 or SIRT2, markedly reduced cell viability, particularly in the presence of Duvelisib (Figure 8C). Consistently, exposure to the combination of a SIRT inhibitor and of Duvelisib completely blocked AKT activation. Similar results were obtained using genetic silencing of both enzymes (Figure 8D-E).

5.6 In vivo combination of OT-82 and Duvelisib treatments induce a significant block in tumor growth and reduction in cellular sirtuins activity

The efficacy of the PI3Ki/NAMPTi drug combination was then validated using our RS-PDX models. RS cells were subcutaneously injected in 8-week-old male NSG mice and left to engraft until tumor masses were at least 0.2 cm^3. Mice were then randomized in 4 groups and treated for three weeks with vehicle, OT-82 (40mg/kg), Duvelisib (100mg/kg) or the combination of both drugs.[208]

Treatments were administered for three consecutive days, leaving a 4 day-washout period between treatment cycles. To increase the efficacy of OT-82 in vivo, two days before starting the treatment we substituted the regular mice diet, supplemented with 115 mg/kg of niacin, with a custom diet containing 30 mg/kg of niacin, as previously described.[214]

At the end of the treatment, mice were sacrificed, and tumor masses recovered. In all the RS models we could already noticed that the combination treatment was more effective than the individual treatment measuring volume and weight of the masses (Figure 9-12A-B). We

then performed APC-Annexin V/PI apoptosis assay to evaluate the viability of the recovered cells, which again showed that the viability of RS-PDX cells was remarkably reduced in the masses treated with the drug combination (Figure 9-12C). We also evaluated NAD^+ and ATP levels in the isolated RS-PDX cells. Our measurements confirmed the results obtained in vitro: NAD^+ and ATP levels were drastically decreased by the combination of dual PI3Ki and NAMPTi, in line with the more robust apoptosis observed in these samples (Figure 9-12D-E). Sirtuin activity was also measured and again confirmed the in vitro findings, with the activity of the deacetylases maximally reduced upon combination treatment (Figure 9-12F). Finally, to corroborate the flow cytometry apoptosis data, we also performed immunohistochemistry assay for cleaved Caspase 3 on representative tissue samples. As expected, we observed, a predominant increase in cleaved Caspase 3 in mice treated with the combination of the two drugs (Figure 9-12G). These in vivo results confirmed how the combined use of these two drugs is much more effective than the individual treatments in reducing tumor progression.

Discussion

This work identifies for the first time a possible therapeutic role for the NAMPT inhibitor OT-82 in PDX models of Richter's syndrome. NAMPT is an inhibitor of the NAM pathway of NAD^+ synthesis and a promising tumor target. It has been extensively studied as an anti-tumor target in several different clinical trials, which, however, were marred by the occurrence of severe side effects, including thrombocytopenia and gastrointestinal toxicity.

The modest success of NAMPT inhibitors as monotherapy in cancer patients, may be explained by the activation of rescue pathways that can overcome NAMPT block and restore NAD^+ levels through alternative routes. Most important in this context is NAPRT, the rate-limiting enzyme in the metabolism of dietary NA into NAD^+.

In this work, we show activity of the novel OT-82 NAMPT inhibitor in combination with a PI3K inhibitor, demonstrating anti-tumor activity independently of NAPRT or NRK expression.

Notably, OT-82 has shown both tissue and cancer specificity in hematological tumors, and no adverse effects in murine models of disease compared to first-generation NAMPTis.[102,103]

In addition, several clinical trials are currently underway in patients with RS, in which the efficacy of several BCR pathway inhibitors is being evaluated, including the dual PI3K inhibitor, Duvelisib (NCT03892044).[190–192]

However, patients with RS are often unresponsive and develop resistance to treatments used as monotherapy, probably due to a more complex genetic background or karyotype, which cause these cells to be more aggressive. Therefore, combining BCR pathway inhibitors with other drugs targeting different molecular pathways could be an effective strategy to overcome resistance.

Building upon these findings, we decided to characterize the reciprocal crosstalk between NAD^+ metabolism and BCR signaling using our RS-PDX models, which have proved to be valuable for the discovery of new therapeutic strategies for RS.[197,203]

The analysis of the expression data, both in primary RS samples and in RS-PDX models, of the four different NAD^+ biosynthetic enzymes showed that NAMPT is significantly more expressed than the other enzymes, although its expression levels are heterogeneous.

Of note, upon BCR cross-linking we observed a marked increase in NAMPT expression in all RS-PDX models. In contrast, the expression of NAPRT and NMRK does not appear to be modulated by the activation or inhibition of BCR signaling in RS cells, as expected given their ubiquitous expression pattern.[214–216]

These results suggest that NAMPT is the rate-limiting enzyme in NAD^+ biosynthesis in RS cells. Many of the effects stemming from NAMPT upregulation, and the subsequent increase in NAD^+ levels, are mediated by the increase in the deacetylating activity of sirtuins on their protein targets.[217]

From this point of view, NAMPT is considered the main regulator of sirtuin activity. On the one hand, it is able to generate NAD^+ from NAM, which is necessary for the activity of these enzymes. On the other, NAM is a well-established non-competitive inhibitor of the end product of the sirtuin family.

Sirtuins apparently play contradictory roles in cancer: on one hand, some sirtuins influence cellular responses to genomic instability by regulating the cell cycle, DNA repair, cell survival, and apoptosis, thus having critical roles in cancer progression and metastasis.[217,218] Specifically, SIRT1 can induce chromatin silencing and regulates a wide variety of biological processes and cellular functions by deacetylating a large number of non-histonic proteins, including AKT.[213] SIRT2 is also a key regulator of multiple physiological pathways. In the

cytoplasm, where it is predominantly localized, SIRT2 acts on a variety of substrates, among these it also activates AKT by deacetylating it at the same lysine residues as SIRT1.[50] In addition, SIRT2 can transiently translocate to the nucleus during the G2/M transition to regulate the mitotic chromosome segregation through the deacetylation of histone H4 at Lys16.[74]

In some types of cancer, SIRT3 functions as a tumoral promoter since it keeps ROS levels under a certain threshold compatible with cell viability and proliferation. On the contrary, other studies describe SIRT3 as a tumoral suppressor, as SIRT3 could trigger cell death under stress conditions. Thus, SIRT3 could have a dual role in cancer.[83]

The mitochondrial sirtuins, SIRT4 and SIRT5, can regulate cell-cycle progression, genomic fidelity in response to DNA damage and are involved in metabolic reprogramming. Different evidence that SIRT4 is a tumor suppressor, in fact, it is downregulated in most cancer types, and loss of it increases the risk of spontaneous tumors throughout life.[219] While, SIRT5, as well as, SIRT6 impact in cancer biology in a context-specific manner, in some situations, promoting cancer cell survival and proliferation and, in others, functioning to restrict cancer growth.[92] SIRT7 is involved in diverse cellular processes, including energy homeostasis, chromatin regulation, gene regulation and ribosome biogenesis. The importance of SIRT7 in DNA damage repair suggests that this enzyme might function as a tumor suppressor. However, SIRT7 is overexpressed in various cancers. Thus, SIRT7 might have opposing effects on cancer initiation and progression.[220]

Several different studies have highlighted the central role of SIRT1 and SIRT2 in hematological malignancies and the overexpression of SIRT1 and SIRT2 has also been reported in CLL and DLBCL. Elevated SIRT1 expression is associated with poor prognosis in CLL, AML, CML, and DLBCL.[221,222]

Promising results have also been obtained from studies investigating the therapeutic potential of sirtuin inhibitors both in solid and hematological neoplasia. The SIRT1 inhibitor Selisistat exhibited a strong anti-proliferative effect in multiple leukemia cell lines, while the antitumor activity of the SIRT1/2 inhibitor cambinol has been demonstrated on BCL6-expressing Burkitt lymphoma cells and xenografts.[223224]

Sirtinol, a SIRT1 inhibitor, treatment induced growth arrest and apoptosis in human breast cancer cells, lung cancer cells, and leukemic cells, and led to increased sensitivity to chemotherapy in prostate cancer cell lines.[225–227]

Lastly, the SIRT2 inhibitor TM strongly reduced the viability of leukemic cell lines compared to non-hematopoietic cancer cell lines.[71]

Together, these and other studies support SIRT1 and SIRT2 inhibition as a promising therapeutic vulnerability in solid and hematological cancers. However, the translation of *in vitro* and *in vivo* results into small molecule sirtuin inhibitors with the potential to be tested in clinical trials has been hampered by a variety of difficulties, among them the lack of isoform specificity, limited potency and bioavailability, and poor pharmacokinetics and pharmacodynamic of the candidates advanced to the trial stage. [228,229]

In fact, no sirtuin inhibitors have been approved for clinical trials for the treatment of solid and hematological cancers. Some of the possible explanations are that sirtuins could be redundant in their actions, with significant overlaps in substrate specificity; or that, since some of their cellular roles are not dependent on enzymatic activity, enzymatic inhibition alone exhibits only moderate efficacy.

Based on these considerations and observations, it is reasonable to speculate that reducing NAD^+ levels, through NAMPT inhibition, could have a polypharmacological effect on the activity of the whole sirtuin family, in turn modulating their targets, including AKT.

In fact, treatment with SIRT1 or SIRT2 inhibitors has been observed to negatively regulate AKT activation in several disease models.[209,210,230–232]

Activation of Akt occurs through its binding to phosphatidylinositol 3,4,5-trisphosphate (PIP3), where the Pleckstrin homology domain (PH) is modified. These modifications allow its translocation from the cytosol to the membrane and its activation due to the phosphorylation at Thr308 and Ser473 by the upstream kinase, phosphoinositide-dependent protein kinase 1 (PDK1).[233] Acetylation of the PH domain at specific residues, lysines 14 and 20, neutralizes their positive charge by affecting their structure and rendering them unable to bind to PIP3.[234]

Given the convergency of NAD^+ metabolism and BCR signaling, via PI3K, on AKT, in this study, we explored the potential targeting synergy arising from BCR signaling inhibition via Duvelisib combined with OT-82-mediated NAMPT inhibition in RS. The dual treatment induces strong apoptosis in vitro in all the RS-PDX models tested. We also confirmed the same finding in vivo, observing a striking tumor regression in all RS-PDX models, independently of their genetic background.

Of note, OT-82-treated mice showed a significant response compared to duvelisib treatment alone, highlighting the key role of NAD^+ metabolism in RS. Importantly, we showed that the combined administration of Duvelisib and OT-82 converges on AKT activation, through the modulation of SIRT1/2 activity obtained by decreasing NAD^+ levels (Figure 13).

We also highlighted the critical role that SIRT1 and SIRT2 play in RS cells, especially when they are targeted in combination with BCR signaling, either by pharmacologically inhibiting their activities or by silencing their expression using siRNA. It must be noted that, although we corroborated the role of AKT in the synergy established between OT-82 and Duvelisib, we cannot in principle exclude that the depletion of NAD^+ through NAMPT inhibition also has an

impact on multiple other targets and pathways, which could also play a role in this context. For example, SIRT1 has been reported to induce c-Myc overexpression, while SIRT2 promotes tumor growth by increasing c-Myc stabilization.[70]

Further studies are needed also to address the specific role of individual sirtuins, besides SIRT1 and SIRT2, in RS cells.

In conclusion, our data emphasize the crucial nature of NAMPT as the main NAD^+ biosynthetic enzyme and prove how NAD^+ levels, especially in the context of BCR inhibition, are a potential metabolic Achilles' heel of RS, which could be exploited therapeutically. OT-82 and Duvelisib cooperate in turning off central pro-neoplastic cellular pathways, which promote RS proliferation and survival, and their co-administration should be further investigated and potentially translated to clinical applications.

References

1 Canto C, Menzies KJ, Auwerx J. NAD(+) Metabolism and the Control of Energy Homeostasis: A Balancing Act between Mitochondria and the Nucleus. *Cell Metab* 2015; **22**: 31–53.

2 Houtkooper RH, Canto C, Wanders RJ, Auwerx J. The secret life of NAD+: an old metabolite controlling new metabolic signaling pathways. *Endocr Rev* 2010; **31**: 194–223.

3 Berger F, Ramirez-Hernandez MH, Ziegler M. The new life of a centenarian: signalling functions of NAD(P). *Trends Biochem Sci* 2004; **29**: 111–118.

4 Yaku K, Okabe K, Nakagawa T. NAD metabolism: Implications in aging and longevity. *Ageing Res Rev* 2018; **47**: 1–17.

5 Xiao W, Wang RS, Handy DE, Loscalzo J. NAD(H) and NADP(H) Redox Couples and Cellular Energy Metabolism. *Antioxid Redox Signal* 2018; **28**: 251–272.

6 Kunjithapatham R, Ganapathy-Kanniappan S. GAPDH with NAD(+)-binding site mutation competitively inhibits the wild-type and affects glucose metabolism in cancer. *Biochim Biophys Acta Gen Subj* 2018; **1862**: 2555–2563.

7 Doherty JR, Cleveland JL. Targeting lactate metabolism for cancer therapeutics. *J Clin Invest* 2013; **123**: 3685–3692.

8 Akram M. Citric acid cycle and role of its intermediates in metabolism. *Cell Biochem Biophys* 2014; **68**: 475–478.

9 Sazanov LA. A giant molecular proton pump: structure and mechanism of respiratory complex I. *Nat Rev Mol Cell Biol* 2015; **16**: 375–388.

10 le Belle JE, Orozco NM, Paucar AA, Saxe JP, Mottahedeh J, Pyle AD *et al.* Proliferative neural stem cells have high endogenous ROS levels that regulate self-renewal and neurogenesis in a PI3K/Akt-dependant manner. *Cell Stem Cell* 2011; **8**: 59–71.

11 Moldogazieva NT, Mokhosoev IM, Feldman NB, Lutsenko S v. ROS and RNS signalling: adaptive redox switches through oxidative/nitrosative protein modifications. *Free Radic Res* 2018; **52**: 507–543.

12 Miller CG, Schmidt EE. Disulfide reductase systems in liver. *Br J Pharmacol* 2019; **176**: 532–543.

13 Filomeni G, de Zio D, Cecconi F. Oxidative stress and autophagy: the clash between damage and metabolic needs. *Cell Death Differ* 2015; **22**: 377–388.

14 Chen SH, Yu X. Human DNA ligase IV is able to use NAD+ as an alternative adenylation donor for DNA ends ligation. *Nucleic Acids Res* 2019; **47**: 1321–1334.

15 Hassinen IE. Signaling and Regulation Through the NAD(+) and NADP(+) Networks. *Antioxid Redox Signal* 2019; **30**: 857–874.

16 Verdin E. NAD(+) in aging, metabolism, and neurodegeneration. *Science (1979)* 2015; **350**: 1208–1213.

17 Chiarugi A, Dolle C, Felici R, Ziegler M. The NAD metabolome--a key determinant of cancer cell biology. *Nat Rev Cancer* 2012; **12**: 741–752.

18 Cambronne XA, Kraus WL. Location, Location, Location: Compartmentalization of NAD(+) Synthesis and Functions in Mammalian Cells. *Trends Biochem Sci* 2020; **45**: 858–873.

19 Cambronne XA, Stewart ML, Kim D, Jones-Brunette AM, Morgan RK, Farrens DL *et al.* Biosensor reveals multiple sources for mitochondrial NAD(+). *Science (1979)* 2016; **352**: 1474–1477.

20 Rajman L, Chwalek K, Sinclair DA. Therapeutic Potential of NAD-Boosting Molecules: The In Vivo Evidence. *Cell Metab* 2018; **27**: 529–547.

21 di Stefano M, Conforti L. Diversification of NAD biological role: the importance of location. *FEBS J* 2013; **280**: 4711–4728.

22 Liu L, Su X, Quinn 3rd WJ, Hui S, Krukenberg K, Frederick DW *et al.* Quantitative Analysis of NAD Synthesis-Breakdown Fluxes. *Cell Metab* 2018; **27**: 1067-1080 e5.

23 Minhas PS, Liu L, Moon PK, Joshi AU, Dove C, Mhatre S *et al.* Macrophage de novo NAD(+) synthesis specifies immune function in aging and inflammation. *Nat Immunol* 2019; **20**: 50–63.

24 Zamporlini F, Ruggieri S, Mazzola F, Amici A, Orsomando G, Raffaelli N. Novel assay for simultaneous measurement of pyridine mononucleotides synthesizing activities allows dissection of the NAD(+) biosynthetic machinery in mammalian cells. *FEBS J* 2014; **281**: 5104–5119.

25 Magni G, Amici A, Emanuelli M, Orsomando G, Raffaelli N, Ruggieri S. Enzymology of NAD+ homeostasis in man. *Cell Mol Life Sci* 2004; **61**: 19–34.

26 Bieganowski P, Brenner C. Discoveries of nicotinamide riboside as a nutrient and conserved NRK genes establish a Preiss-Handler independent route to NAD+ in fungi and humans. *Cell* 2004; **117**: 495–502.

27 Preiss J, Handler P. Biosynthesis of diphosphopyridine nucleotide. I. Identification of intermediates. *J Biol Chem* 1958; **233**: 488–492.

28 Audrito V, Manago A, Gaudino F, Sorci L, Messana VG, Raffaelli N *et al.* NAD-Biosynthetic and Consuming Enzymes as Central Players of Metabolic Regulation of Innate and Adaptive Immune Responses in Cancer. *Front Immunol* 2019; **10**: 1720.

29 Audrito V, Manago A, la Vecchia S, Zamporlini F, Vitale N, Baroni G *et al.* Nicotinamide Phosphoribosyltransferase (NAMPT) as a Therapeutic Target in BRAF-Mutated Metastatic Melanoma. *J Natl Cancer Inst* 2018; **110**. doi:10.1093/jnci/djx198.

30 Revollo JR, Grimm AA, Imai S. The NAD biosynthesis pathway mediated by nicotinamide phosphoribosyltransferase regulates Sir2 activity in mammalian cells. *J Biol Chem* 2004; **279**: 50754–50763.

31 Sauve AA. NAD+ and vitamin B3: from metabolism to therapies. *J Pharmacol Exp Ther* 2008; **324**: 883–893.

32 Revollo JR, Korner A, Mills KF, Satoh A, Wang T, Garten A *et al.* Nampt/PBEF/Visfatin regulates insulin secretion in beta cells as a systemic NAD biosynthetic enzyme. *Cell Metab* 2007; **6**: 363–375.

33 Rongvaux A, Andris F, van Gool F, Leo O. Reconstructing eukaryotic NAD metabolism. *Bioessays* 2003; **25**: 683–690.

34 Audrito V, Messana VG, Deaglio S. NAMPT and NAPRT: Two Metabolic Enzymes With Key Roles in Inflammation. *Front Oncol* 2020; **10**: 358.

35 Garten A, Schuster S, Penke M, Gorski T, de Giorgis T, Kiess W. Physiological and pathophysiological roles of NAMPT and NAD metabolism. *Nat Rev Endocrinol* 2015; **11**: 535–546.

36 Moschen AR, Gerner RR, Tilg H. Pre-B cell colony enhancing factor/NAMPT/visfatin in inflammation and obesity-related disorders. *Curr Pharm Des* 2010; **16**: 1913–1920.

37 Audrito V, Serra S, Brusa D, Mazzola F, Arruga F, Vaisitti T *et al.* Extracellular nicotinamide phosphoribosyltransferase (NAMPT) promotes M2 macrophage polarization in chronic lymphocytic leukemia. *Blood* 2015; **125**: 111–123.

38 Soncini D, Caffa I, Zoppoli G, Cea M, Cagnetta A, Passalacqua M *et al.* Nicotinamide phosphoribosyltransferase promotes epithelial-to-mesenchymal transition as a soluble factor independent of its enzymatic activity. *J Biol Chem* 2014; **289**: 34189–34204.

39 Carbone F, Liberale L, Bonaventura A, Vecchie A, Casula M, Cea M *et al.* Regulation and Function of Extracellular Nicotinamide Phosphoribosyltransferase/Visfatin. *Compr Physiol* 2017; **7**: 603–621.

40 Camp SM, Ceco E, Evenoski CL, Danilov SM, Zhou T, Chiang ET *et al.* Unique Toll-Like Receptor 4 Activation by NAMPT/PBEF Induces NFkappaB Signaling and Inflammatory Lung Injury. *Sci Rep* 2015; **5**: 13135.

41 Cairns RA, Harris IS, Mak TW. Regulation of cancer cell metabolism. *Nat Rev Cancer* 2011; **11**: 85–95.

42 Chalkiadaki A, Guarente L. The multifaceted functions of sirtuins in cancer. *Nat Rev Cancer* 2015; **15**: 608–624.

43 Guarente L. Sirtuins, aging, and metabolism. *Cold Spring Harb Symp Quant Biol* 2011; **76**: 81–90.

44 Huffman DM, Grizzle WE, Bamman MM, Kim JS, Eltoum IA, Elgavish A *et al.* SIRT1 is significantly elevated in mouse and human prostate cancer. *Cancer Res* 2007; **67**: 6612–6618.

45 Liu G, Yuan X, Zeng Z, Tunici P, Ng H, Abdulkadir IR *et al.* Analysis of gene expression and chemoresistance of CD133+ cancer stem cells in glioblastoma. *Mol Cancer* 2006; **5**: 67.

46 Huang FT, Sun J, Zhang L, He X, Zhu YH, Dong HJ *et al.* Role of SIRT1 in hematologic malignancies. *J Zhejiang Univ Sci B* 2019; **20**: 391–398.

47 Luo J, Nikolaev AY, Imai S, Chen D, Su F, Shiloh A *et al.* Negative control of p53 by Sir2alpha promotes cell survival under stress. *Cell* 2001; **107**: 137–148.

48 Wales MM, Biel MA, el Deiry W, Nelkin BD, Issa JP, Cavenee WK *et al.* p53 activates expression of HIC-1, a new candidate tumour suppressor gene on 17p13.3. *Nat Med* 1995; **1**: 570–577.

49 Grahnert A, Grahnert A, Klein C, Schilling E, Wehrhahn J, Hauschildt S. Review: NAD +: a modulator of immune functions. *Innate Immun* 2011; **17**: 212–233.

50 Moore AM, Zhou L, Cui J, Li L, Wu N, Yu A *et al.* NAD(+) depletion by type I interferon signaling sensitizes pancreatic cancer cells to NAMPT inhibition. *Proc Natl Acad Sci U S A* 2021; **118**. doi:10.1073/pnas.2012469118.

51 Sampath D, Zabka TS, Misner DL, O'Brien T, Dragovich PS. Inhibition of nicotinamide phosphoribosyltransferase (NAMPT) as a therapeutic strategy in cancer. *Pharmacol Ther* 2015; **151**: 16–31.

52 Maldi E, Travelli C, Caldarelli A, Agazzone N, Cintura S, Galli U *et al.* Nicotinamide phosphoribosyltransferase (NAMPT) is over-expressed in melanoma lesions. *Pigment Cell Melanoma Res* 2013; **26**: 144–146.

53 Reddy PS, Umesh S, Thota B, Tandon A, Pandey P, Hegde AS *et al.* PBEF1/NAmPRTase/Visfatin: a potential malignant astrocytoma/glioblastoma serum marker with prognostic value. *Cancer Biol Ther* 2008; **7**: 663–668.

54 Bi TQ, Che XM, Liao XH, Zhang DJ, Long HL, Li HJ *et al.* Overexpression of Nampt in gastric cancer and chemopotentiating effects of the Nampt inhibitor FK866 in combination with fluorouracil. *Oncol Rep* 2011; **26**: 1251–1257.

55 Folgueira MA, Carraro DM, Brentani H, Patrao DF, Barbosa EM, Netto MM *et al.* Gene expression profile associated with response to doxorubicin-based therapy in breast cancer. *Clin Cancer Res* 2005; **11**: 7434–7443.

56 Nacarelli T, Lau L, Fukumoto T, Zundell J, Fatkhutdinov N, Wu S *et al.* NAD(+) metabolism governs the proinflammatory senescence-associated secretome. *Nat Cell Biol* 2019; **21**: 397–407.

57 Piacente F, Caffa I, Ravera S, Sociali G, Passalacqua M, Vellone VG *et al.* Nicotinic Acid Phosphoribosyltransferase Regulates Cancer Cell Metabolism, Susceptibility to NAMPT Inhibitors, and DNA Repair. *Cancer Res* 2017; **77**: 3857–3869.

58 Duarte-Pereira S, Pereira-Castro I, Silva SS, Correia MG, Neto C, da Costa LT *et al.* Extensive regulation of nicotinate phosphoribosyltransferase (NAPRT) expression in human tissues and tumors. *Oncotarget* 2016; **7**: 1973–1983.

59 Li XQ, Lei J, Mao LH, Wang QL, Xu F, Ran T *et al.* NAMPT and NAPRT, Key Enzymes in NAD Salvage Synthesis Pathway, Are of Negative Prognostic Value in Colorectal Cancer. *Front Oncol* 2019; **9**: 736.

60 Tateishi K, Wakimoto H, Iafrate AJ, Tanaka S, Loebel F, Lelic N *et al.* Extreme Vulnerability of IDH1 Mutant Cancers to NAD+ Depletion. *Cancer Cell* 2015; **28**: 773–784.

61 Franceschini N, Oosting J, Tamsma M, Niessen B, Bruijn IB, van den Akker B *et al.* Targeting the NAD Salvage Synthesis Pathway as a Novel Therapeutic Strategy for Osteosarcomas with Low NAPRT Expression. *Int J Mol Sci* 2021; **22**. doi:10.3390/ijms22126273.

62 Watson M, Roulston A, Belec L, Billot X, Marcellus R, Bedard D *et al.* The small molecule GMX1778 is a potent inhibitor of NAD+ biosynthesis: strategy for enhanced therapy in

nicotinic acid phosphoribosyltransferase 1-deficient tumors. *Mol Cell Biol* 2009; **29**: 5872–5888.

63 Manago A, Audrito V, Mazzola F, Sorci L, Gaudino F, Gizzi K *et al.* Extracellular nicotinate phosphoribosyltransferase binds Toll like receptor 4 and mediates inflammation. *Nat Commun* 2019; **10**: 4116.

64 Chowdhry S, Zanca C, Rajkumar U, Koga T, Diao Y, Raviram R *et al.* NAD metabolic dependency in cancer is shaped by gene amplification and enhancer remodelling. *Nature* 2019; **569**: 570–575.

65 Liberti M v., Locasale JW. The Warburg Effect: How Does it Benefit Cancer Cells? Trends Biochem Sci. 2016; **41**. doi:10.1016/j.tibs.2015.12.001.

66 Menssen A, Hydbring P, Kapelle K, Vervoorts J, Diebold J, Lüscher B *et al.* The c-MYC oncoprotein, the NAMPT enzyme, the SIRT1-inhibitor DBC1, and the SIRT1 deacetylase form a positive feedback loop. *Proc Natl Acad Sci U S A* 2012; **109**. doi:10.1073/pnas.1105304109.

67 Kennedy BE, Sharif T, Martell E, Dai C, Kim Y, Lee PWK *et al.* NAD+ salvage pathway in cancer metabolism and therapy. Pharmacol Res. 2016; **114**. doi:10.1016/j.phrs.2016.10.027.

68 Park SH, Zhu Y, Ozden O, Kim HS, Jiang H, Deng CX *et al.* SIRT2 is a tumor suppressor that connects aging, acetylome, cell cycle signaling, and carcinogenesis. Transl Cancer Res. 2012; **1**. doi:10.3978/j.issn.2218-676X.2012.05.01.

69 Fiskus W, Coothankandaswamy V, Chen J, Ma H, Ha K, Saenz DT *et al.* SIRT2 deacetylates and inhibits the peroxidase activity of peroxiredoxin-1 to sensitize breast cancer cells to oxidant stress-inducing agents. *Cancer Res* 2016; **76**. doi:10.1158/0008-5472.CAN-16-0126.

70 Liu PY, Xu N, Malyukova A, Scarlett CJ, Sun YT, Zhang XD *et al.* The histone deacetylase SIRT2 stabilizes Myc oncoproteins. *Cell Death Differ* 2013; **20**. doi:10.1038/cdd.2012.147.

71 Jing H, Hu J, He B, Negrón Abril YL, Stupinski J, Weiser K *et al.* A SIRT2-Selective Inhibitor Promotes c-Myc Oncoprotein Degradation and Exhibits Broad Anticancer Activity. *Cancer Cell* 2016; **29**. doi:10.1016/j.ccell.2016.02.007.

72 Lobry C, Oh P, Mansour MR, Look AT, Aifantis I. Notch signaling: switching an oncogene to a tumor suppressor. *Blood* 2014; **123**: 2451–2459.

73 Head PE, Zhang H, Bastien AJ, Koyen AE, Withers AE, Daddacha WB *et al.* Sirtuin 2 mutations in human cancers impair its function in genome maintenance. *Journal of Biological Chemistry* 2017; **292**. doi:10.1074/jbc.M116.772566.

74 Kim HS, Vassilopoulos A, Wang RH, Lahusen T, Xiao Z, Xu X *et al.* SIRT2 Maintains Genome Integrity and Suppresses Tumorigenesis through Regulating APC/C Activity. *Cancer Cell* 2011; **20**. doi:10.1016/j.ccr.2011.09.004.

75 Banerjee KK, Deshpande RS, Koppula P, Ayyub C, Kolthur-Seetharam U. Central metabolic sensing remotely controls nutrient-sensitive endocrine response in Drosophila via Sir2/Sirt1-upd2-IIS axis. *Journal of Experimental Biology* 2017; **220**. doi:10.1242/jeb.150805.

76 Scher MB, Vaquero A, Reinberg D. SirT3 is a nuclear NAD+-dependent histone deacetylase that translocates to the mitochondria upon cellular stress. *Genes Dev* 2007; **21**. doi:10.1101/gad.1527307.

77 Ozden O, Park SH, Wagner BA, Song HY, Zhu Y, Vassilopoulos A *et al.* SIRT3 deacetylates and increases pyruvate dehydrogenase activity in cancer cells. *Free Radic Biol Med* 2014; **76**. doi:10.1016/j.freeradbiomed.2014.08.001.

78 Yang Y, Wang W, Xiong Z, Kong J, Qiu Y, Shen F *et al.* Activation of SIRT3 attenuates triptolide-induced toxicity through closing mitochondrial permeability transition pore in cardiomyocytes. *Toxicology in Vitro* 2016; **34**. doi:10.1016/j.tiv.2016.03.020.

79 Cheng Y, Ren X, Gowda ASP, Shan Y, Zhang L, Yuan YS *et al.* Interaction of Sirt3 with OGG1 contributes to repair of mitochondrial DNA and protects from apoptotic cell death under oxidative stress. *Cell Death Dis* 2013; **4**. doi:10.1038/cddis.2013.254.

80 Yang S, Xu M, Meng G, Lu Y. SIRT3 deficiency delays diabetic skin wound healing via oxidative stress and necroptosis enhancement. *J Cell Mol Med* 2020; **24**. doi:10.1111/jcmm.15100.

81 Yang W, Nagasawa K, Münch C, Xu Y, Satterstrom K, Jeong S *et al.* Mitochondrial Sirtuin Network Reveals Dynamic SIRT3-Dependent Deacetylation in Response to Membrane Depolarization. *Cell* 2016; **167**. doi:10.1016/j.cell.2016.10.016.

82 Tao R, Coleman MC, Pennington JD, Ozden O, Park SH, Jiang H *et al.* Sirt3-Mediated Deacetylation of Evolutionarily Conserved Lysine 122 Regulates MnSOD Activity in Response to Stress. *Mol Cell* 2010; **40**. doi:10.1016/j.molcel.2010.12.013.

83 Torrens-Mas M, Oliver J, Roca P, Sastre-Serra J. SIRT3: Oncogene and tumor suppressor in cancer. Cancers (Basel). 2017; **9**. doi:10.3390/cancers9070090.

84 Finley LWS, Carracedo A, Lee J, Souza A, Egia A, Zhang J *et al.* SIRT3 Opposes Reprogramming of Cancer Cell Metabolism through HIF1α Destabilization. *Cancer Cell* 2011; **19**. doi:10.1016/j.ccr.2011.02.014.

85 Son MJ, Ryu JS, Kim JY, Kwon Y, Chung KS, Mun SJ *et al.* Upregulation of mitochondrial NAD+ levels impairs the clonogenicity of SSEA1+ glioblastoma tumor-initiating cells. *Exp Mol Med* 2017; **49**. doi:10.1038/emm.2017.74.

86 Ren T, Zhang H, Wang J, Zhu J, Jin M, Wu Y *et al.* MCU-dependent mitochondrial Ca 2+ inhibits NAD +/SIRT3/SOD2 pathway to promote ROS production and metastasis of HCC cells. *Oncogene* 2017; **36**. doi:10.1038/onc.2017.167.

87 Jeong SM, Hwang S, Seong RH. SIRT4 regulates cancer cell survival and growth after stress. *Biochem Biophys Res Commun* 2016; **470**. doi:10.1016/j.bbrc.2016.01.078.

88 Wood JG, Schwer B, Wickremesinghe PC, Hartnett DA, Burhenn L, Garcia M *et al.* Sirt4 is a mitochondrial regulator of metabolism and lifespan in Drosophila melanogaster. *Proc Natl Acad Sci U S A* 2018; **115**. doi:10.1073/pnas.1720673115.

89 Csibi A, Fendt SM, Li C, Poulogiannis G, Choo AY, Chapski DJ *et al.* Erratum: The mTORC1 pathway stimulates glutamine metabolism and cell proliferation by repressing SIRT4 (A Conserved Dedicated Olfactory Circuit for Detecting Harmful Microbes in Drosophila (2012)

151(6) (1345–1357), (S0092867412013578), (10.1016/j.cell.2012.09.046)). Cell. 2021; **184**. doi:10.1016/j.cell.2021.03.059.

90 Jeong SM, Xiao C, Finley LWS, Lahusen T, Souza AL, Pierce K *et al.* SIRT4 has tumor-suppressive activity and regulates the cellular metabolic response to dna damage by inhibiting mitochondrial glutamine metabolism. *Cancer Cell* 2013; **23**. doi:10.1016/j.ccr.2013.02.024.

91 Zhu Y, Wang G, Li X, Wang T, Weng M, Zhang Y. Knockout of sirt4 decreases chemosensitivity to 5-fu in colorectal cancer cells. *Oncol Lett* 2018; **16**. doi:10.3892/ol.2018.8850.

92 Bringman-Rodenbarger LR, Guo AH, Lyssiotis CA, Lombard DB. Emerging Roles for SIRT5 in Metabolism and Cancer. Antioxid Redox Signal. 2018; **28**. doi:10.1089/ars.2017.7264.

93 Du J, Zhou Y, Su X, Yu JJ, Khan S, Jiang H *et al.* Sirt5 is a NAD-dependent protein lysine demalonylase and desuccinylase. *Science (1979)* 2011; **334**. doi:10.1126/science.1207861.

94 Bhardwaj A, Das S. SIRT6 deacetylates PKM2 to suppress its nuclear localization and oncogenic functions. *Proc Natl Acad Sci U S A* 2016; **113**. doi:10.1073/pnas.1520045113.

95 Sebastián C, Zwaans BMM, Silberman DM, Gymrek M, Goren A, Zhong L *et al.* The histone deacetylase SIRT6 Is a tumor suppressor that controls cancer metabolism. *Cell* 2012; **151**. doi:10.1016/j.cell.2012.10.047.

96 Desantis V, Lamanuzzi A, Vacca A. The role of SIRT6 in tumors. Haematologica. 2018; **103**. doi:10.3324/haematol.2017.182675.

97 Geng CH, Zhang CL, Zhang JY, Gao P, He M, Li YL. Overexpression of Sirt6 is a novel biomarker of malignant human colon carcinoma. *J Cell Biochem* 2018; **119**. doi:10.1002/jcb.26539.

98 Yu J, Qin B, Wu F, Qin S, Nowsheen S, Shan S *et al.* Regulation of Serine-Threonine Kinase Akt Activation by NAD+-Dependent Deacetylase SIRT7. *Cell Rep* 2017; **18**. doi:10.1016/j.celrep.2017.01.009.

99 Blank MF, Grummt I. The seven faces of SIRT7. Transcription. 2017; **8**. doi:10.1080/21541264.2016.1276658.

100 Drevs J, Loser R, Rattel B, Esser N. Antiangiogenic potency of FK866/K22.175, a new inhibitor of intracellular NAD biosynthesis, in murine renal cell carcinoma. *Anticancer Res* 2003; **23**: 4853–4858.

101 Nagashima H, Lee CK, Tateishi K, Higuchi F, Subramanian M, Rafferty S *et al.* Poly(ADP-ribose) Glycohydrolase Inhibition Sequesters NAD(+) to Potentiate the Metabolic Lethality of Alkylating Chemotherapy in IDH-Mutant Tumor Cells. *Cancer Discov* 2020; **10**: 1672–1689.

102 Korotchkina L, Kazyulkin D, Komarov PG, Polinsky A, Andrianova EL, Joshi S *et al.* OT-82, a novel anticancer drug candidate that targets the strong dependence of hematological malignancies on NAD biosynthesis. *Leukemia* 2020; **34**: 1828–1839.

103 Somers K, Evans K, Cheung L, Karsa M, Pritchard T, Kosciolek A *et al.* Effective targeting of NAMPT in patient-derived xenograft models of high-risk pediatric acute lymphoblastic leukemia. *Leukemia* 2020; **34**: 1524–1539.

104 Gibson AE, Yeung C, Issaq SH, Collins VJ, Gouzoulis M, Zhang Y *et al.* Inhibition of nicotinamide phosphoribosyltransferase (NAMPT) with OT-82 induces DNA damage, cell death, and suppression of tumor growth in preclinical models of Ewing sarcoma. *Oncogenesis* 2020; **9**: 80.

105 Nahimana A, Attinger A, Aubry D, Greaney P, Ireson C, Thougaard A v *et al.* The NAD biosynthesis inhibitor APO866 has potent antitumor activity against hematologic malignancies. *Blood* 2009; **113**: 3276–3286.

106 Kozako T, Aikawa A, Ohsugi T, Uchida YI, Kato N, Sato K *et al.* High expression of NAMPT in adult T-cell leukemia/lymphoma and anti-tumor activity of a NAMPT inhibitor. *Eur J Pharmacol* 2019; **865**: 172738.

107 Nahimana A, Aubry D, Breton CS, Majjigapu SR, Sordat B, Vogel P *et al.* The anti-lymphoma activity of APO866, an inhibitor of nicotinamide adenine dinucleotide biosynthesis, is potentialized when used in combination with anti-CD20 antibody. *Leuk Lymphoma* 2014; **55**: 2141–2150.

108 Takao S, Chien W, Madan V, Lin DC, Ding LW, Sun QY *et al.* Targeting the vulnerability to NAD(+) depletion in B-cell acute lymphoblastic leukemia. *Leukemia* 2018; **32**: 616–625.

109 Mitchell SR, Larkin K, Grieselhuber NR, Lai TH, Cannon M, Orwick S *et al.* Selective targeting of NAMPT by KPT-9274 in acute myeloid leukemia. *Blood Adv* 2019; **3**: 242–255.

110 Abril-Rodriguez G, Torrejon DY, Liu W, Zaretsky JM, Nowicki TS, Tsoi J *et al.* Publisher Correction: PAK4 inhibition improves PD-1 blockade immunotherapy. *Nat Cancer* 2020; **1**: 264.

111 Qasim SL, Sierra L, Shuck R, Kurenbekova L, Patel TD, Rajapakshe K *et al.* p21-activated kinases as viable therapeutic targets for the treatment of high-risk Ewing sarcoma. *Oncogene* 2021; **40**: 1176–1190.

112 Ravaud A, Cerny T, Terret C, Wanders J, Bui BN, Hess D *et al.* Phase I study and pharmacokinetic of CHS-828, a guanidino-containing compound, administered orally as a single dose every 3 weeks in solid tumours: an ECSG/EORTC study. *Eur J Cancer* 2005; **41**: 702–707.

113 Olesen UH, Thougaard A v, Jensen PB, Sehested M. A preclinical study on the rescue of normal tissue by nicotinic acid in high-dose treatment with APO866, a specific nicotinamide phosphoribosyltransferase inhibitor. *Mol Cancer Ther* 2010; **9**: 1609–1617.

114 Beauparlant P, Bedard D, Bernier C, Chan H, Gilbert K, Goulet D *et al.* Preclinical development of the nicotinamide phosphoribosyl transferase inhibitor prodrug GMX1777. *Anticancer Drugs* 2009; **20**: 346–354.

115 Misner DL, Kauss MA, Singh J, Uppal H, Bruening-Wright A, Liederer BM *et al.* Cardiotoxicity Associated with Nicotinamide Phosphoribosyltransferase Inhibitors in Rodents and in Rat and Human-Derived Cells Lines. *Cardiovasc Toxicol* 2017; **17**: 307–318.

116 Cassar S, Dunn C, Olson A, Buck W, Fossey S, Ramos MF *et al.* From the Cover: Inhibitors of Nicotinamide Phosphoribosyltransferase Cause Retinal Damage in Larval Zebrafish. *Toxicol Sci* 2018; **161**: 300–309.

117 Swerdlow SH, Campo E, Pileri SA, Harris NL, Stein H, Siebert R *et al.* The 2016 revision of the World Health Organization classification of lymphoid neoplasms. *Blood* 2016; **127**: 2375–2390.

118 Richter MN. Generalized Reticular Cell Sarcoma of Lymph Nodes Associated with Lymphatic Leukemia. *Am J Pathol* 1928; **4**: 285-292 7.

119 Lortholary P, Boiron M, Ripault P, Levy JP, Manus A, Bernard J. [Chronic Lymphoid Leukemia Secondarily Associated with a Malignant Reticulopathy: Richter's Syndrome]. *Nouv Rev Fr Hematol* 1964; **4**: 621–644.

120 Bockorny B, Codreanu I, Dasanu CA. Hodgkin lymphoma as Richter transformation in chronic lymphocytic leukaemia: a retrospective analysis of world literature. *Br J Haematol* 2012; **156**: 50–66.

121 Parikh SA, Kay NE, Shanafelt TD. How we treat Richter syndrome. *Blood* 2014; **123**: 1647–1657.

122 Maddocks-Christianson K, Slager SL, Zent CS, Reinalda M, Call TG, Habermann TM *et al.* Risk factors for development of a second lymphoid malignancy in patients with chronic lymphocytic leukaemia. *Br J Haematol* 2007; **139**: 398–404.

123 Rossi D, Cerri M, Capello D, Deambrogi C, Rossi FM, Zucchetto A *et al.* Biological and clinical risk factors of chronic lymphocytic leukaemia transformation to Richter syndrome. *Br J Haematol* 2008; **142**: 202–215.

124 Jamroziak K, Grzybowska-Izydorczyk O, Jesionek-Kupnicka D, Gora-Tybor J, Robak T. Poor prognosis of Hodgkin variant of Richter transformation in chronic lymphocytic leukemia treated with cladribine. *Br J Haematol* 2012; **158**: 286–288.

125 Mao Z, Quintanilla-Martinez L, Raffeld M, Richter M, Krugmann J, Burek C *et al.* IgVH mutational status and clonality analysis of Richter's transformation: diffuse large B-cell lymphoma and Hodgkin lymphoma in association with B-cell chronic lymphocytic leukemia (B-

CLL) represent 2 different pathways of disease evolution. *Am J Surg Pathol* 2007; **31**: 1605–1614.

126 Rossi D, Spina V, Deambrogi C, Rasi S, Laurenti L, Stamatopoulos K *et al.* The genetics of Richter syndrome reveals disease heterogeneity and predicts survival after transformation. *Blood* 2011; **117**: 3391–3401.

127 Tsimberidou AM, O'Brien S, Khouri I, Giles FJ, Kantarjian HM, Champlin R *et al.* Clinical outcomes and prognostic factors in patients with Richter's syndrome treated with chemotherapy or chemoimmunotherapy with or without stem-cell transplantation. *J Clin Oncol* 2006; **24**: 2343–2351.

128 Gine E, Martinez A, Villamor N, Lopez-Guillermo A, Camos M, Martinez D *et al.* Expanded and highly active proliferation centers identify a histological subtype of chronic lymphocytic leukemia ('accelerated' chronic lymphocytic leukemia) with aggressive clinical behavior. *Haematologica* 2010; **95**: 1526–1533.

129 Soilleux EJ, Wotherspoon A, Eyre TA, Clifford R, Cabes M, Schuh AH. Diagnostic dilemmas of high-grade transformation (Richter's syndrome) of chronic lymphocytic leukaemia: results of the phase II National Cancer Research Institute CHOP-OR clinical trial specialist haemato-pathology central review. *Histopathology* 2016; **69**: 1066–1076.

130 Bruzzi JF, Macapinlac H, Tsimberidou AM, Truong MT, Keating MJ, Marom EM *et al.* Detection of Richter's transformation of chronic lymphocytic leukemia by PET/CT. *J Nucl Med* 2006; **47**: 1267–1273.

131 Tsimberidou AM, O'Brien S, Kantarjian HM, Koller C, Hagemeister FB, Fayad L *et al.* Hodgkin transformation of chronic lymphocytic leukemia: the M. D. Anderson Cancer Center experience. *Cancer* 2006; **107**: 1294–1302.

132 Ohno T, Smir BN, Weisenburger DD, Gascoyne RD, Hinrichs SD, Chan WC. Origin of the Hodgkin/Reed-Sternberg cells in chronic lymphocytic leukemia with 'Hodgkin's transformation'. *Blood* 1998; **91**: 1757–1761.

133 Fayad L, Robertson LE, O'Brien S, Manning JT, Wright S, Hagemeister F *et al.* Hodgkin's disease variant of Richter's syndrome: experience at a single institution. *Leuk Lymphoma* 1996; **23**: 333–337.

134 Rossi D, Gaidano G. Richter syndrome: pathogenesis and management. *Semin Oncol* 2016; **43**: 311–319.

135 Solh M, Rai KR, Peterson BL, Kolitz JE, Appelbaum FR, Tallman MS *et al.* The impact of initial fludarabine therapy on transformation to Richter syndrome or prolymphocytic leukemia in patients with chronic lymphocytic leukemia: analysis of an intergroup trial (CALGB 9011). *Leuk Lymphoma* 2013; **54**: 252–254.

136 Mauro FR, Foa R, Giannarelli D, Cordone I, Crescenzi S, Pescarmona E *et al.* Clinical characteristics and outcome of young chronic lymphocytic leukemia patients: a single institution study of 204 cases. *Blood* 1999; **94**: 448–454.

137 Ding W. Richter transformation in the era of novel agents. *Hematology Am Soc Hematol Educ Program* 2018; **2018**: 256–263.

138 Brown JR, Hillmen P, O'Brien S, Barrientos JC, Reddy NM, Coutre SE *et al.* Extended follow-up and impact of high-risk prognostic factors from the phase 3 RESONATE study in patients with previously treated CLL/SLL. *Leukemia* 2018; **32**: 83–91.

139 Chigrinova E, Rinaldi A, Kwee I, Rossi D, Rancoita PM, Strefford JC *et al.* Two main genetic pathways lead to the transformation of chronic lymphocytic leukemia to Richter syndrome. *Blood* 2013; **122**: 2673–2682.

140 Eyre TA, Schuh A. An update for Richter syndrome - new directions and developments. *Br J Haematol* 2017; **178**: 508–520.

141 Fabbri G, Khiabanian H, Holmes AB, Wang J, Messina M, Mullighan CG *et al.* Genetic lesions associated with chronic lymphocytic leukemia transformation to Richter syndrome. *J Exp Med* 2013; **210**: 2273–2288.

142 te Raa GD, Kater AP. TP53 dysfunction in CLL: Implications for prognosis and treatment. *Best Pract Res Clin Haematol* 2016; **29**: 90–99.

143 Schick M, Habringer S, Nilsson JA, Keller U. Pathogenesis and therapeutic targeting of aberrant MYC expression in haematological cancers. *Br J Haematol* 2017; **179**: 724–738.

144 Rossi D, Berra E, Cerri M, Deambrogi C, Barbieri C, Franceschetti S *et al.* Aberrant somatic hypermutation in transformation of follicular lymphoma and chronic lymphocytic leukemia to diffuse large B-cell lymphoma. *Haematologica* 2006; **91**: 1405–1409.

145 Rossi D, Rasi S, Fabbri G, Spina V, Fangazio M, Forconi F *et al.* Mutations of NOTCH1 are an independent predictor of survival in chronic lymphocytic leukemia. *Blood* 2012; **119**: 521–529.

146 Fabbri G, Rasi S, Rossi D, Trifonov V, Khiabanian H, Ma J *et al.* Analysis of the chronic lymphocytic leukemia coding genome: role of NOTCH1 mutational activation. *J Exp Med* 2011; **208**: 1389–1401.

147 Lobry C, Oh P, Mansour MR, Look AT, Aifantis I. Notch signaling: switching an oncogene to a tumor suppressor. *Blood* 2014; **123**: 2451–2459.

148 del Giudice I, Rossi D, Chiaretti S, Marinelli M, Tavolaro S, Gabrielli S *et al.* NOTCH1 mutations in +12 chronic lymphocytic leukemia (CLL) confer an unfavorable prognosis, induce a distinctive transcriptional profiling and refine the intermediate prognosis of +12 CLL. *Haematologica* 2012; **97**: 437–441.

149 del Giudice I, Rossi D, Chiaretti S, Marinelli M, Tavolaro S, Gabrielli S *et al.* NOTCH1 mutations in +12 chronic lymphocytic leukemia (CLL) confer an unfavorable prognosis, induce a distinctive transcriptional profiling and refine the intermediate prognosis of +12 CLL. *Haematologica* 2012; **97**: 437–441.

150 Chakraborty S, Martines C, Porro F, Fortunati I, Bonato A, Dimishkovska M *et al.* B-cell receptor signaling and genetic lesions in TP53 and CDKN2A/CDKN2B cooperate in Richter transformation. *Blood* 2021; **138**: 1053–1066.

151 Kohlhaas V, Blakemore SJ, Al-Maarri M, Nickel N, Pal M, Roth A *et al.* Active Akt signaling triggers CLL toward Richter transformation via overactivation of Notch1. *Blood* 2021; **137**: 646–660.

152 Rossi D, Spina V, Cerri M, Rasi S, Deambrogi C, de Paoli L *et al.* Stereotyped B-cell receptor is an independent risk factor of chronic lymphocytic leukemia transformation to Richter syndrome. *Clin Cancer Res* 2009; **15**: 4415–4422.

153 Nadeu F, Royo R, Massoni-Badosa R, Playa-Albinyana H, Garcia-Torre B, Duran-Ferrer M *et al.* Detection of early seeding of Richter transformation in chronic lymphocytic leukemia. *Nat Med* 2022; **28**: 1662–1671.

154 Puente XS, Bea S, Valdes-Mas R, Villamor N, Gutierrez-Abril J, Martin-Subero JI *et al.* Non-coding recurrent mutations in chronic lymphocytic leukaemia. *Nature* 2015; **526**: 519–524.

155 Kasar S, Kim J, Improgo R, Tiao G, Polak P, Haradhvala N *et al.* Whole-genome sequencing reveals activation-induced cytidine deaminase signatures during indolent chronic lymphocytic leukaemia evolution. *Nat Commun* 2015; **6**: 8866.

156 Maura F, Degasperi A, Nadeu F, Leongamornlert D, Davies H, Moore L *et al.* A practical guide for mutational signature analysis in hematological malignancies. *Nat Commun* 2019; **10**: 2969.

157 Arthur SE, Jiang A, Grande BM, Alcaide M, Cojocaru R, Rushton CK *et al.* Genome-wide discovery of somatic regulatory variants in diffuse large B-cell lymphoma. *Nat Commun* 2018; **9**: 4001.

158 Alexandrov LB, Kim J, Haradhvala NJ, Huang MN, Tian Ng AW, Wu Y *et al.* The repertoire of mutational signatures in human cancer. *Nature* 2020; **578**: 94–101.

159 Kucab JE, Zou X, Morganella S, Joel M, Nanda AS, Nagy E *et al.* A Compendium of Mutational Signatures of Environmental Agents. *Cell* 2019; **177**: 821-836 e16.

160 Kwok M, Wu CJ. Clonal Evolution of High-Risk Chronic Lymphocytic Leukemia: A Contemporary Perspective. *Front Oncol* 2021; **11**: 790004.

161 Parikh SA, Shanafelt TD. Risk factors for Richter syndrome in chronic lymphocytic leukemia. *Curr Hematol Malig Rep* 2014; **9**: 294–299.

162 Tzankov A, Fong D. Hodgkin's disease variant of Richter's syndrome clonally related to chronic lymphocytic leukemia arises in ZAP-70 negative mutated CLL. *Med Hypotheses* 2006; **66**: 577–579.

163 Aydin S, Rossi D, Bergui L, D'Arena G, Ferrero E, Bonello L *et al.* CD38 gene polymorphism and chronic lymphocytic leukemia: a role in transformation to Richter syndrome? *Blood* 2008; **111**: 5646–5653.

164 Timar B, Fulop Z, Csernus B, Angster C, Bognar A, Szepesi A *et al.* Relationship between the mutational status of VH genes and pathogenesis of diffuse large B-cell lymphoma in Richter's syndrome. *Leukemia* 2004; **18**: 326–330.

165 Parikh SA, Rabe KG, Call TG, Zent CS, Habermann TM, Ding W *et al.* Diffuse large B-cell lymphoma (Richter syndrome) in patients with chronic lymphocytic leukaemia (CLL): a cohort study of newly diagnosed patients. *Br J Haematol* 2013; **162**: 774–782.

166 Catovsky D, Richards S, Matutes E, Oscier D, Dyer M, Bezares RF *et al.* Assessment of fludarabine plus cyclophosphamide for patients with chronic lymphocytic leukaemia (the LRF CLL4 Trial): a randomised controlled trial. *Lancet* 2007; **370**: 230–239.

167 Condoluci A, Rossi D. Treatment of Richter's Syndrome. *Curr Treat Options Oncol* 2017; **18**: 75.

168 Tsimberidou AM, O'Brien S, Khouri I, Giles FJ, Kantarjian HM, Champlin R *et al.* Clinical outcomes and prognostic factors in patients with Richter's syndrome treated with chemotherapy or chemoimmunotherapy with or without stem-cell transplantation. *J Clin Oncol* 2006; **24**: 2343–2351.

169 Dabaja BS, O'Brien SM, Kantarjian HM, Cortes JE, Thomas DA, Albitar M *et al.* Fractionated cyclophosphamide, vincristine, liposomal daunorubicin (daunoXome), and dexamethasone (hyperCVXD) regimen in Richter's syndrome. *Leuk Lymphoma* 2001; **42**: 329–337.

170 Tsimberidou AM, Kantarjian HM, Cortes J, Thomas DA, Faderl S, Garcia-Manero G *et al.* Fractionated cyclophosphamide, vincristine, liposomal daunorubicin, and dexamethasone plus rituximab and granulocyte-macrophage-colony stimulating factor (GM-CSF) alternating with methotrexate and cytarabine plus rituximab and GM-CSF in patients with Richter syndrome or fludarabine-refractory chronic lymphocytic leukemia. *Cancer* 2003; **97**: 1711–1720.

171 Langerbeins P, Busch R, Anheier N, Durig J, Bergmann M, Goebeler ME *et al.* Poor efficacy and tolerability of R-CHOP in relapsed/refractory chronic lymphocytic leukemia and Richter transformation. *Am J Hematol* 2014; **89**: E239-43.

172 Tsimberidou AM, Wierda WG, Plunkett W, Kurzrock R, O'Brien S, Wen S *et al.* Phase I-II study of oxaliplatin, fludarabine, cytarabine, and rituximab combination therapy in patients with Richter's syndrome or fludarabine-refractory chronic lymphocytic leukemia. *J Clin Oncol* 2008; **26**: 196–203.

173 Tsimberidou AM, Wierda WG, Wen S, Plunkett W, O'Brien S, Kipps TJ *et al.* Phase I-II clinical trial of oxaliplatin, fludarabine, cytarabine, and rituximab therapy in aggressive relapsed/refractory chronic lymphocytic leukemia or Richter syndrome. *Clin Lymphoma Myeloma Leuk* 2013; **13**: 568–574.

174 Jenke P Busch R et al. EB. Cyclophosphamide, adriamycin, vincristine and predni sone plus rituximab (CHOP-R) in fludarabine (F) refractory chronic lymphocytic leukemia (CLL) or CLL with autoimmune cytopenia (AIC) or Richter's transformation (RT): final analysis of a phase II study of the German CLL study group. *Blood (ASH Annual Meeting Abstracts)* 2011; **2011;118:2860**.

175 Al-Sawaf O, Robrecht S, Bahlo J, Fink AM, Cramer P, Tresckow VJ *et al.* Richter transformation in chronic lymphocytic leukemia (CLL)-a pooled analysis of German CLL Study Group (GCLLSG) front line treatment trials. *Leukemia* 2021; **35**: 169–176.

176 Kim HT, Baker PO, Parry E, Davids M, Alyea EP, Ho VT *et al.* Allogeneic hematopoietic cell transplantation outcomes in patients with Richter's transformation. *Haematologica* 2021; **106**: 3219–3222.

177 Lahoud OB, Devlin SM, Maloy MA, Roeker LE, Dahi PB, Ponce DM *et al.* Reduced-intensity conditioning hematopoietic stem cell transplantation for chronic lymphocytic leukemia and Richter's transformation. *Blood Adv* 2021; **5**: 2879–2889.

178 Sochacka-Cwikla A, Maczynski M, Regiec A. FDA-Approved Drugs for Hematological Malignancies-The Last Decade Review. *Cancers (Basel)* 2021; **14**. doi:10.3390/cancers14010087.

179 Giri S, Hahn A, Yaghmour G, Martin MG. Ibrutinib has some activity in Richter's syndrome. *Blood Cancer J* 2015; **5**: e277.

180 Master S, Leary C, Takalkar A, Coltelingam J, Mansour R, Mills GM *et al.* Successful Treatment of Richter Transformation with Ibrutinib in a Patient with Chronic Lymphocytic Leukemia following Allogeneic Hematopoietic Stem Cell Transplant. *Case Rep Oncol* 2017; **10**: 534–541.

181 Eyre TA, Schuh A, Wierda WG, Brown JR, Ghia P, Pagel JM *et al.* Acalabrutinib monotherapy for treatment of chronic lymphocytic leukaemia (ACE-CL-001): analysis of the Richter transformation cohort of an open-label, single-arm, phase 1-2 study. *Lancet Haematol* 2021; **8**: e912–e921.

182 Woyach J Flinn IW Bhat SA Savage RE Chai F Eathiraj S Granlund L Szuszkiewicz LA Schwartz B Byrd JC. SDM. Final results of phase 1, dose escalation study evaluating ARQ 531 in patients with relapsed or refractory B-cell lymphoid malignancies. *Blood* 2019; **Blood 2019;134.**

183 Visentin A, Imbergamo S, Scomazzon E, Pravato S, Frezzato F, Bonaldi L *et al.* BCR kinase inhibitors, idelalisib and ibrutinib, are active and effective in Richter syndrome. *Br J Haematol* 2019; **185**: 193–197.

184 Scheffold A, Stilgenbauer S. Revolution of Chronic Lymphocytic Leukemia Therapy: the Chemo-Free Treatment Paradigm. *Curr Oncol Rep* 2020; **22**: 16.

185 Stamatopoulos B, Antoniou P, Vavoulis D, Eyre TA, Clifford R, Cabes M *et al.* Characterization of Recurrent Mutations in Patient with a Richter Syndrome By Targeted Next Generation Sequencing. *Blood* 2016; **128**. doi:10.1182/blood.v128.22.3200.3200.

186 Nilsson S, Stein A, Rolfo C, Kranich AL, Mann J, Papadimitriou K *et al.* Selinexor (KPT-330), an Oral Selective Inhibitor of Nuclear Export (SINE) Compound, in Combination with FOLFOX in Patients with Metastatic Colorectal Cancer (mCRC) - Final Results of the Phase I Trial SENTINEL. *Curr Cancer Drug Targets* 2020; **20**: 811–817.

187 Holstein SA, Lunning MA. CAR T-Cell Therapy in Hematologic Malignancies: A Voyage in Progress. Clin Pharmacol Ther. 2020; **107**. doi:10.1002/cpt.1674.

188 Gauthier J, Hirayama A v., Purushe J, Hay KA, Lymp J, Li DH *et al.* Feasibility and efficacy of CD19-targeted CAR T cells with concurrent ibrutinib for CLL after ibrutinib failure. In: *Blood*. 2020 doi:10.1182/BLOOD.2019002936.

189 Benjamini O, Rokach L, Itchaki G, Braester A, Shvidel L, Goldschmidt N *et al.* Safety and efficacy of the BNT162b mRNA COVID-19 vaccine in patients with chronic lymphocytic leukemia. *Haematologica* 2022; **107**. doi:10.3324/haematol.2021.279196.

190 Jaglowski SM, Jones JA, Nagar V, Flynn JM, Andritsos LA, Maddocks KJ *et al.* Safety and activity of BTK inhibitor ibrutinib combined with ofatumumab in chronic lymphocytic leukemia: A phase 1b/2 study. *Blood* 2015; **126**. doi:10.1182/blood-2014-12-617522.

191 Lamar Z, Kennedy L, Kennedy B, Lynch M, Goad A, Hurd D *et al.* Ibrutinib and rituximab induced rapid response in refractory Richter syndrome. *Clin Case Rep* 2015; **3**: 615–617.

192 Younes A, Brody J, Carpio C, Lopez-Guillermo A, Ben-Yehuda D, Ferhanoglu B *et al.* Safety and activity of ibrutinib in combination with nivolumab in patients with relapsed non-Hodgkin lymphoma or chronic lymphocytic leukaemia: a phase 1/2a study. *Lancet Haematol* 2019; **6**: e67–e78.

193 Appleby N, Eyre TA, Cabes M, Jackson A, Boucher R, Yates F *et al.* The STELLAR trial protocol: a prospective multicentre trial for Richter's syndrome consisting of a randomised trial

investigation CHOP-R with or without acalabrutinib for newly diagnosed RS and a single-arm platform study for evaluation of novel agents in relapsed disease. *BMC Cancer* 2019; **19**: 471.

194 Stilgenbauer S, Eichhorst B, Schetelig J, Hillmen P, Seymour JF, Coutre S *et al.* Venetoclax for Patients With Chronic Lymphocytic Leukemia With 17p Deletion: Results From the Full Population of a Phase II Pivotal Trial. *J Clin Oncol* 2018; **36**: 1973–1980.

195 Davids MS, Rogers KA, Tyekucheva S, Wang Z, Pazienza S, Renner SK *et al.* Venetoclax plus dose-adjusted R-EPOCH for Richter syndrome. *Blood* 2022; **139**: 686–689.

196 Iannello A, Deaglio S, Vaisitti T. Novel Approaches for the Treatment of Patients with Richter's Syndrome. *Curr Treat Options Oncol* 2022; **23**: 526–542.

197 Vaisitti T, Braggio E, Allan JN, Arruga F, Serra S, Zamo A *et al.* Novel Richter Syndrome Xenograft Models to Study Genetic Architecture, Biology, and Therapy Responses. *Cancer Res* 2018; **78**: 3413–3420.

198 Al-Shawi R, Ashton S v, Underwood C, Simons JP. Expression of the Ror1 and Ror2 receptor tyrosine kinase genes during mouse development. *Dev Genes Evol* 2001; **211**: 161–171.

199 Dave H, Anver MR, Butcher DO, Brown P, Khan J, Wayne AS *et al.* Restricted cell surface expression of receptor tyrosine kinase ROR1 in pediatric B-lineage acute lymphoblastic leukemia suggests targetability with therapeutic monoclonal antibodies. *PLoS One* 2012; **7**: e52655.

200 Fukuda T, Chen L, Endo T, Tang L, Lu D, Castro JE *et al.* Antisera induced by infusions of autologous Ad-CD154-leukemia B cells identify ROR1 as an oncofetal antigen and receptor for Wnt5a. *Proc Natl Acad Sci U S A* 2008; **105**: 3047–3052.

201 Daneshmanesh AH, Porwit A, Hojjat-Farsangi M, Jeddi-Tehrani M, Tamm KP, Grander D *et al.* Orphan receptor tyrosine kinases ROR1 and ROR2 in hematological malignancies. *Leuk Lymphoma* 2013; **54**: 843–850.

202 Zhang S, Chen L, Wang-Rodriguez J, Zhang L, Cui B, Frankel W *et al.* The onco-embryonic antigen ROR1 is expressed by a variety of human cancers. *Am J Pathol* 2012; **181**: 1903–1910.

203 Vaisitti T, Arruga F, Vitale N, Lee TT, Ko M, Chadburn A *et al.* ROR1 targeting with the antibody-drug conjugate VLS-101 is effective in Richter syndrome patient-derived xenograft mouse models. *Blood* 2021; **137**: 3365–3377.

204 Vaisitti T, Vitale N, Micillo M, Brandimarte L, Iannello A, Papotti MG *et al.* Anti-CD37 alpha-amanitin conjugated antibodies as potential therapeutic weapons for Richter's Syndrome. *Blood* 2022. doi:10.1182/blood.2022016211.

205 Barrena S, Almeida J, Yunta M, Lopez A, Fernandez-Mosteirin N, Giralt M *et al.* Aberrant expression of tetraspanin molecules in B-cell chronic lymphoproliferative disorders and its correlation with normal B-cell maturation. *Leukemia* 2005; **19**: 1376–1383.

206 Beckwith KA, Byrd JC, Muthusamy N. Tetraspanins as therapeutic targets in hematological malignancy: a concise review. *Front Physiol* 2015; **6**: 91.

207 Xu-Monette ZY, Li L, Byrd JC, Jabbar KJ, Manyam GC, Maria de Winde C *et al.* Assessment of CD37 B-cell antigen and cell of origin significantly improves risk prediction in diffuse large B-cell lymphoma. *Blood* 2016; **128**: 3083–3100.

208 Iannello A, Vitale N, Coma S, Arruga F, Chadburn A, di Napoli A *et al.* Synergistic efficacy of the dual PI3K-delta/gamma inhibitor duvelisib with the Bcl-2 inhibitor venetoclax in Richter syndrome PDX models. *Blood* 2021; **137**: 3378–3389.

209 Cha Y, Kim T, Jeon J, Jang Y, Kim PB, Lopes C *et al.* SIRT2 regulates mitochondrial dynamics and reprogramming via MEK1-ERK-DRP1 and AKT1-DRP1 axes. *Cell Rep* 2021; **37**. doi:10.1016/j.celrep.2021.110155.

210 Pillai VB, Sundaresan NR, Gupta MP. Regulation of Akt signaling by sirtuins its implication in cardiac hypertrophy and aging. Circ Res. 2014; **114**. doi:10.1161/CIRCRESAHA.113.300536.

211 Ramakrishnan G, Davaakhuu G, Kaplun L, Chung WC, Rana A, Atfi A *et al.* Sirt2 deacetylase is a novel AKT Binding partner critical for AKT activation by insulin. *Journal of Biological Chemistry* 2014; **289**. doi:10.1074/jbc.M113.537266.

212 Qian B, Yang Y, Tang N, Wang J, Sun P, Yang N *et al.* M1 macrophage-derived exosomes impair beta cell insulin secretion via miR-212-5p by targeting SIRT2 and inhibiting Akt/GSK-3β/β-catenin pathway in mice. *Diabetologia* 2021; **64**. doi:10.1007/s00125-021-05489-1.

213 Sundaresan NR, Pillai VB, Wolfgeher D, Samant S, Vasudevan P, Parekh V *et al.* The deacetylase SIRT1 promotes membrane localization and activation of Akt and PDK1 during tumorigenesis and cardiac hypertrophy. *Sci Signal* 2011; **4**. doi:10.1126/scisignal.2001465.

214 Terakata M, Fukuwatari T, Kadota E, Sano M, Kanai M, Nakamura T *et al.* The niacin required for optimum growth can be synthesized from l-tryptophan in growing mice lacking tryptophan-2,3-dioxygenase. *Journal of Nutrition* 2013; **143**. doi:10.3945/jn.113.176875.

215 Tempel W, Rabeh WM, Bogan KL, Belenky P, Wojcik M, Seidle HF *et al.* Nicotinamide riboside kinase structures reveal new pathways to NAD +. *PLoS Biol* 2007; **5**. doi:10.1371/journal.pbio.0050263.

216 Ruggieri S, Orsomando G, Sorci L, Raffaelli N. Regulation of NAD biosynthetic enzymes modulates NAD-sensing processes to shape mammalian cell physiology under varying biological cues. Biochim Biophys Acta Proteins Proteom. 2015; **1854**. doi:10.1016/j.bbapap.2015.02.021.

217 Chen X, Sun K, Jiao S, Cai N, Zhao X, Zou H *et al.* High levels of SIRT1 expression enhance tumorigenesis and associate with a poor prognosis of colorectal carcinoma patients. *Sci Rep* 2014; **4**. doi:10.1038/srep07481.

218 Alhazzazi TY, Kamarajan P, Verdin E, Kapila YL. Sirtuin-3 (SIRT3) and the Hallmarks of Cancer. *Genes Cancer* 2013; **4**. doi:10.1177/1947601913486351.

219 Bai Y, Yang J, Cui Y, Yao Y, Wu F, Liu C *et al.* Research Progress of Sirtuin4 in Cancer. Front Oncol. 2021; **10**. doi:10.3389/fonc.2020.562950.

220 Tang M, Tang H, Tu B, Zhu WG. SIRT7: A sentinel of genome stability. Open Biol. 2021; **11**. doi:10.1098/rsob.210047.

221 Li L, Osdal T, Ho Y, Chun S, McDonald T, Agarwal P *et al.* SIRT1 activation by a c-MYC oncogenic network promotes the maintenance and drug resistance of human FLT3-ITD acute myeloid leukemia stem cells. *Cell Stem Cell* 2014; **15**. doi:10.1016/j.stem.2014.08.001.

222 Kan Y, Ge P, Wang X, Xiao G, Zhao H. SIRT1 rs3758391 polymorphism and risk of diffuse large B cell lymphoma in a Chinese population. *Cancer Cell Int* 2018; **18**. doi:10.1186/s12935-018-0659-z.

223 Cea M, Soncini D, Fruscione F, Raffaghello L, Garuti A, Emionite L *et al.* Synergistic interactions between HDAC and sirtuin inhibitors in human leukemia cells. *PLoS One* 2011; **6**. doi:10.1371/journal.pone.0022739.

224 Heltweg B, Gatbonton T, Schuler AD, Posakony J, Li H, Goehle S *et al.* Antitumor activity of a small-molecule inhibitor of human silent information regulator 2 enzymes. *Cancer Res* 2006; **66**. doi:10.1158/0008-5472.CAN-05-3617.

225 Wang D, Hu Z, Hao J, He B, Gan Q, Zhong X *et al.* SIRT1 inhibits apoptosis of degenerative human disc nucleus pulposus cells through activation of Akt pathway. *Age (Omaha)* 2013; **35**. doi:10.1007/s11357-012-9474-y.

226 Ota H, Tokunaga E, Chang K, Hikasa M, Iijima K, Eto M *et al.* Sirt1 inhibitor, Sirtinol, induces senescence-like growth arrest with attenuated Ras-MAPK signaling in human cancer cells. *Oncogene* 2006; **25**. doi:10.1038/sj.onc.1209049.

227 Kojima K, Ohhashi R, Fujita Y, Hamada N, Akao Y, Nozawa Y *et al.* A role for SIRT1 in cell growth and chemoresistance in prostate cancer PC3 and DU145 cells. *Biochem Biophys Res Commun* 2008; **373**. doi:10.1016/j.bbrc.2008.06.045.

228 Curry AM, Cohen I, Zheng S, Wohlfahrt J, White DS, Donu D *et al.* Profiling sirtuin activity using Copper-free click chemistry. *Bioorg Chem* 2021; **117**. doi:10.1016/j.bioorg.2021.105413.

229 Curry AM, White DS, Donu D, Cen Y. Human Sirtuin Regulators: The “Success” Stories. Front Physiol. 2021; **12**. doi:10.3389/fphys.2021.752117.

230 Li XH, Chen C, Tu Y, Sun HT, Zhao ML, Cheng SX *et al.* Sirt1 promotes axonogenesis by deacetylation of akt and inactivation of GSK3. Mol Neurobiol. 2013; **48**. doi:10.1007/s12035-013-8437-3.

231 Dan L, Klimenkova O, Klimiankou M, Klusman JH, van den Heuvel-Eibrink MM, Reinhardt D *et al.* The role of sirtuin 2 activation by nicotinamide phosphoribosyltransferase in the aberrant proliferation and survival of myeloid leukemia cells. *Haematologica* 2012; **97**. doi:10.3324/haematol.2011.055236.

232 Peng J, Li Q, Li K, Zhu L, Lin X, Lin X *et al.* Quercetin Improves Glucose and Lipid Metabolism of Diabetic Rats: Involvement of Akt Signaling and SIRT1. *J Diabetes Res* 2017; **2017**. doi:10.1155/2017/3417306.

233 Kohn AD, Takeuchi F, Roth RA. Akt, a pleckstrin homology domain containing kinase, is activated primarily by phosphorylation. *Journal of Biological Chemistry* 1996; **271**. doi:10.1074/jbc.271.36.21920.

234 Rebecchi MJ, Scarlata S. Pleckstrin homology domains: A common fold with diverse functions. Annu Rev Biophys Biomol Struct. 1998; **27**. doi:10.1146/annurev.biophys.27.1.503.

Figures

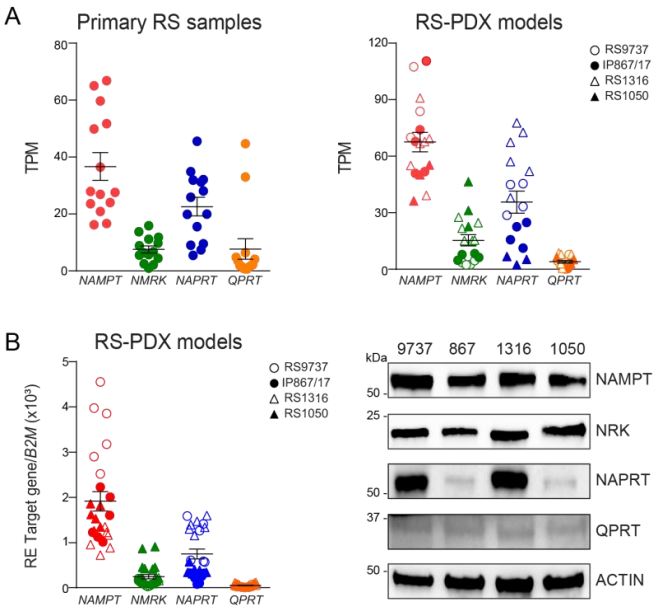

Figure 1. Expression of NAD$^+$ Biosynthetic Enzymes (NBEs) in Richter Syndrome.
(A) NBEs expression obtained from RNA-sequencing data (RNA Seq) in a cohort of 14 primary samples and 4 RS-PDX models (RS9737, IP867/17, RS1316 and RS1050) taken at different passages. The data show the expression of NAMPT (red), NMRK (green), NAPRT (blue) and QPRT (orange) as a scattered plot with mean ± SEM. (B) qRT-PCR analysis and Western blot panels showing NAD$^+$ machinery expression in the available RS-PDX models (RS9737, IP867/17, RS1316, RS1050). The expression of messenger RNA is normalized to β-2-microglobulin (B2M). Actin was used as a loading control in western blot.

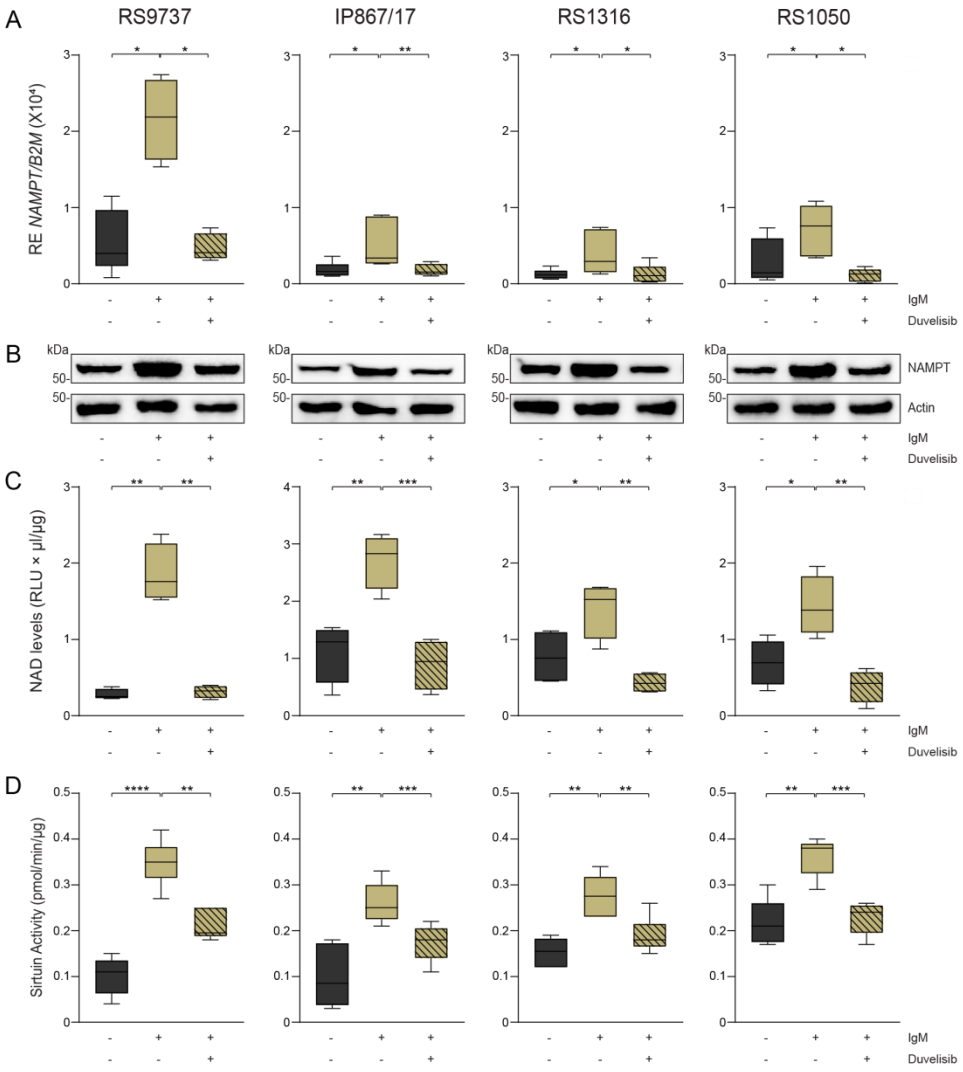

Figure 2. BCR engagement induces an increase expression and activity of NAMPT modulating NAD^+ levels and sirtuins activity in RS cells.

RS cells, freshly purified from tumor masses, were stimulated with a polyclonal anti-IgM for 24 hours in presence or not of Duvelisib, as indicated by the legend. (A) qRT-PCR analysis showing expression of NAMPT in RS cells. Messenger RNA expression is normalized over β-2-microglobulin (B2M). (B)Western blots data showing the expression of NAMPT. Actin was used as a loading control in western blot. (C) Box plots representing NAD^+ luminescence. NAD^+ levels was normalized on protein levels (RLU x µl/µg; $x10^4$). (D) Sirtuin activity analysis in RS cells. The specific activity of sirtuins was calculated by performing B/ T*S (pmol/min/ µg) and was normalized on protein levels. Statistical analysis was performed using a multiple Student t test; *P <0,05, **P <0,01 ***P<0,001****P<0,0001.

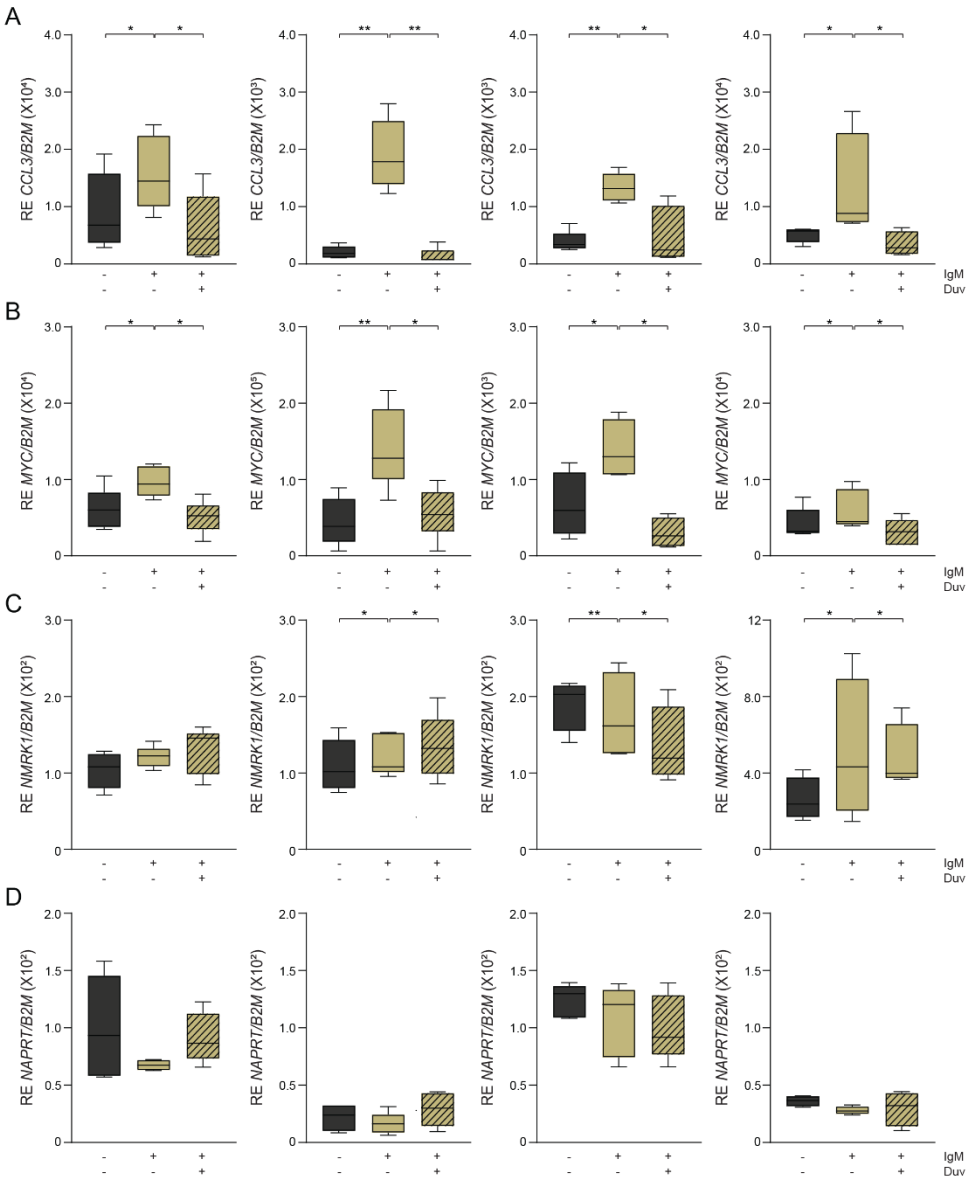

Figure 3. BCR activation in RS cells do not modulate the other NAD⁺ biosynthetic enzymes.
RS cells, freshly purified from tumor masses, were stimulated with a polyclonal anti-IgM for 24 hours in presence or not of Duvelisib, as indicated by the legend. (A-D) qRT-PCR analysis showing expression of CCL3, MYC, NMRK1 and NAPRT in RS cells. Messenger RNA expression is normalized over β-2-microglobulin (B2M). Statistical analysis was performed using a multiple Student t test; *P <0,05, **P <0,01 ***P<0,001****P<0,0001.

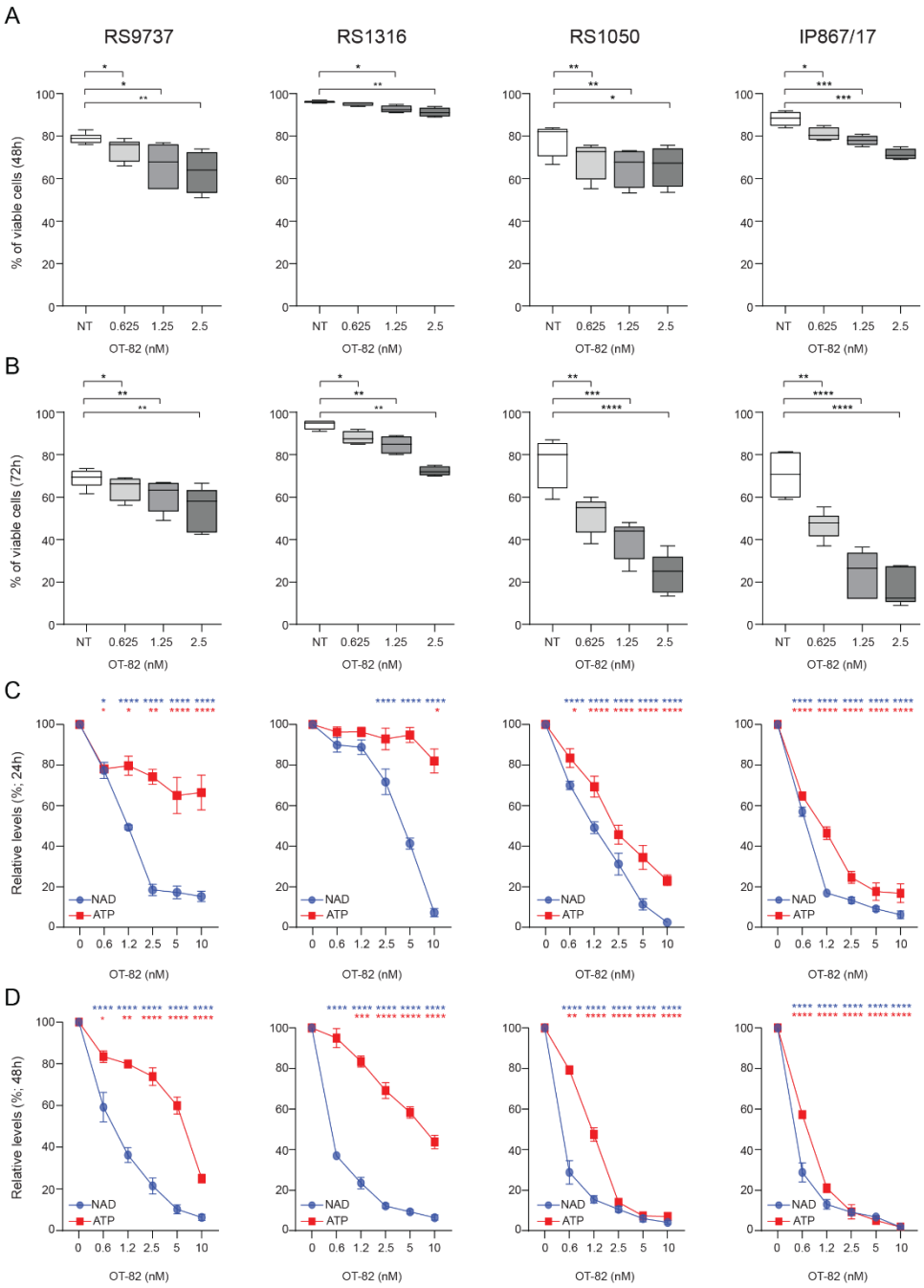

Figure 4. OT-82 decrease cell viability and NAD⁺ levels in RS cells dose-escalation manner.
(A-B) Analyses of the percentage of apoptotic cells, obtained by flow cytometry, after ex vivo incubation of RS cells for 48 and 72 hours with vehicle (black), OT-82 (0.625nM, 1.25nM, 2.5nM). Box plots of apoptotic data show the distribution of values: median, interquartile range, minimum and maximum values. (C-D) Box plots representing NAD^+ luminescence at 24 and 48 hours. NAD^+ levels was normalized on protein levels (RLU x µl/µg; $x10^4$). Statistical analysis was performed using paired Student t test; *P <0,05, **P <0,01 ***P<0,001****P<0,0001.

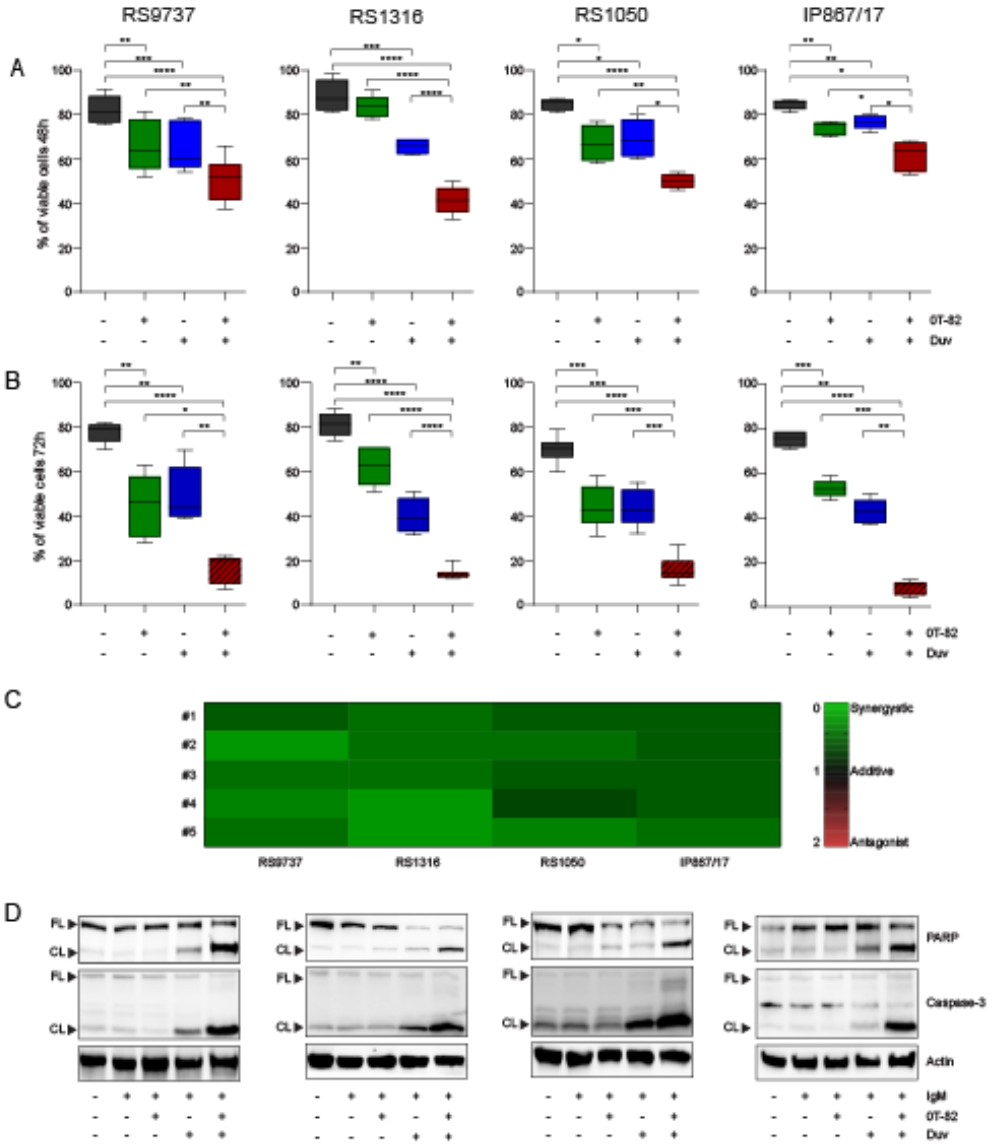

Figure 5. Induction of apoptosis in RS cells ex vivo treated with OT-82, Duvelisib and their combination.
(A-B) Analyses of the percentage of apoptotic cells, obtained by flow cytometry, after ex vivo incubation of RS cells for 48 and 72 hours with vehicle (black), OT-82 (2.5nM for RS9737 and RS136; 0.625nM for RS1050 and IP867/17) (green), Duvelisib (blue), and their combination (red). Box plots of apoptotic data show the distribution of values: median, interquartile range, minimum and maximum values. (C) CI analysis. CI was calculated using the Bliss Independence model to compute the effect of OT-82 and Duvelisib combination. Synergistic effect is defined as CI less than 1 (green), while additive effect is CI around 1 (black) and antagonist effect is CI more than 1 (red). (D) Expression levels of cleaved (Cl.) and total Caspase-3 and PARP1 in RS cells after treatment with OT-82, Duvelisib, and their combination. Data from at least 3 independent experiments. Statistical analysis was performed using paired Student t test; *P <0,05, **P <0,01 ***P<0,001****P<0,0001.

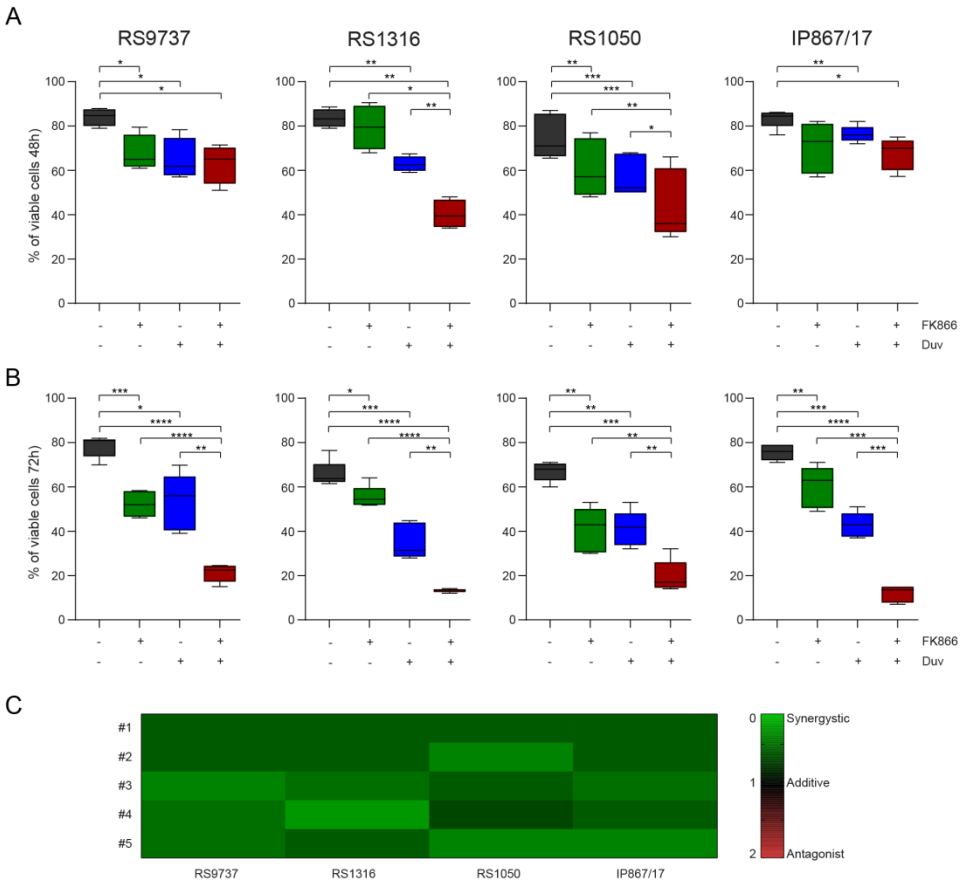

Figure 6. Induction of apoptosis in RS cells ex vivo treated with FK866, Duvelisib and their combination.
(A-B) Analyses of the percentage of apoptotic cells, obtained by flow cytometry, after ex vivo incubation of RS cells for 48 and 72 hours with vehicle (black), FK688 (25nM for RS9737 and RS136; 6.25nM for RS1050 and IP867/17) (green), Duvelisib (blue), and their combination (red). Box plots of apoptotic data show the distribution of values: median, interquartile range, minimum and maximum values. (C) CI analysis. CI was calculated using the Bliss Independence model to compute the effect of FK866 and Duvelisib combination. Synergistic effect is defined as CI less than 1 (green), while additive effect is CI around 1 (black) and antagonist effect is CI more than 1 (red). (D) Expression levels of cleaved (Cl.) and total Caspase-3 and PARP1 in RS cells after treatment with FK866, Duvelisib, and their combination. Data from at least 3 independent experiments. Statistical analysis was performed using paired Student t test; *P <0,05, **P <0,01 ***P<0,001****P<0,0001.

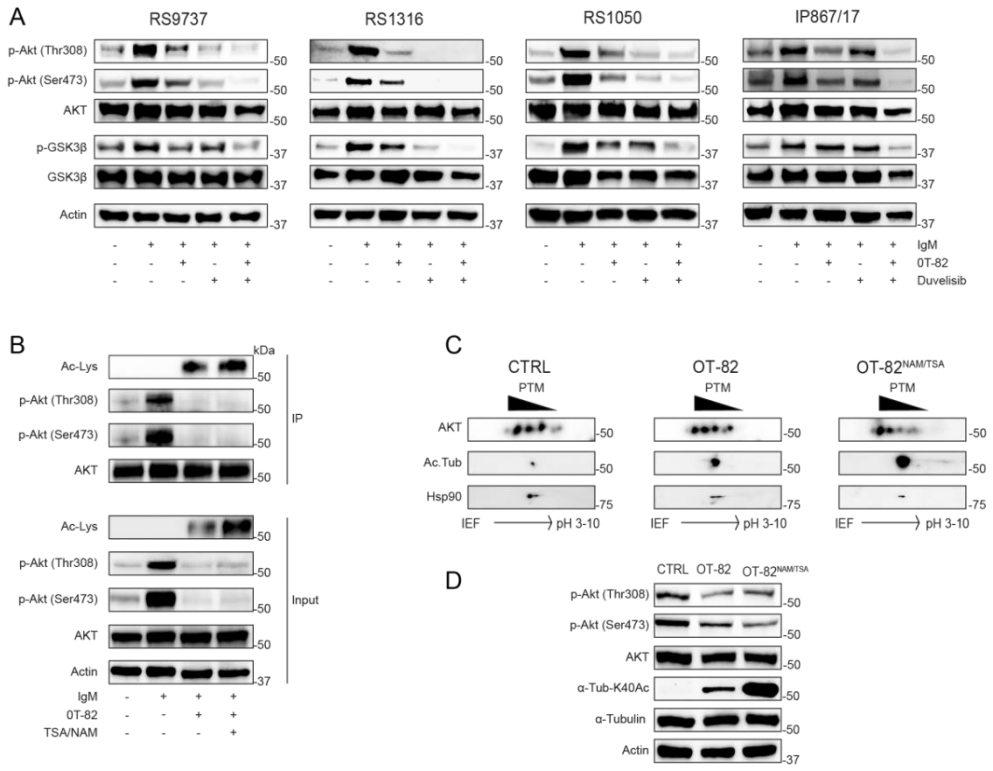

Figure 7. Synergism between PI3Ki and NAMPTi converges in downmodulating AKT signaling.
(A) Expression levels and activation status of AKT and GSK3β in RS cells after ex-vivo stimulation with at polyclonal anti-IgM for 5 minutes and pre-treatments for 24 hour with OT-82, Duvelisib, their combination, or dimethyl sulfoxide (DMSO). (B) Anti-AKT immunoprecipitation followed by immunoblotting for Anti-Acetylated lysine, p-AKT(Thr308) or p-Akt (Ser473), AKT, in RS cells after ex-vivo stimulation with polyclonal anti-IgM for 24 hours and treated with OT-82(0.625 or 2.5 nM), TSA (40μM) and NAM (200 mM) and their combination, or DMSO. Actin was used as a loading control in input samples. (C-D) IEF/SDS-PAGE 2D electrophoresis and its 2D blot followed by immunoblotting p-AKT(Thr308) or p-Akt (Ser473), AKT, Acetyl-α-Tubulin. HSP90 and Actin was used as a loading control in IEF/SDS-PAGE 2D and western blot, respectively.

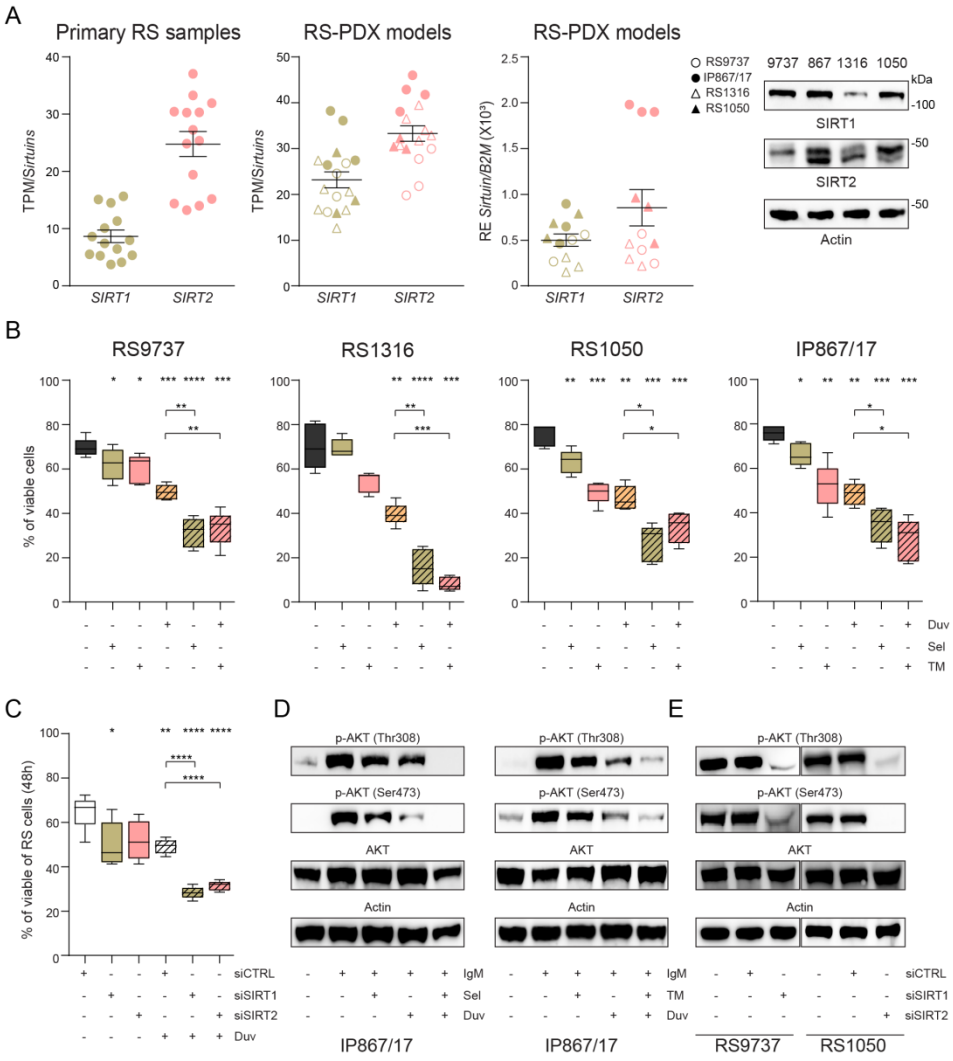

Figure 8. Effect of SIRT1/2 modulation in RS-PDX models.
(A)Expression of SIRT1 and SIRT2 obtain from RNA-sequencing (RNA Seq) data in a cohort of 14 primary samples and 4 RS-PDX models (RS9737, IP867/17, RS1316, and RS1050) take at different passages. Data report the expression of SIRT1 (gold), and SIRT2 (pink) as scattered plot with mean ± SEM. qRT-PCR analysis showing expression of SIRT1 (gold) and SIRT2 (pink) in RS cells. Messenger RNA expression is normalized over β-2-microglobulin (B2M). Western blot panels showing expression of SIRT1 and SIRT2 in the available RS-PDX models (RS9737, IP867/17, RS1316, RS1050). Actin was used as a loading control. (B) Percentage of viable RS cells after 72 hours of treatment with vehicle (black), Selisistat (gold), TM (pink), Duvelisib (orange) and their combination (fill pattern gold and pink). Box plots of apoptotic data show the distribution of values: median, interquartile range, minimum and maximum values. (C) Percentage of viable RS cells after nucleofection with short interfering RNA for SIRT1 (gold), SIRT2 (pink), or control (white) and then treated with Duvelisib (fill pattern) for 48 hours. Box plots of apoptotic data show the distribution of values: median, interquartile range, minimum and maximum values. (D) Expression levels and activation status of AKT in RS cells after ex-vivo stimulation with at polyclonal anti-IgM for 5 minutes and pre-treatments for 24 hour with Selisistat, TM, Duvelisib, their combination, or dimethyl sulfoxide (DMSO). (E) Expression levels and activation status of AKT in RS cells after nucleofection with short interfering RNA for SIRT1 (gold), SIRT2 (pink), or control (white). Actin was used as a loading control. Data from at least 3 independent experiments. Actin was used as a loading control. Statistical analysis was performed using paired Student t test; *P <0,05, **P <0,01 ***P<0,001****P<0,0001.

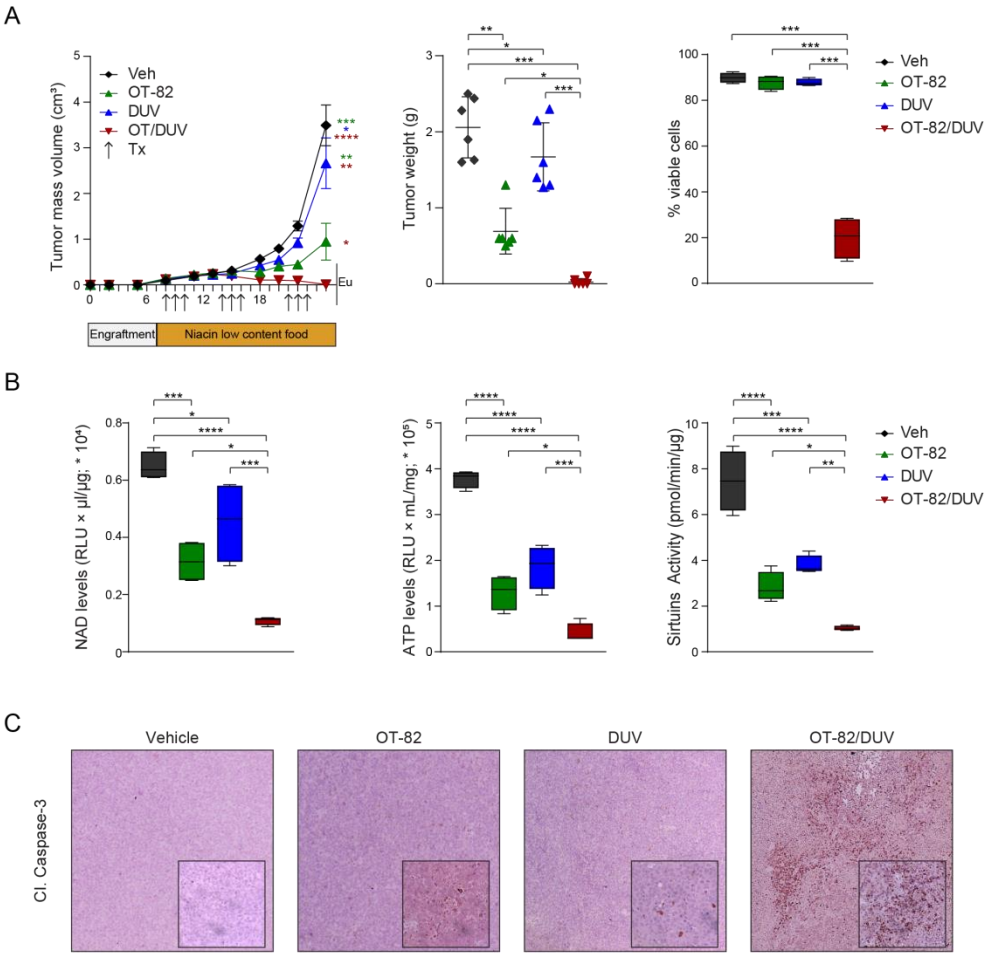

Figure 9. Tumor growth kinetics of RS9737 SC models treated with OT-82, Duvelisib, and their combination.
(A) RS cells were subcutaneously injected into both flanks of NSG mice. After palpable tumors were evident (tumor volume of 0.2 cm3), animals were randomly assigned to vehicle, OT-82 40 mg/kg, Duvelisib 100 mg/kg, or their combination. 2 days before starting the treatment we substituted the regular mice diet, with a custom diet lower of Niacin. Drugs were OG administered for three consecutive days as indicated by arrows (Tx), leaving a 4 day-washout period between treatment cycles. Tumor masses were measured using a digital caliper. Left panels display mean and standard error of the mean values for tumor masses with data evaluated using the multiple-sample Paired t tests. Center panels display individual mean and standard deviation values for tumor masses at the end of treatment on days 25 with data evaluated using Paired t tests. Right panels display the percentage of viable RS cells at the end of treatment with vehicle (black), OT-82 (green), Duvelisib (blue), and their combination (red). Data are reported as mean 6 SEM. (B) NAD^+ levels, ATP levels and Sirtuin activity of RS cells at the end of treatment. NAD^+ levels was normalized on protein levels (RLU x µl/µg; $x10^4$). ATP levels was normalized on protein levels (RLU × mL/mg; $x10^5$). Sirtuin activity was calculated by performing B/ T*S (pmol/min/ µg) and was normalized on protein levels. Statistical analysis was performed using a multiple Student t test; *P <0,05, **P <0,01 ***P<0,001****P<0,0001. (C) Expression level of cleaved (Cl.) Caspase-3 signal, obtained by immunohistochemistry performed on tumor masses, represented as percentage of positive area (magnification x20 and x40).

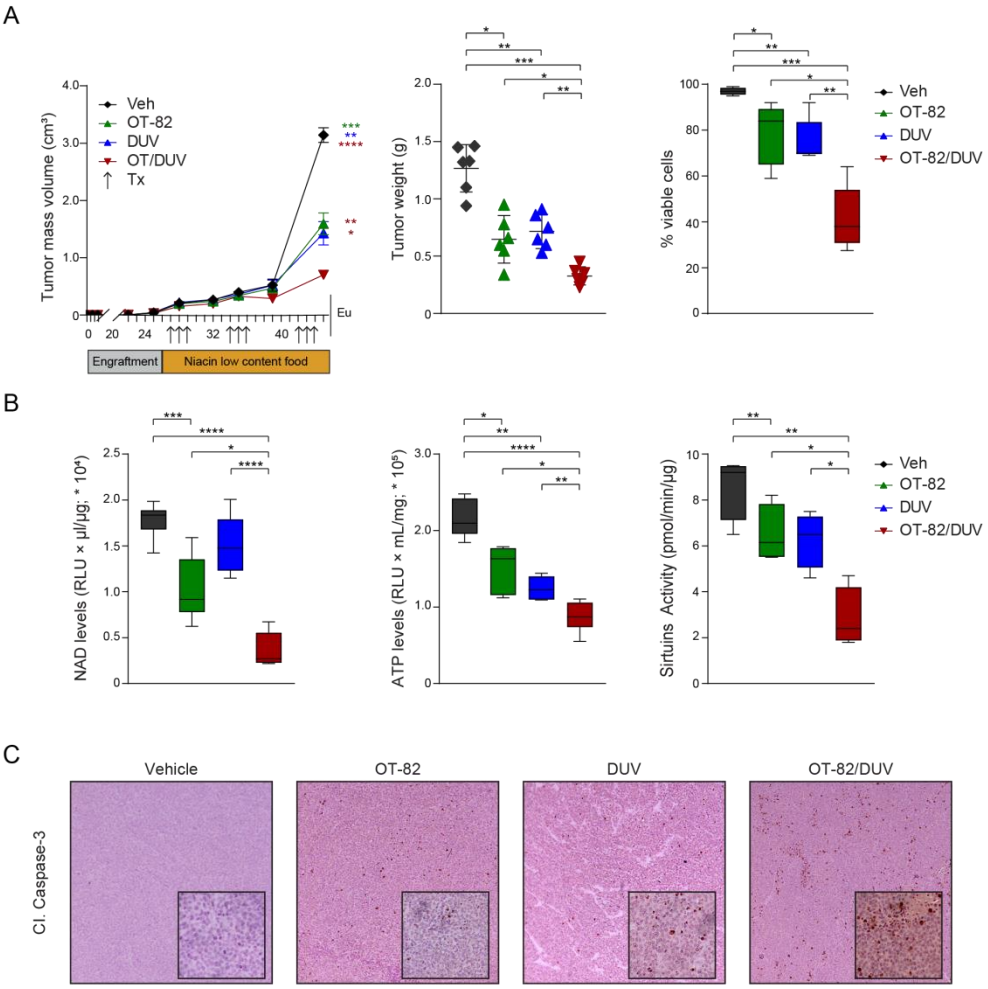

Figure 10. Tumor growth kinetics of RS1316 SC models treated with OT-82, Duvelisib, and their combination.
(A) RS cells were subcutaneously injected into both flanks of NSG mice. After palpable tumors were evident (tumor volume of 0.2 cm3), animals were randomly assigned to vehicle, OT-82 40 mg/kg, Duvelisib 100 mg/kg, or their combination. 2 days before starting the treatment we substituted the regular mice diet, with a custom diet lower of Niacin. Drugs were OG administered for three consecutive days as indicated by arrows (Tx), leaving a 4 day-washout period between treatment cycles. Tumor masses were measured using a digital caliper. Left panels display mean and standard error of the mean values for tumor masses with data evaluated using the multiple-sample Paired t tests. Center panels display individual mean and standard deviation values for tumor masses at the end of treatment on days 25 with data evaluated using Paired t tests. Right panels display the percentage of viable RS cells at the end of treatment with vehicle (black), OT-82 (green), Duvelisib (blue), and their combination (red). Data are reported as mean 6 SEM. (B) NAD^+ levels, ATP levels and Sirtuin activity of RS cells at the end of treatment. NAD^+ levels was normalized on protein levels (RLU x µl/µg; $x10^4$). ATP levels was normalized on protein levels (RLU × mL/mg; $x10^5$). Sirtuin activity was calculated by performing B/ T*S (pmol/min/ µg) and was normalized on protein levels. Statistical analysis was performed using a multiple Student t test; *P <0,05, **P <0,01 ***P<0,001****P<0,0001. (C) Expression level of cleaved (Cl.) Caspase-3 signal, obtained by immunohistochemistry performed on tumor masses, represented as percentage of positive area (magnification x20 and x40).

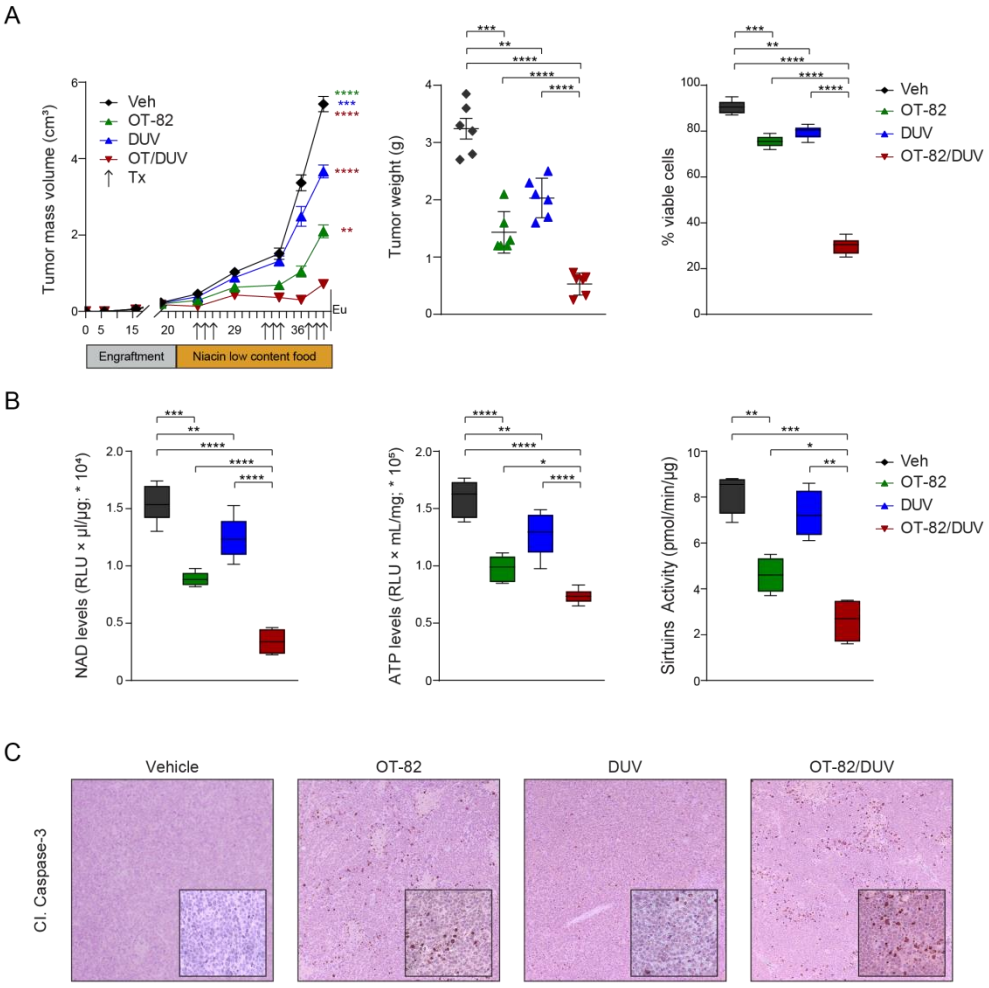

Figure 11. Tumor growth kinetics of RS1050 SC models treated with OT-82, Duvelisib, and their combination.
(A) RS cells were subcutaneously injected into both flanks of NSG mice. After palpable tumors were evident (tumor volume of 0.2 cm3), animals were randomly assigned to vehicle, OT-82 40 mg/kg, Duvelisib 100 mg/kg, or their combination. 2 days before starting the treatment we substituted the regular mice diet, with a custom diet lower of Niacin. Drugs were OG administered for three consecutive days as indicated by arrows (Tx), leaving a 4 day-washout period between treatment cycles. Tumor masses were measured using a digital caliper. Left panels display mean and standard error of the mean values for tumor masses with data evaluated using the multiple-sample Paired t tests. Center panels display individual mean and standard deviation values for tumor masses at the end of treatment on days 25 with data evaluated using Paired t tests. Right panels display the percentage of viable RS cells at the end of treatment with vehicle (black), OT-82 (green), Duvelisib (blue), and their combination (red). Data are reported as mean 6 SEM. (B) NAD^+ levels, ATP levels and Sirtuin activity of RS cells at the end of treatment. NAD^+ levels was normalized on protein levels (RLU x µl/µg; $x10^4$). ATP levels was normalized on protein levels (RLU × mL/mg; $x10^5$). Sirtuin activity was calculated by performing B/ T*S (pmol/min/ µg) and was normalized on protein levels. Statistical analysis was performed using a multiple Student t test; *P <0,05, **P <0,01 ***P<0,001****P<0,0001. (C) Expression level of cleaved (Cl.) Caspase-3 signal, obtained by immunohistochemistry performed on tumor masses, represented as percentage of positive area (magnification x20 and x40).

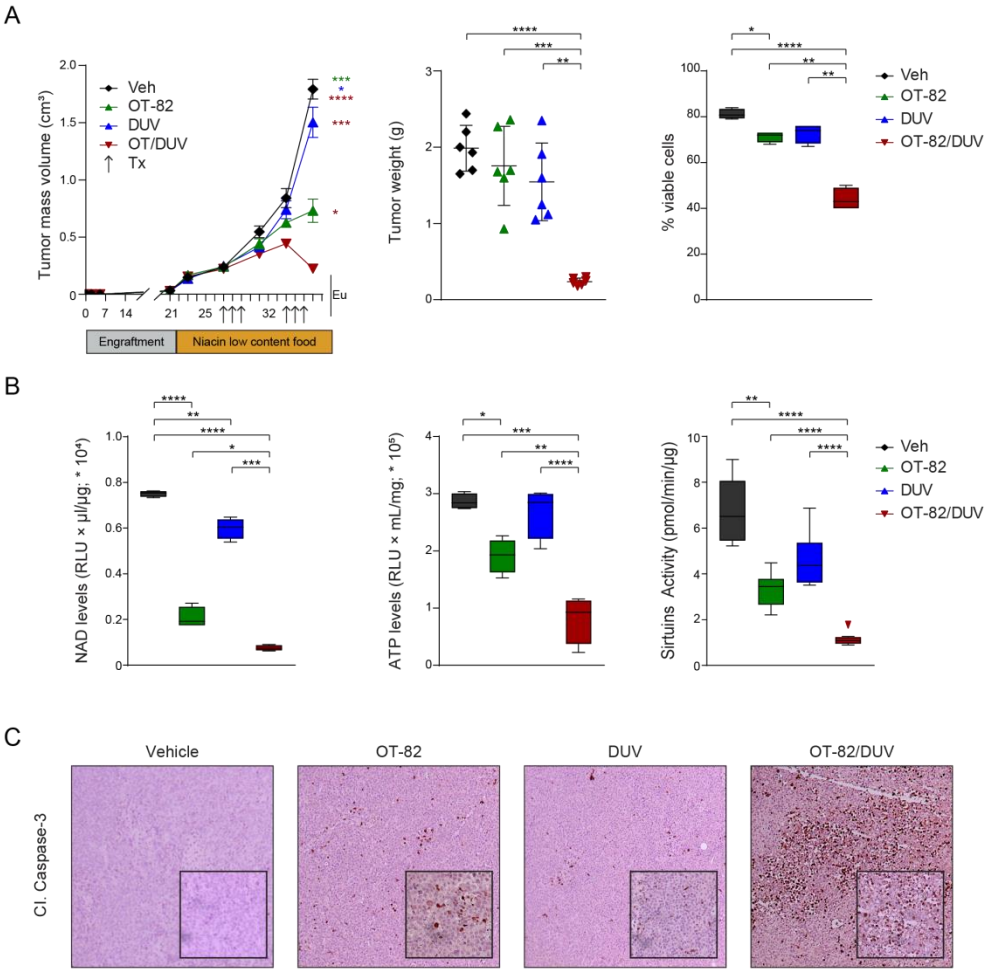

Figure 10. Tumor growth kinetics of IP867/17 SC models treated with OT-82, Duvelisib, and their combination.
(A) RS cells were subcutaneously injected into both flanks of NSG mice. After palpable tumors were evident (tumor volume of 0.2 cm3), animals were randomly assigned to vehicle, OT-82 40 mg/kg, Duvelisib 100 mg/kg, or their combination. 2 days before starting the treatment we substituted the regular mice diet, with a custom diet lower of Niacin. Drugs were OG administered for three consecutive days as indicated by arrows (Tx), leaving a 4 day-washout period between treatment cycles. Tumor masses were measured using a digital caliper. Left panels display mean and standard error of the mean values for tumor masses with data evaluated using the multiple-sample Paired t tests. Center panels display individual mean and standard deviation values for tumor masses at the end of treatment on days 25 with data evaluated using Paired t tests. Right panels display the percentage of viable RS cells at the end of treatment with vehicle (black), OT-82 (green), Duvelisib (blue), and their combination (red). Data are reported as mean 6 SEM. (B) NAD^+ levels, ATP levels and Sirtuin activity of RS cells at the end of treatment. NAD^+ levels was normalized on protein levels (RLU x µl/µg; $x10^4$). ATP levels was normalized on protein levels (RLU × mL/mg; $x10^5$). Sirtuin activity was calculated by performing B/ T*S (pmol/min/ µg) and was normalized on protein levels. Statistical analysis was performed using a multiple Student t test; *P <0,05, **P <0,01 ***P<0,001****P<0,0001. (C) Expression level of cleaved (Cl.) Caspase-3 signal, obtained by immunohistochemistry performed on tumor masses, represented as percentage of positive area (magnification x20 and x40).

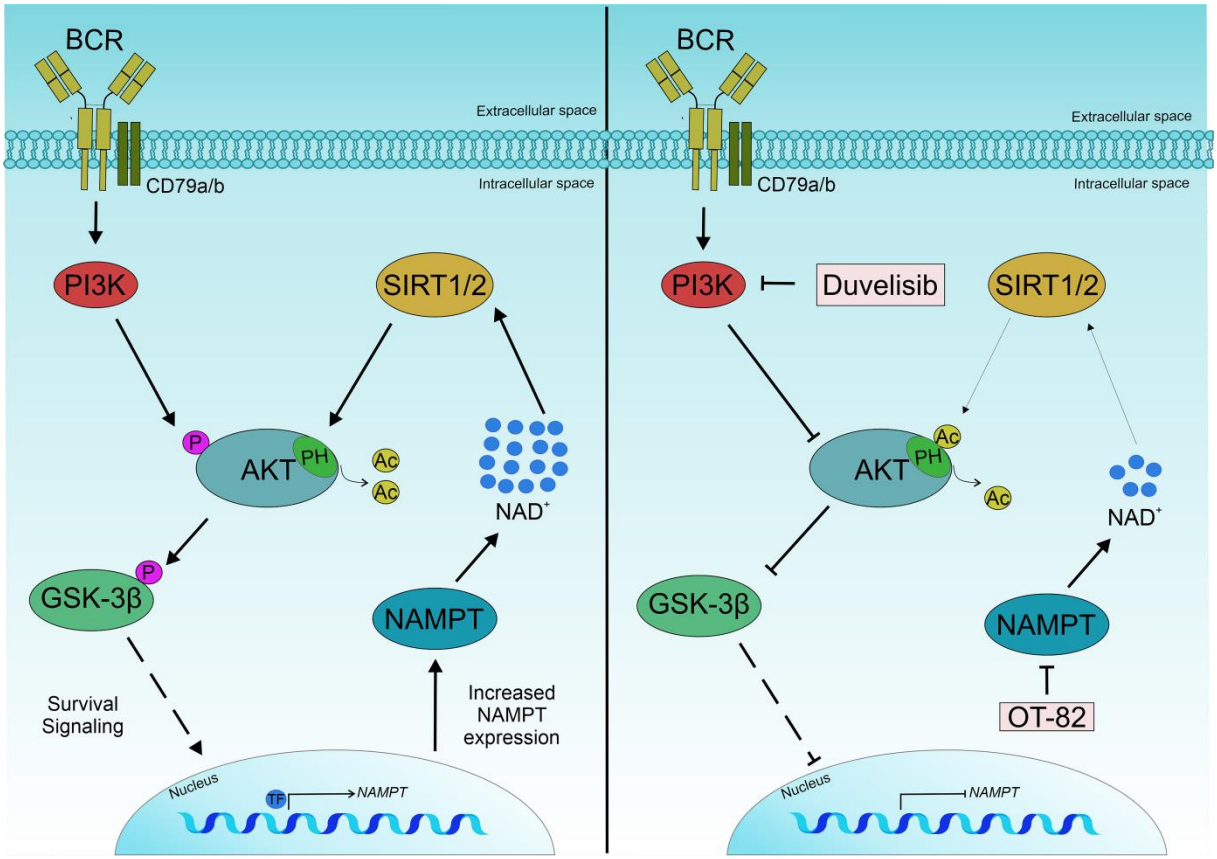

Figure 13: Representation of the molecular mechanism being the synergy between Duvelisib and OT-82.
Activation of the BCR receptor positive modulate PI3K/AKT/NAMPT/SIRT1-SIRT2 axis. Duvelisib treatment decrease AKT phosphorylation and NAMPT expression, resulting in reduced SIRT1 and SIRT2 activity. The concomitant inhibition of OT-82 further sustain the drop in SIRT1 and SIRT2 activity followed thought an increase in AKT acetylation improving RS cells apoptosis.

Publications of this PhD thesis

Title: Simultaneous inhibition of the B cell receptor signaling pathway and NAMPT enzymatic activity shows potent anti-tumor activity in Richter's syndrome patient-derived xenografts

Authors: Vincenzo Gianluca Messana, Nicoletta Vitale, Matteo Rovere, Andrea Iannello, Noemi Anna Pesce, Matilde Micillo, Claudio Martines, Dimitar Efremov, Tiziana Vaisitti, Silvia Deaglio

Individual Contribution:

This work was build and developed as the main research project of my PhD course. Supported by the experience of the Professor Silvia Deaglio and Professor Tiziana Vaisitti, I designed and performed all the experiments shown in the manuscript, thanks to the collaboration of Nicoletta Vitale, Matteo Rovere, Andrea Iannello, Noemi Anna Pesce, Matilde Micillo, Claudio Martines and Dimitar Efremov. Together with Professor Tiziana Vaisitti and Silvia Deaglio I interpreted data and wrote the manuscript.

Acknowledgements:

First, I want to thanks my mentor Prof. Dr. Silvia Deaglio for giving me the opportunity to accomplish my PhD studies at the laboratory for the Molecular Biotechnology Center (MBC) Guido Tatore, as well as for her excellent scientific input and for the inspiring and challenging approaches.

However, my deepest gratitude here goes to Prof. Tiziana Vaisitti and Dr. Valentina Audrito for being not only my tutors but also my guide through my PhD thesis by proving high expertise and invaluable advice.

I also thanks my groups collegues, Federica Gaudino, Antonella Managò, Nicoletta Vitale, Andrea Iannello, Marcello Lingua, Matteo Rovere, Martina Migliorero, Noemi Anna Pesce, Lorenzo Brandimarte, Monica Sorbini, Benjamin Baffour Gyau, Adriana Saba and Francesca Arruga

List of publications

(chronological order, 2018-to date, during PhD)

1. Tumors carrying BRAF-mutations over-express NAMPT that is genetically amplified and possesses oncogenic properties. Audrito V, Moiso E, Ugolini F, Messana VG, Brandimarte L, Manfredonia I, Bianchi S, De Logu F, Nassini R, Szumera-Ciećkiewicz A, Taverna D, Massi D, Deaglio S. J Transl Med. 2022 Mar 10;20(1):118. doi: 10.1186/s12967-022-03315-9. PMID: 35272691 Free PMC article.

2. The Extracellular NADome Modulates Immune Responses. Audrito V, Messana VG, Brandimarte L, Deaglio S. Front Immunol. 2021 Aug 4;12:704779. doi: 10.3389/fimmu.2021.704779. eCollection 2021. PMID: 34421911 Free PMC article. Review.

3. NAMPT Over-Expression Recapitulates the BRAF Inhibitor Resistant Phenotype Plasticity in Melanoma. Audrito V, Messana VG, Moiso E, Vitale N, Arruga F, Brandimarte L, Gaudino F, Pellegrino E, Vaisitti T, Riganti C, Piva R, Deaglio S. Cancers (Basel). 2020 Dec 20;12(12):3855. doi: 10.3390/cancers12123855. PMID: 33419372 Free PMC article.

4. NAMPT and NAPRT: Two Metabolic Enzymes With Key Roles in Inflammation. Audrito V, Messana VG, Deaglio S. Front Oncol. 2020 Mar 19;10:358. doi: 10.3389/fonc.2020.00358. eCollection 2020.PMID: 32266141 Free PMC article. Review.

5. NAD-Biosynthetic and Consuming Enzymes as Central Players of Metabolic Regulation of Innate and Adaptive Immune Responses in Cancer. Audrito V, Managò A, Gaudino F, Sorci L, Messana VG, Raffaelli N, Deaglio S. Front Immunol. 2019 Jul 25;10:1720. doi: 10.3389/fimmu.2019.01720. eCollection 2019. PMID: 31402913 Free PMC article. Review.